Distribution Agreement

In presenting this thesis or dissertation as a partial fulfillment of the requirements for an advanced degree from Emory University, I hereby grant to Emory University and its agents the non-exclusive license to archive, make accessible, and display my thesis or dissertation in whole or in part in all forms of media, now or hereafter known, including display on the world wide web. I understand that I may select some access restrictions as part of the online submission of this thesis or dissertation. I retain all ownership rights to the copyright of the thesis or dissertation. I also retain the right to use in future works (such as articles or books) all or part of this thesis or dissertation.

Signature:

_____ _____

Lukas Hoffmann Date

Complex sensorimotor processing and neural plasticity in the Bengalese finch song system during vocal learning and error correction

Lukas Alexander Hoffmann
Doctor of Philosophy
Graduate Division of Biological and Biomedical Sciences
Neuroscience

_____
Samuel J. Sober
Advisor

_____
Dieter Jaeger
Committee Member

_____
Robert Liu
Committee Member

_____
Ilya Nemenman
Committee Member

_____
Lena Ting
Committee Member

Accepted:

_____
Lisa A. Tedesco, Ph.D.
Dean of the James T. Laney School of Graduate Studies

_____
Date

Complex sensorimotor processing and neural plasticity in the Bengalese finch song system during vocal learning and error correction

By

Lukas Alexander Hoffmann

B.S., University of Pittsburgh, 2010

Advisor: Samuel J. Sober, Ph.D.

An abstract of
A dissertation submitted to the Faculty of the
James T. Laney School of Graduate Studies of Emory University
in partial fulfillment of the requirements for the degree of
Doctor of Philosophy
in Neuroscience
2017

Abstract

Complex sensorimotor processing and neural plasticity in the Bengalese finch song system during vocal learning and error correction

By Lukas Alexander Hoffmann

A major goal of neuroscience is to understand how the brain learns to change motor behavior in response to sensory input. Moreover, the ability to learn and adapt complex vocalizations is critical for communication. Although the brain uses auditory feedback to calibrate vocal performance, the neural substrates of vocal learning remain unclear. Therefore, to fully understand the mechanisms of vocal plasticity, we must determine how the brain learns to change vocal motor output using auditory feedback. This dissertation uses Bengalese finches (*Lonchura striata*), a vocal learning species, to answer three questions: the rules of generalization in adaptive error correction, whether dopamine in the learning-specialized basal ganglia nucleus Area X is required for vocal learning, and how dopamine affects Area X's neural activity.

We first showed that adaptive error correction of a vocal gesture (song syllable) in a sequence of gestures generalized to other gestures. Using miniaturized headphones, we perturbed pitch in real time as birds were singing a particular song syllable, which gradually caused compensatory pitch changes. Then, we measured generalization by quantifying pitch changes in non-perturbed syllables. We found that learning to change pitch on one gesture generalized to the same type of gesture produced in other contexts, learning generalized anti-adaptively to different gestures, and the magnitude of generalization decreased with increasing sequential distance. Next, we demonstrated that learning to change pitch depends on intact dopamine signaling in Area X, a basal ganglia nucleus critical for vocal learning. We drove pitch changes on single song syllables with negative reinforcement (aversive blasts of white noise when pitch was above or below a threshold). Finally, we performed preliminary experiments to investigate how partial loss of dopamine inputs to Area X affected its spontaneous and song-playback-evoked neural firing and local field potential. This is a first step towards investigating how dopamine guides neural firing changes during vocal learning. By finding that generalization depends on vocal gestures' type and position within a sequence and that intact dopamine signaling is required for negative-reinforcement-driven vocal learning, this dissertation lays a foundation for future studies into the rules of vocal learning and the role of dopamine.

Complex sensorimotor processing and neural plasticity in the Bengalese finch song system during vocal learning and error correction

By

Lukas Alexander Hoffmann

B.S., University of Pittsburgh, 2010

Advisor: Samuel J. Sober, Ph.D.

A dissertation submitted to the Faculty of the
James T. Laney School of Graduate Studies of Emory University
in partial fulfillment of the requirements for the degree of
Doctor of Philosophy
in Neuroscience
2017

ACKNOWLEDGMENTS

The old saying goes “It takes a village to raise a child”. I think it is also true that it takes a village to make a PhD. Certain people in that village have been especially important in my quest for a doctorate.

First, I would like to thank my PI, Dr. Sam Sober. You have always been there to give me guidance and to nudge me onto more productive trajectories when I was off course. Your cheerful personality, enthusiasm and scientific ideas have always sparked my own motivation and encouraged me to keep finding a way forward. You gave me the freedom to pursue my own research and career goals. You have taught me how to compose good scientific questions, design experiments, write papers and think critically. Finally, you made it fun to work in the lab, and social events like Lab Retreat and Sausagefest helped the lab come together as a team. I consider you a colleague and a friend and I hope I can be as good of a boss in the future as you have been.

Thanks to my dissertation committee: Dr. Dieter Jaeger, Dr. Robert Liu, Dr. Ilya Nemenman and Dr. Lena Ting. You have given me great critical feedback at every meeting and made sure I stayed on track. I appreciate your support and advice regarding my plans for a career outside academia. I especially thank Dr. Jaeger for being a co-sponsor on my NRSA grant and Dr. Liu for taking me on as a rotation student in 2010. Each committee member’s expertise and guidance has strengthened the quality of my work.

I would also like to thank the many current and past Sober lab members: Emily Berthiaume, Diala Chehayeb, Bryce Chung, Amanda Jacob, Conor Kelly, Ben Kuebrich, James MacGregor, David Nicholson, Andrea Pack, Jonah Queen, Sevara Rakhimova, Varun Saravanan, Reid Schwartz, Jeffrey Simpson, Kyle Srivastava, Claire Tang, Laura Waters-Goggins, Lyndie Wood and MacKenzie Wyatt. Some of you were there from the start and others joined as I was finishing up, but you all made positive contributions. I want to give a special thanks to my fellow grad

students who were always ready to help, argue about science, make bad jokes, have the occasional beer (or three) and make our lab a fun place to spend 7 years. I will miss you.

I appreciate all my personal friends in the Neuroscience Program and the Neuroscience faculty and staff. Starting when I was a nervous recruit, you have always made me feel part of a family. This Program has been a great nurturing environment for my development as a scientist. Hanging out with everyone through these years let me have a fun time and many happy memories. You all helped me do the improbable: be a grad student and be happy at the same time. I hope I have done the same for you.

Thanks to my mom and dad (Doris and Ken) for your hard work in bringing me up and supporting me all these years. As a little kid, I wanted to be a "fizissist" just like my dad, but later I decided to slack off and get a PhD in a less (mathematically) challenging field. Sorry for disappointing you, Dad. Thanks also to my siblings Anna, Eva, Phillip and Elisa for always being there, and the rest of my extended family.

My girlfriend Tish Wolfe has been with me through the second half of my PhD. She has been my biggest emotional support and inspires me every day to improve myself and how I do my work. I am grateful to have her in my life.

Thanks to the Grace Masters Toastmasters Club, who have taught me much about public speaking and leadership. Being a successful scientist requires these "soft skills" as much as everything else.

Finally, I would like to thank my funding sources at the NIH, from whom I received a two-year NRSA, and Emory's Udall Center for Excellence in Parkinson's Disease Research. As with most grants, I was not able to complete every experiment exactly as written, but I accomplished most what I set out to do. I also thank the US taxpayers that ultimately funded me. I hope my research will end up paying for itself. If not, it has at least given me the skill set to be a very productive member of society going forward.

TABLE OF CONTENTS

LIST OF FIGURES AND TABLES

LIST OF ABBREVIATIONS

4-AP	4-Aminopyridine
6-OHDA	6-hydroxydopamine
ABC	Avidin-biotin complex
AFP	Anterior Forebrain Pathway
AP	Anterior/posterior axis
BG	Basal ganglia
BOS	Bird's own song (playback stimulus)
BOSdown	Bird's own song, pitch-shifted downwards (playback stimulus)
BOSup	Bird's own song, pitch-shifted upwards (playback stimulus)
BOSwn	Bird's own song, some syllables interrupted with white noise (playback stimulus)
BSA	Bovine serum albumin
DA	Dopamine
DAB	Diaminobenzidine
DARPP-32	Dopamine- and cyclic AMP-regulated neuronal phosphoprotein
DLM	Dorsolateral nucleus of the anterior thalamus
DV	Dorsal/ventral axis
EDTA	Ethylenediaminetetraacetic acid
FS	Fast-spiking interneurons
FOXP2	Forkhead box protein P2
GABA	gamma-aminobutyric acid
GPe	External globus pallidus
GPi	Internal globus pallidus
HPLC	High-performance liquid chromatography
HRP	Horseradish peroxidase

HVC	Used as a proper name, a premotor nucleus projecting to RA and Area X
LANT6	Lys8-asn9-neurotensin8–13
LC	Locus coeruleus
LFP	Local field potential
LMAN	Lateral magnocellular nucleus of the anterior nidopallium
LSVT	Lee Silverman Voice Treatment (subtypes: LOUD and BIG)
LTP	Long-term potentiation
LTS	Low-threshold spiking neurons
ML	Medial/lateral axis
MPP^+	N-Methyl-4-phenylpyridine
MPTP	1-methyl-4-phenyl-1,2,3,6-tetrahydropyridine
MSN	Medium spiny neuron
NE	Norepinephrine
NeuN	Neuronal nuclei protein
nXIIts	Tracheosyringeal portion of the hypoglossal nucleus
OD	Optical density
PB	Phosphate buffer solution
PD	Parkinson's disease
RA	Robust nucleus of arcopallium
REV	Reversed bird's own song (playback stimulus)
ROI	Region of interest
RPE	Reward prediction error
RS	Response strength (see Section 5.2)
SIL	Silence (playback stimulus)
SNc	Substantia nigra pars compacta
STN	Subthalamic nucleus

TAN	Tonically active neurons
TH	Tyrosine hydroxylase
VP	Ventral pallidum
VTA	Ventral tegmental area
WN	White noise

CHAPTER 1

INTRODUCTION AND LITERATURE REVIEW

Humans and other animals learn to perform complex behaviors by modifying motor commands in response to sensory input. A major goal in neuroscience is to understand the neural substrates of motor plasticity and the computational rules by which it proceeds. Vocal learning is an excellent model of complex motor skill learning. In order to speak, humans must learn to adeptly manipulate the vocal organs (lungs, vocal cords, tongue, lips and other articulators) [1,2]. This skill is acquired and maintained using sensory feedback, including auditory feedback [3–5]. Songbirds likewise produce complex, learned vocalizations that are maintained with sensory feedback [6–9]. By studying how vocal learning works in songbirds and humans, we can get insight into the principles of complex sensorimotor plasticity. Vocal learning is also a relevant subject of study in its own right because speech is critical for communication and various disorders damage the ability to learn, produce and maintain normal vocalizations [10–13]. For example, Parkinson's disease (PD) symptoms, caused by deficiencies in the modulatory neurotransmitter dopamine (DA) in the basal ganglia (BG), include monotonic quiet speech [14] along with other motor control problems.

Despite much work investigating motor plasticity and vocal learning, we still do not understand the general rules by which learning proceeds and how neurons implement these rules. A better understanding could lead to more effective treatments for disorders affecting speech and other motor behaviors. Two important aspects of vocal learning need to be clarified: how it generalizes across contexts and the role of DA in the BG during sensorimotor learning. This dissertation will use a songbird model of vocal learning to demonstrate novel rules of generalization, show that DA in the BG is necessary for vocal learning using auditory feedback, and explore DA-dependent aspects of songbird BG neural activity. This lays the groundwork for future studies of DA's role in sensorimotor learning and generalization.

1.1 Songbirds as a model system

Vocal learning is a rare behavior seen only in a few species including humans, songbirds [15], bats [16], elephants [17] and cetaceans [18]. Many animals, including mice and nonhuman primates, produce innate non-learned vocalizations [19,20] but juvenile humans and songbirds learn to speak and sing from tutors of the same species during a critical period [6,21]. Human speech and birdsong share many common mechanisms [21,22]. In particular both produce spectrally complex and sequenced vocalizations, depend on auditory feedback to maintain stable vocalizations [7–9,23–25], and evolved specialized brain networks for controlling vocal learning and production [22,26].

Songbirds possess several key advantages as a model system for complex motor plasticity, including vocal plasticity [27]. First, songbirds have well-characterized neural anatomy specialized for singing behavior called the "song system", which includes Area X, a BG nucleus specialized to guide vocal learning (see Section 1.4). Second, song is highly amenable to statistical analysis, since each bird has a limited repertoire of song syllables (**Fig. 1.1a**) whose acoustic features remain consistent [28] and are under precise neural control. For example, in the motor and premotor nuclei RA (robust nucleus of arcopallium) and LMAN (lateral magnocellular nucleus of the anterior nidopallium) (**Fig. 1.1b**), neural firing correlates with trial-by-trial variability in acoustic features and microstimulating LMAN drives pitch and amplitude changes [29,30]. Conveniently, invasive manipulations of the song system do not affect non-vocal behaviors [31,32] and we can drive sensorimotor error correction or operant learning by manipulating auditory feedback, i.e. shifting subjectively experienced pitch with headphones or driving pitch changes with aversive white noise (WN) reinforcement [7,33]. The favorable combination of anatomy, acoustic properties and experimental accessibility makes songbirds an excellent model system to study the principles of vocal plasticity. It is also a good model for general motor learning since songbirds learn complex sequenced behaviors.

1.2 Generalization of motor learning

Generalization, or the ability to transfer learning from one context to another, is a fundamental feature of motor learning. The ability to generalize makes it easier to learn and maintain complex behaviors in a variable environment whether reaching, speaking or performing other motor actions. For example, when study subjects make perturbed reaching movements (so that the hand arrives off target), they learn to alter their movement to arrive on target. This learning generalizes to nearby movement directions [34–36]. When human subjects wearing headphones are exposed to artificial pitch shifts they adaptively change their vocal output to reduce experienced auditory error [3,4,24]. This learning can transfer to the same vowel in a different word or other vowels that are acoustically similar [3,4,23,37,38].

Computational models of vocal generalization are limited because the rules of generalization remain unclear for speech and other movements. While some speech studies have suggested error-corrective learning does not generalize [39–41] or generalizes based on acoustic similarity to training utterances [37], these studies have not examined generalization across the natural vocal repertoire such as during conversational speech. Across a variety of motor tasks including walking, throwing, catching, lifting, drawing and piano playing, several studies have found that learning generalizes mostly to similar movements [42–48] but others have shown it can transfer across context, muscle groups (such as one arm to another) and to different movements depending on the task [49–55]. Generalization patterns can also be modulated by contextual cues. Subjects can learn two or more transformations at once when provided with salient cues [56–61], such as instantly compensating to leftward or rightward force fields when they are predicted by differently-colored lights [58]. This complexity and task-dependency of learning transfer demonstrates more work is needed to quantify its rules.

One barrier to understanding is that studies typically use a small set of training and transfer movements (or utterances). For broad movement classes such as arm-reaching or speech, it is difficult to explore the large repertoire of natural movements (or speech utterances) and sequences

of movements (or phonemes). It is therefore also unclear how generalization occurs across all naturally produced movements and motor sequences, including vocalizations. Also, in humans (unlike animals), we must use non-invasive methods or take advantage of existing conditions, such as recording during medical surgeries or investigating behavioral deficits related to neurological diseases. This work addresses the knowledge gap by exploring generalization patterns across the full range of natural vocal behavior in an experimentally accessible songbird model.

Observing generalization patterns for sequences of natural behavior could lead to new hypotheses of how generalization is implemented in motor circuits. To provide contextual background we will briefly review current computational models. Generalization to similar movements and phonemes could be implemented via neural tuning curves and population coding in the motor cortex [54,56,62]. A computational model showed that when simulated subjects changed reaching movements to compensate for a force field, this learning generalized less to nearby reaching targets (such as 45° degrees counterclockwise) when simulated motor neurons had narrow tuning curves, meaning they were activated only for a narrow range of reach directions [63]. More complex generalization patterns could result from higher-level controllers gating multiple internal models via computational processes such as mixture-of-experts [64] or "MOSAIC" [58,65,66] which we will not discuss further here.

1.3 Dopamine and vocal learning

DA, a neurotransmitter that modulates neural firing and synaptic plasticity [67], has long been thought to help guide learning, especially through its actions in the BG [68]. In mammals, many midbrain DA neurons encode the difference between predicted and experienced reward (i.e. reward prediction error or RPE), leading to a prominent hypothesis that these signals guide reinforcement learning [69–72]. This dissertation does not examine whether DAergic motor learning is implemented consistent with a specific computational model. However, one example of how DA could be used to guide learning is Temporal Difference, where DAergic RPE is used to update predictions of future

rewards, which makes reward-predicting stimuli become associated with reward [73,74]. DA has also been linked to aversive reinforcement learning [75], motivation or "wanting" [76], motor skill learning in the motor cortex [77], movement vigor [78], attention to novel stimuli [79] and supporting normal patterns of BG activity that maintain motor control [80]. Since DA signaling is complex and seems to have several important roles, much remains unclear about its function in sensorimotor learning.

It is difficult to test BG DA's specific contributions to motor learning in humans and mammalian models, especially its role in modifying long-established motor skills acquired during development. DA lesions in the mammalian BG cause severe motor performance deficits [81,82] as does the DAergic deficiency in PD. Studies of vocal learning in PD [83,84] may be confounded not only by motor control deficits but also by extensive non-DAergic disruptions [85,86]. Furthermore, the effects of DAergic manipulation are not limited to the behavior being examined because the mammalian BG modulates a wide range of behaviors. When motor learning deficits are studied, they are often assessed using highly artificial tasks learned later in life such as operant reinforcement or serial reaction time (i.e. learning to press keys in response to stimuli that occur in a repeating sequence[87]) [88–90], instead of naturally produced motor behaviors. Finally, DA's contribution to vocal learning cannot be studied in nonlearning species, which include rodents and nonhuman primates [19,20]. This work overcomes these barriers by creating a DA-depleted state in a songbird BG circuit specialized for vocal learning (but not required for vocal performance or nonsinging behavior – see Section 1.4) and studying how this affects the ability to modify natural vocalizations.

Several mammalian studies have investigated DA's role in motor learning despite the aforementioned difficulties. Skill learning tasks such as trying to balance on a rotating rotarod [91] cause striatal synaptic plasticity [92] and depend on D_1 receptor signaling [93] and DA-deficient rodents showed learning deficits on these tasks [91,94–97]. Other studies have shown DA in the motor cortex is required for learning skilled tasks, such as modifying forelimb pronation/supination to reach around obstacles to obtain food rewards [77,97–99]. Interestingly, increasing evidence suggests loss of DA may

cause an active aberrant learning process, suggesting it is important for not only acquisition but also active maintenance of learned motor skills [100–103]. In other words, practicing motor tasks in the absence of DA may generate abnormal corticostriatal plasticity that leads to gradual deterioration of task performance. While these findings support the hypothesized role of DA in motor skill learning, it remains difficult to disentangle learning and performance functions and DA's role in vocal learning remains particularly understudied.

DA is hypothesized to guide vocal learning in songbirds [104–107], but there has been no direct evidence it is necessary for learning via external reinforcement. To summarize this model, learning is hypothesized to occur via an Actor-Critic mechanism: an "actor" in motor circuitry generates exploratory behavioral variability, followed by BG DAergic "critic" signals that drive adaptive learning by strengthening activity patterns yielding better outcomes [108,109]. In this model, DA neurons from the songbird VTA/SNc (ventral tegmental area and substantia nigra pars compacta; **Fig. 1.1b**) [110] provide phasic RPE signals indicating good or bad song performance as determined by the internal template [111] or external reinforcing stimuli including aversive WN [33]. In Area X brain slices, phasic DA release peaks at ~0.3 seconds after electrical stimulation and has an exponential decay time constant of ~0.5 sec (how long it takes to decay to ~36.8% of peak DA concentration), which is similar to mammalian striatum [112]. Area X medium spiny neurons (MSNs) receive the DA signals and glutamatergic motor efference copies from HVC (used as a proper name), LMAN and RA (via RA's projection to DLM – the dorsolateral nucleus of the anterior thalamus [109,113]; not shown in **Fig. 1.1b**). This leads to DA-dependent synaptic plasticity and causes Area X to bias downstream motor output and drive learning [114]. This model is supported by the fact that songbird VTA/SNc neurons have RPE-like signals during song [115]. Additionally, DA modulates Area X MSN excitability via D_1 and D_2 receptors [116], presynaptically modulates the strength of MSN inputs from HVC/LMAN [117] and is required for inducing long-term potentiation (LTP) onto MSNs via D_1 receptors [118,119]. VTA/SNc neurons are well placed to provide RPE signals because they receive auditory information via their bisynaptic inputs from Area X [120] and auditory

nuclei [121] whose neurons react to errors in predicted auditory feedback [121,122]. Despite this promising evidence, there has not been a direct test whether DA in the songbird BG is required for vocal learning.

In the song system DA also regulates song variability. The acoustic features of female-directed song are less variable than undirected song [123] and this "social-context-dependent variability" could represent the switch between motor exploration (finding actions resulting in good song performance) and exploitation (performing the favorable actions). DA levels rise for female-directed song [124,125] and D_1 receptor activation is required for social-context-dependent variability [126,127]. Higher DA could cause lower song variability by decorrelating MSN activity within Area X, leading to increased downstream firing precision [128]. A recent study also found a 6-hydroxydopamine (6-OHDA) lesion in Area X (chronic ~50% DA depletion) caused reduced variability in undirected song [129]. DA's functions in variability and learning are probably separate. Variability is likely controlled by tonic DA levels, whereas learning is more linked to phasic DA signals [130].

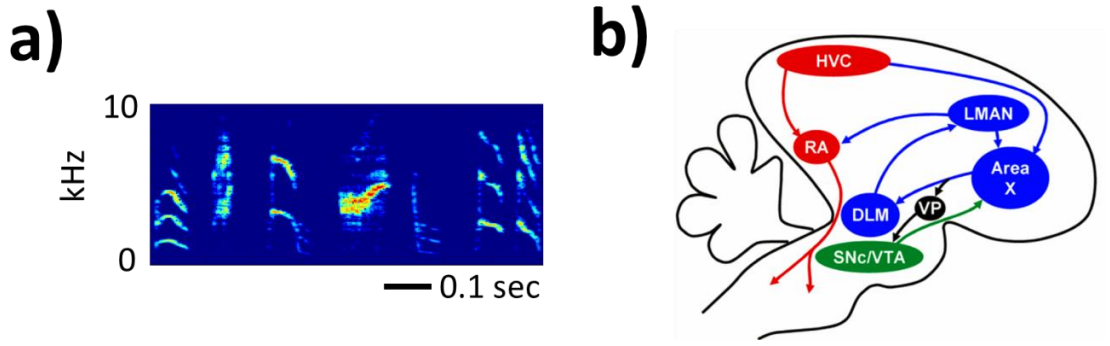

Figure 1.1. Song syllables and the song system. **(A)**, Spectrogram of seven song syllables. Brighter colors indicate higher power at the frequencies indicated on the Y axis. **(B)**, Simplified schematic of the song system, reprinted from [120] (© 2008 Wiley-Liss, Inc, used with permission). A vocal motor pathway (red) descends from HVC (used as a proper name) to the robust nucleus of the arcopallium (RA), which sends output to brainstem nuclei connected to vocal musculature including the tracheosyringeal portion of the hypoglossal nucleus (nXIIts; not shown). A second circuit (blue), known as the anterior forebrain pathway (AFP), receives excitatory input from HVC and includes the BG nucleus Area X, the dorsolateral nucleus of the anterior thalamus (DLM) and the lateral magnocellular nucleus of the nidopallium (LMAN). DAergic neurons (green) from the ventral tegmental area (VTA) and the substantia nigra pars compacta (SNc) project strongly to Area X. Area X sends inhibitory collaterals to the ventral pallidum (VP; black) which projects to SNc/VTA. VTA and SNc also receive input from a region (not shown here) that is connected to auditory cortical areas [120,121].

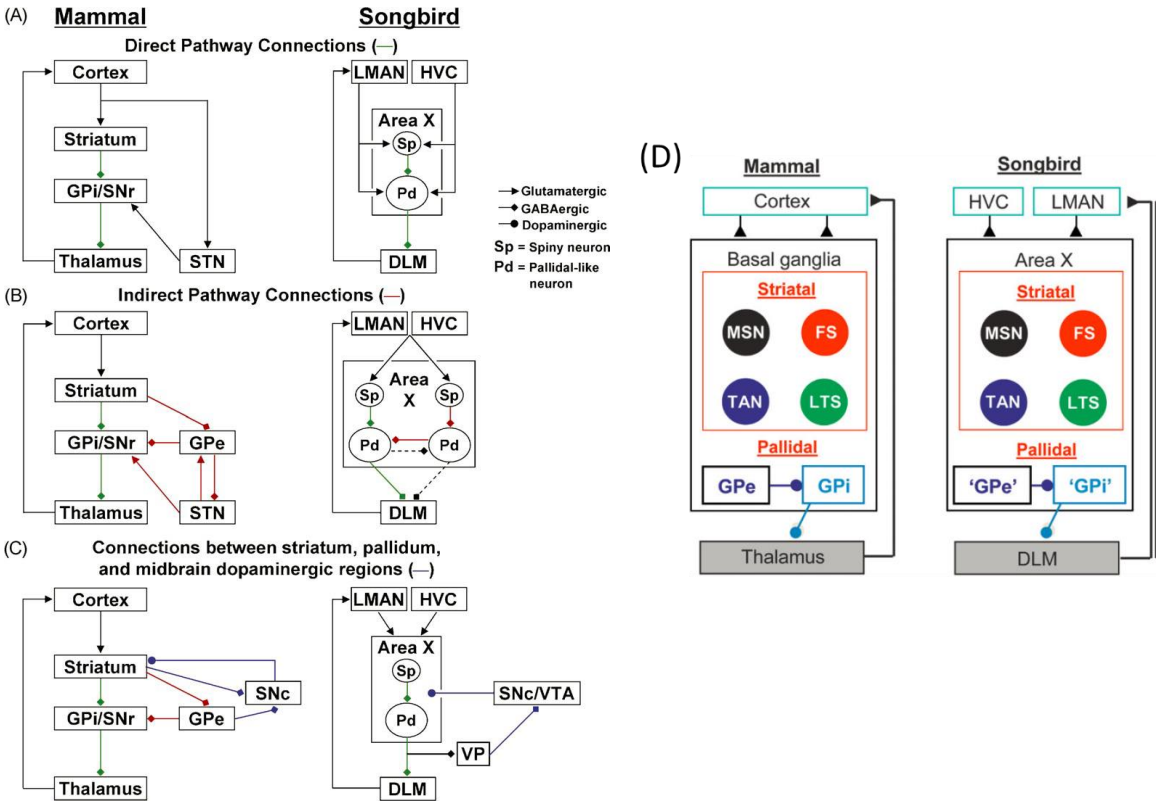

Figure 1.2. Comparison of mammalian BG and Area X circuitry. Figure and captions reprinted from [27,131], with permission. "The schematics of mammalian pathways focus on dorsal striatal and pallidal pathways and use primate terminology for the globus pallidus; internal and external portions (GPi and GPe) correspond to rodent entopeduncular nucleus and globus pallidus, respectively. **(A)** The direct pathway through the mammalian BG and songbird Area X (green lines). **(B)** The indirect pathway in mammals and a putative indirect pathway in Area X (red lines). The indirect pathway in Area X could be mediated via pallidal-like neurons that do not project to thalamus; alternatively, thalamus-projecting pallidal-like neurons could be interconnected (dashed lines). **(C)** Anatomical pathways among striatum, pallidum, and midbrain DAergic neurons differ in mammals and songbird Area X (blue lines). The SNc in mammals also receives BG input from the subthalamic nucleus (STN) and collaterals of SNr, but not GPi, neurons (not shown)." **(D)** "The avian Area X is homologous to the mammalian BG and includes striatal and pallidal cell types. The BG forms part of a highly conserved anatomical loop through several stations, from cortex to the BG (striatum and pallidum), then to thalamus and back to cortex. Similar loops are seen in the songbird: the cortical analogue nucleus LMAN projects to Area X, the pallidal components of which project to the thalamic nucleus DLM, which projects back to LMAN. Like the mammalian BG, Area X contains medium spiny neurons (MSN), fast-spiking interneurons (FS), tonically active neurons (TAN), and low-threshold spikers (LTS). Area X also contains GPi-like pallidal neurons that project to the thalamus, and GPe-like pallidal neurons that project within Area X. Note that there are some differences between Area X and mammalian BG. For example, Area X does not appear to contain, or interact with, neurons homologous to those of the mammalian subthalamic nucleus (STN; not shown), nor does Area X have a direct projection to midbrain DAergic areas (not shown)." ***A***, ***B***, *and* ***C*** *and their captions were reprinted from* [131]*: Journal of Chemical Neuroanatomy, Vol 39, Issue 2, Samuel Gale & David Perkel, Anatomy of a songbird basal ganglia circuit essential for vocal learning and plasticity, p. 126, © 2009 Elsevier B.V, used with permission from Elsevier.* ***D*** *and its caption was reprinted from* [27]*: Michale Fee & Constance Scharff, The songbird as a model for the generation and learning of complex sequential behaviors, ILAR Journal, © 2010, Vol 51, Issue 4, p. 366, used with permission of Oxford University Press.*

1.4 The song system and Area X

A network of interconnected nuclei known as the song system enables song learning and production (**Fig. 1.1b**). Song is produced via the vocal motor pathway (**Fig. 1.1b, red**) which sends output to brainstem motoneurons activating vocal muscles [132]. The vocal motor pathway is connected to the anterior forebrain pathway (AFP) [133] (**Fig. 1.1b, blue**), which is not essential for song production but is required for both juvenile song learning and adult song plasticity [109,134,135]. The AFP actively generates exploratory song variability, adaptively biases vocal plasticity and consolidates learning via LMAN input to RA [30,109,136,137]. The mechanisms by which the AFP guides vocal plasticity are under active investigation.

In this dissertation we focus on the song system's nucleus Area X [32] – a large, anatomically well-defined nucleus within the avian BG which, despite being a single nucleus, is homologous to mammalian BG (**Fig. 1.2**) [138–140]. Although it is a single nucleus and does not connect to the rest of the avian BG, Area X shares important features with several mammalian BG nuclei [138–140]. These include simple direct and indirect pathways [141] (**Fig. 1.2a,b**), similar striatal and pallidal cell types [142–144] (**Fig. 1.2d**), topographic projections within a cortico-BG-thalamo-cortical loop (Area X's anatomical subregions project to DLM subregions, which project to LMAN subregions, which send collaterals back to the same Area X subregions) [145,146] and genes underlying vocal learning including the speech-related gene FOXP2 (Forkhead box protein P2) [147]. Of course there are some differences between songbird and mammalian BG, including the absence of the subthalamic nucleus (STN) in song system circuitry [27,131,148] and the lack of direct reciprocal projections between Area X and its DAergic input [120] (**Fig. 1.2c**). However, despite its simpler internal circuitry [149] Area X shares many core features with mammalian BG.

Area X is an excellent model for the BG's role in motor skill learning and maintenance [138,149]. Area X and mammalian BG share functional features related to learning [149]. For example, the topographic cortico-BG loops in both mammals [150,151] and songbirds [30,134,152] are linked to guided amplification of behaviors associated with reward, which in both groups is followed by a process

of consolidation [149,153]. However, while the BG of other model systems is involved in a diversity of motor functions, Area X is dedicated to just one precisely-controlled and highly quantifiable behavior: song [149]. Evidence for this includes the findings that Area X is absent in non-singing females [154] and that Area X immediate early gene expression occurs only during song, not during other motor behaviors or sensory stimuli [31]. This allows the experimenter to selectively access BG circuitry involved in a single learned behavior.

Area X has an additional unique advantage: it is specialized for vocal learning [134,136,155] but not required for vocal performance [156,157]. It is necessary for song learning in young birds [156,157], pitch learning driven by aversive WN cues [158] and song degradation after deafening [152]. Importantly, lesions of Area X or its DAergic input have little effect on song performance [156,157], except for small vocal variability changes or temporary increases in syllable repetitions reminiscent of stuttering [129,159]. Since disturbing songbird cortico-BG circuits disrupts learning but barely affects performance [30,134,152,157,158], this removes the confound of motor control deficits. This advantage has been exploited to produce new insights that can be translated to research in other species, including the finding that songbird cortico-BG circuitry actively generates variability in acoustic features during motor exploration [30,136]. Thus, manipulating Area X allows us to selectively study the BG's role in vocal learning, which can lead to new insights on how the BG helps guide complex motor skill learning.

Area X's neural subtypes and their anatomical connections are relatively well characterized. Area X contains six types of neurons that are similar to their counterparts in mammalian striatum, external globus pallidus (GPe) and internal globus pallidus (GPi): striatal-like MSNs, three types of striatal-like interneurons, GPe-like neurons and GPi-like neurons [141–144,160] (**Fig. 1.2d**). ***Henceforth we will refer to these as "striatal", "pallidal", "GPe" and "GPi" neurons even though they are all located in the same nucleus***. In extracellular recordings pallidal neurons can be easily distinguished from striatal neurons based on their high spontaneous firing rates [127,144], and all six subtypes can be distinguished using additional features of their firing patterns

(such as burstiness) and spike waveforms (broad or narrow) [143,144]. Although there are many similarities between Area X and mammalian BG neurons, there are also some differences [131,138,142]. For example, Area X firing rates during song are 3-4x higher than mammalian BG firing rates during behavior [143,144]. Although this dissertation focused only on pallidal neurons (see Study 3, Chapter 5), we review each neuron type below.

As in mammalian striatum, most Area X neurons are inhibitory gamma-aminobutyric acid (GABA)ergic MSNs that have small somata, spiny dendrites and express the MSN markers Substance P, enkephalin and DARPP-32 (dopamine- and cyclic AMP-regulated neuronal phosphoprotein) [160,161]. Roughly 80% of all Area X neurons are MSNs [160]. Both mammalian and Area X MSNs have fast inward rectification upon hyperpolarization *in vitro* (decreased membrane resistance, blockable with Cs^+) and ramping responses upon depolarization (rapid membrane voltage increases that semi-plateau before the action potential, blockable with 4-aminopyridine, or 4-AP) [142]. During song MSNs fire brief bursts time-locked to individual syllables, similar to mammalian MSNs that have sparse firing locked to behavioral events [143]. However, some mammalian MSNs fire spontaneously at ~5 spikes/sec, while Area X MSNs fire only during song [143]. This could be related to Area X's specialized function since it is uninvolved in non-singing behavior [31].

Area X contains three types of aspiny interneurons similar to those in mammalian striatum. They express the striatal interneuron markers LANT6 (Lys8-Asn9-neurotensin8–13) and/or parvalbumin [160]. The first type is fast-spiking interneurons (FS) [142] with narrow spike waveforms, as in mammals [143]. Their firing *in vitro* is similar to mammalian FS neurons: brief ramping responses and bursts of spikes upon depolarization that can turn into continuous firing when injected current is high enough. However, Area X FS neurons have more depolarized resting membrane potentials than in mammals [142]. In awake birds they fire spontaneously (~8 spikes/sec) and throughout song they increase firing rate (~19 spikes/sec) & exhibit short bursts [143]. This is similar to rodent FS activity during behavior [143]. The second type is tonically active cholinergic

interneurons (TAN) [142,160,161]. As in mammals they are spontaneously active at low rates *in vitro*, have a long-lasting afterhyperpolarization after action potentials and exhibit rebound depolarization when an injected hyperpolarizing current stops [142]. In awake birds TANs fire spontaneously (~12 spikes/sec), do not burst, have a long refractory period (~4 ms) and during song increase firing rate (~65 spikes/sec) [143]. Mammalian TANs have qualitatively similar firing patterns and long refractory periods [143]. However, unlike mammalian TANs, Area X TANs do not have wide & complex spike waveforms and fire at much higher rates during behavior (~60 spikes/sec vs. ~10-20 spikes/sec for mammalian TANs) [143]. The third type is low-threshold spiking interneurons (LTS) [142] which label for somatostatin as in mammals [160]. *In vitro*, mammalian and Area X LTS neurons fire a series of action potentials at a membrane voltage plateau (starting with a fast spike at the start) and have relatively slow inward rectification & rebound spikes in response to hyperpolarization [142]. In awake birds they rarely fire spontaneously but throughout song they produce long high-frequency bursts (~950 spikes/sec during burst) [143]. *In vivo* firing patterns of mammalian LTS neurons are not well studied [162] so we cannot make a direct comparison.

As in mammalian pallidum, Area X's GABAergic GPe and GPi neurons are large, aspiny and spontaneously active at high rates (>60 spikes/sec) [142,144,160,161] that increase further during song [163]. They have some striatal-like properties; for example, they express the neuropeptide enkephalin (found in mammalian striatal neurons) [161] but not the pallidal marker gene Nkx2.1 [161]. However, GPi neurons do express the pallidal marker LANT6 [160]. Additionally, Area X GPi neurons and rat entopeduncular neurons (equivalent to primate GPi) exhibit similar properties *in vitro*: relatively slow inward rectification upon hyperpolarization, rebound firing after hyperpolarization, depolarizing membrane voltage bumps once depolarizing current starts and ability to sustain high firing rates [142]. As occurs in the output of mammalian BG circuits, Area X GPi neurons strongly inhibit the thalamus (i.e. DLM) [164–166], but unlike in mammals they form large terminals covering the soma of DLM neurons and each DLM neuron receives input from only one or two GPi neurons [165]. Area X GPe/GPi firing patterns in awake birds are similar to awake primate GPe/GPi [144]. GPe

neurons (which do not project to the thalamus; **Fig. 1.2d**) fire in a pattern of bursts and pauses, while GPi neurons (which project to the thalamus) fire continuously without bursting [144]. Likewise, both primate and Area X GPi neurons fire asynchronously and have less interspike interval variation and narrower autocorrelation peaks than GPe neurons [144]. There are some activity differences: for instance, Area X's pallidal neuron firing rates are approximately 1.5-3.5x higher than in primates (~120-300 vs. ~85 spikes/sec) and typical primate GPe pauses (~470 ms) are much longer than Area X GPe pauses (~50 ms) [144].

Thus, although Area X and mammalian BG neurons differ in some respects, their basic properties are broadly similar despite Area X's specialized function for vocal learning.

Current evidence suggests Area X MSNs and pallidal neurons are linked in a simple direct/indirect pathway architecture [141,148] (**Fig. 1.2a,b**). First, they receive excitatory inputs from HVC and LMAN [141,167]. On a minor note, Area X also has weak noradrenergic input from locus coeruleus (LC) [168], and DA reuptake is handled by the norepinephrine (NE) transporter because the DA transporter gene is absent in birds [112,169]. Inhibitory MSNs project to GPe and GPi neurons. Inhibitory GPe neurons project within Area X, including onto GPi neurons [141]. Inhibitory GPi neurons project within Area X and/or to ventral pallidum (VP) and DLM [120,141,164,170]. DLM then sends excitatory projections to LMAN, which sends excitatory projections to RA and collaterals to Area X in a closed topographic loop [145]. Thus, MSN-GPi projections form a "direct pathway" roughly analogous to mammalian BG, whose activation would generally lead to cortical (i.e. LMAN/RA) excitation (**Fig. 1.2a**). Likewise, MSN-GPe-GPi projections form an "indirect pathway" roughly analogous to mammalian BG, whose activation would generally lead to cortical (i.e. LMAN/RA) inhibition (**Fig. 1.2b**). Finally, Area X MSNs receive extensive DA input from VTA/SNc [118,171] as discussed in Section 1.3.

We will now summarize additional Area X firing properties of interest. While pallidal neurons and some striatal interneurons fire spontaneously, MSNs fire exclusively during singing [142–144,172]. A subset of striatal interneurons and pallidal neurons respond to song playback stimuli in

anesthetized (but not awake) birds by increasing their firing rates [127,173–177]. During singing, Area X neurons increase their firing rates, and for spontaneously active neurons this increased firing begins and ends several hundred milliseconds before and after song [143,144,163]. Area X's neural firing patterns tend to be locked to individual song syllables with some trial-to-trial variability, but the degree of stereotypy depends on type of neuron and developmental stage [143,144,163]. Mammalian striatal and pallidal neuron firing is also time-locked to behavioral tasks with trial-to-trial variability [143,144]. Interestingly, although Area X is specialized for singing behavior [31], its neural activity can be modulated by food rewards [178], which could be merely vestigial because the song system evolved from pre-existing BG circuitry. Finally, one study found DA injections raise pallidal firing rate, decrease pallidal firing variability and reduce bird's own song (BOS)-selective responsivity [127]. However, it remains largely unknown which Area X firing patterns are DA-dependent and how neural firing is related to vocal learning. In Study 3 (Chapter 5) we began investigating these questions by recording in DA-depleted Area X.

Unlike Area X's basic neural firing properties, its local field potential (LFP) signaling is largely unexplored. Broadly speaking, the LFP (0-300 Hz) has many potential functions and can indirectly give insight onto neural firing patterns [179–183]. The only published study of Area X LFP found increased high-gamma oscillations (80-160 Hz) in sleeping birds and that Area X spikes were phase-locked to the gamma rhythm, which may be related to off-line processing to help consolidate adult vocal plasticity [184]. In mammalian BG nuclei, DA depletion leads to increased power in beta band oscillations (approx. 13-30 Hz) [185–190] but it is unknown in a similar phenomenon would occur in DA-depleted Area X. In Study 3 (Chapter 5) we performed a preliminary analysis of Area X's LFP in normal and DA-depleted states to help fill this knowledge gap.

1.5 Clinical Significance

Diverse neurological disorders cause vocal learning and production deficits. This includes speech disorders [191], stroke [192] and disruptions in BG DAergic signaling such as in PD [14] and Huntington's

disease [193]. These can have devastating effects on patients' ability to communicate and perform normal movements. The search for more effective treatments is inhibited by lack of understanding the mechanisms of vocal plasticity. Understanding how neural circuits control vocal learning could lead to improved therapies for treating speech disorders.

Importantly, by studying vocal plasticity in the songbird model system, we can also discover more of the general principles of motor learning. The mechanisms of learning during natural behavior, motor practice and motor rehabilitation remain largely unknown. As described in Sections 1.1-1.4, songbirds are ideal for studying not only vocal learning, but also motor learning in voluntary skilled motor behaviors. Investigating the rules of vocal generalization (Study 1; Chapter 3) and Area X DA's role in vocal learning (Studies 2 & 3; Chapters 4 & 5) could lead to new insights on vertebrate motor learning principles, such as the finding that songbird motor circuits actively generate exploratory variability to help guide learning [27]. This could lead to improved therapies for motor rehabilitation in general, not just speech disorders.

For example, investigating DA's role in songbird vocal learning could ultimately lead to better therapies for PD, which is accompanied by many motor deficits. Among these are vocal performance problems (soft voice, monotone & imprecise articulation [14]) and impairments in the sensorimotor learning processes used to maintain the accuracy of skilled behaviors [103,194–200], including aberrant vocal learning such as excessive or reduced compensation to pitch and formant shifts [83,84]. These deficiencies depend on the type of learning task, differing disease subtypes and disease progression status of study subjects [194,201]. Current PD therapies such as levodopa [202], deep-brain stimulation [203], exercise [204], dancing [205] and LSVT LOUD/BIG (Lee Silverman Voice Treatment) [206,207] can be effective but do not work permanently for everyone or eliminate all symptoms. For example, LSVT LOUD outcomes are poor in subjects with more severe speech deficits, and optimizing treatment efficacy is limited by our ignorance of the neural mechanisms underlying LSVT-related improvements [207]. To optimize delivery of current PD therapies and develop the next generation of therapies we must understand more about how DA helps guide motor

behaviors. The songbird model system is excellent for isolating DA's role in learning and maintaining natural skilled sensorimotor behaviors. However, to learn more about DA's role in this system we must first characterize vocal learning in DA-depleted states, which is a key motivation of Study 2 (Chapter 4). Understanding more about how DA contributes to motor learning could lead to better rehabilitation paradigms for PD and other motor disorders.

CHAPTER 2

DISSERTATION OVERVIEW

This project's overall goal is to determine the neural mechanisms by which auditory feedback guides vocal plasticity. The *main objective* of this dissertation is to first reveal the rules underlying vocal plasticity and then begin exploring the neural basis of these rules by determining whether vocal learning depends on DA signaling in the BG. The *central hypothesis* is that sensorimotor error correction on one vocal gesture generalizes to other gestures and that DA in the BG is necessary to guide vocal learning. Using the Bengalese Finch (*Lonchura striata*) as a model system, we approached this problem at three levels: behavioral (Study 1; Chapter 3), systems (Study 2; Chapter 4) and neurophysiological (Study 3; Chapter 5). We drove vocal learning using behavioral paradigms customized for songbirds (Study 1 and 2), developed a new lesioning technique to study DA's role in the BG (Study 2 and 3) and used acute electrophysiology to study DA's effect on BG neural activity (Study 3).

2.1 Study 1: Quantify the behavioral rules for songbird vocal error correction

Although songbirds and humans are known to engage in sensorimotor error correction [3,7,24], it is unclear how learning to change one vocal gesture generalizes to other gestures in the vocal repertoire. Some studies suggested learning to change one vowel transfers to vowels in other words and other contexts [3,23,37,38]. In these experiments, subjects wore headphones that played back frequency-altered versions of their voices as they spoke specific utterances (such as "pan") and they learned to compensate to correct perceived errors. Some studies suggested error-corrective learning generalizes in a limited way to vowels in other words ("pen", "pin", "ken", "gen") with more generalization to utterances that are acoustically similar to the training utterance [37]. However, others found learning does not generalize [39–41]. Although these studies provide valuable insights, it

is not known how learning generalizes across the full vocal repertoire (instead of limited sets of training and test utterances) or whether rules of generalization are the same across vocal learning species.

To address this knowledge gap, we fitted Bengalese finches with custom-built headphones and changed the fundamental frequency (pitch) of their song in real-time [208]. This created a sensory error by providing pitch-shifted auditory feedback only when they sung particular vocal gestures, or song syllables. We quantified how well they learned to correct this error and how this learning generalized to the unmanipulated syllables. *We hypothesized that learning to change pitch on one syllable would generalize to the same syllable produced in other contexts but would not generalize to the other syllables in the repertoire.* Therefore, this Study tested whether error-corrective vocal learning proceeds by independently fine-tuning each gesture or uses specific rules of generalization across contexts and gestures. As predicted, we found learning generalized to the same syllables in different contexts. Surprisingly, we also found that learning generalized to different syllables, and this generalization was in the anti-adaptive direction. Also, unexpectedly, we found there was more generalization for syllables produced near to the target syllable within the motif. For detailed results, see Section 3.4.

2.2 Study 2: Determine dopamine's contribution to songbird vocal learning

DA and the BG have been extensively linked to reinforcement learning, including the influential RPE Hypothesis where DA encodes the difference between expected and received rewards [73,209] and the Incentive Salience Hypothesis where DA encodes motivation or "wanting" [76]. However, much less work has been done on DA's role in sensorimotor learning and generalization or its contribution to vocal learning. Some results from PD patients and DA-depleted rodents suggested motor learning and generalization deficits, but other studies found no deficits (see Section 1.3). DA's role in motor learning and vocal learning has been difficult to test due to motor control

deficits, experimental paradigms used, the complexity of PD and the fact that commonly used animal models of PD do not exhibit vocal learning (see Section 1.3).

In this Study, we addressed this gap by determining whether DA in the BG nucleus Area X is necessary for reinforcement-driven learning. Area X is a nucleus in a BG-thalamocortical loop involved in learning and is necessary for song learning (see Section 1.4). DA's well-established association with reinforcement learning has prompted hypotheses that DAergic afferents to Area X guide vocal learning in songbirds via RPE signals [104,105]. However, to my knowledge DA's contribution to vocal learning has not been directly tested.

We used a neurotoxin to selectively reduce Area X's DAergic input and quantified the effects on vocal learning. We drove learning using a negative reinforcement paradigm in which birds received aversive WN blasts when syllable pitches were beyond a threshold [33]. *We hypothesized that partial lesions of Area X's DAergic input would decrease learning magnitude.* This addressed the second part of the central hypothesis and paved the way for future studies into DA's role in vocal plasticity, including the internally guided sensorimotor error correction studied in Study 1 (Chapter 3). As predicted, we found learning deficits after Area X DA depletion. This provided the first direct evidence that DA in the songbird BG is necessary for vocal learning. For detailed results, see Section 4.4.

2.3 Study 3: Identify dopamine-dependent features of basal ganglia neural activity

To understand how DA helps guide vocal learning, it is important to quantify how BG activity changes after loss of DA and relate this to learning deficits. In songbirds we can do this in several ways, beginning with measuring spontaneous and auditory-stimulus-evoked activity in DA-depleted Area X and proceeding towards quantifying activity during vocal learning. Area X responds to playbacks of auditory stimuli, especially bird's own song (BOS) [173,174,177], and responses are suppressed by DA and D_1 receptor agonists [127]. Area X spikes are phase-locked to high-gamma LFP oscillations during sleep, which may be related to off-line processing needed for

song maintenance [184]. However, it is not known how playback-evoked Area X firing or LFP oscillations are affected by chronic loss of DA input or how activity changes during learning in a DA-dependent manner.

Although increasing evidence suggests loss of DA causes aberrant motor learning as well as performance deficits [101–103,210], it can be difficult to dissociate performance- and learning-related pathological BG activity in mammals. However, in songbirds D_1 receptor antagonists and 6-OHDA lesions do not affect vocal performance other than relatively small changes to song variability [126,127,129] and complete Area X lesions only temporarily affect performance in adults [156,157,159]. After considering DA-dependent song variability, Area X activity changes after loss of DA are more likely related to learning deficits. By comparing to activity changes in mammalian striatum and pallidum, such as performance-related pathological bursting and synchronized beta band oscillations [185–189,211,212], we can help dissociate DA-dependent motor learning and motor performance activity in the BG.

As a first step towards investigating DA-dependent neurophysiology during vocal learning, we performed a pilot study of how DA depletion affects spontaneous activity in Area X. We reduced DAergic afferents into Area X unilaterally, followed by recording Area X neurons and LFP signals in anesthetized birds. We quantified spontaneous neural firing rates and LFP power in the DA-depleted hemispheres, and compared this to activity in the sham-lesioned hemispheres. We also quantified firing rates and LFP power evoked by song playbacks in sham- and 6-OHDA-lesioned hemispheres. *We hypothesized that after partial depletion of Area X's DAergic input, pallidal neuron firing rates would become less responsive to playbacks of BOS and that LFP power in the 13-30 Hz range would increase as in PD and mammalian PD models* [185–189]. Contrary to our hypothesis, we found no significant differences in pallidal neuron firing rates or Area X LFP power after 6-OHDA lesions compared to sham-lesioned controls. For detailed results and discussion why this may have occurred, see Sections 5.3-5.4. Although a full investigation of DA's role would require recording in awake birds during vocal learning, this Study provides pilot data for future

studies of neural activity during learning and preliminary comparisons to neurophysiological effects of DA lesion in other model systems and PD.

CHAPTER 3

VOCAL GENERALIZATION DEPENDS ON GESTURE IDENTITY AND SEQUENCE*

A similar version of this chapter was originally published in [213].

3.1 Abstract

Generalization, the brain's ability to transfer motor learning from one context to another, occurs in a wide range of complex behaviors. However, the rules of generalization in vocal behavior are poorly understood, and it is unknown how vocal learning generalizes across an animal's entire repertoire of natural vocalizations and sequences. Here, we asked whether generalization occurs in a nonhuman vocal learner and quantified its properties. We hypothesized that adaptive error correction of a vocal gesture produced in one sequence would generalize to the same gesture produced in other sequences. To test our hypothesis, we manipulated the fundamental frequency (pitch) of auditory feedback in Bengalese finches (*Lonchura striata*) to create sensory errors during vocal gestures (song syllables) produced in particular sequences. As hypothesized, error-corrective learning on pitch-shifted vocal gestures generalized to the same gestures produced in other sequential contexts. Surprisingly, generalization magnitude depended strongly on sequential distance from the pitch-shifted syllables, with greater adaptation for gestures produced near to the pitch-shifted syllable. A further unexpected result was that nonshifted syllables changed their pitch in the direction opposite from the shifted syllables. This apparently antiadaptive pattern of generalization could not be explained by correlations between generalization and the acoustic similarity to the pitch-shifted syllable. These findings therefore suggest that generalization depends on the type of vocal gesture and its sequential context relative to other gestures and may reflect an advantageous strategy for vocal learning and maintenance.

* Modified from: **Hoffmann L.A.** & Sober S.J. (2014). Vocal generalization depends on gesture identity and sequence. *Journal of Neuroscience* 34:5564–5574.

3.2 Introduction

Generalization, the ability to transfer motor adaptation to a new context, is crucial for learning and maintaining complex behaviors. Generalization is especially important in vocal behavior, during which vocal muscles must be precisely activated to reach time-varying acoustic targets. Because complex vocal behaviors involve producing the same vocal gesture within many different sequences, generalization would allow adaptive modifications of a gesture to transfer to the same gesture produced in other sequences, improving performance.

What are the properties of vocal generalization? In humans, learned changes to one vowel can transfer to the same vowel produced in other words and to other vowels [3,23,37,38]. Furthermore, generalization lessens with increasing acoustic distance between training and transfer utterances [37,38]. Such results parallel findings in limb movement studies, where generalization depends on the similarity between training and transfer movements [34,55]. However, other speech studies have suggested that learning is instance-specific with no generalization [39–41]. Thus, the rules of vocal generalization are not well understood. One reason for this could be that speech studies typically use a small set of training and transfer utterances. It is therefore also unclear how generalization occurs across the full natural range of vocalizations and sequences.

Songbirds have provided insight into the neural basis of vocal behavior. Speech and birdsong share numerous parallels [21,22], which include using auditory feedback to correct vocal errors [3,7,24]. Physiological studies in songbirds have proposed models of how neural circuits shape the sequencing and acoustic structure of vocal gestures [29,30,214–216]. However, although such models can suggest how adaptive vocal changes might be implemented in neural circuits, our poor understanding of the behavioral structure of vocal learning leaves such models badly underconstrained. In this study, we therefore investigated a fundamental question about the computations underlying vocal error correction by asking whether generalization occurs in songbirds or instead might be a unique feature of human speech.

We used Bengalese finches to ask whether generalization occurs in a nonhuman vocal learner and to quantify the properties of generalization in a natural vocal repertoire. We hypothesized that, when feedback errors are experienced for a song syllable appearing in a particular sequential context, error correction on the perturbed syllable would generalize to the same syllable produced in other contexts. Our hypothesis was based on similarities between other forms of vocal learning in humans and songbirds [3,7,24] as well as data showing that neural activity is strongly associated with song syllable identity across contexts [215–217]. We fitted songbirds with miniaturized headphones [208] and shifted the pitch of auditory feedback from single syllables in particular sequential contexts (**Fig. 3.1**). We then quantified how birds adapted to the shifts and how this error correction generalized across other vocal gestures and contexts.

3.3 Materials and Methods

Six adult (>135-d-old) male Bengalese finches (*Lonchura striata var. domestica*) were used. Throughout the experiment, birds were isolated in sound-attenuating chambers and maintained on a 14 h:10 h light/dark cycle, with lights on from 7 A.M. to 9 P.M. All recordings analyzed here are from undirected song (i.e., no other bird was present). All procedures were approved by the Emory University Institutional Animal Care and Use Committee.

Experimental procedure. Online, real-time manipulations of auditory feedback were used to induce adaptive changes in song pitch. As described previously [208], custom-built headphones were attached to each bird's head. Sound-processing hardware shifted the pitch of acoustic signals and immediately relayed them to the headphone speakers. There was a mean delay of 8.5 ms from the time the bird sang a syllable to the time that syllable was played through the speakers. Vocal pitch in Bengalese finches remains stable when headphones are used to deliver auditory feedback that has not been pitch-shifted [7], so changes in vocal pitch reflect responses to pitch manipulation.

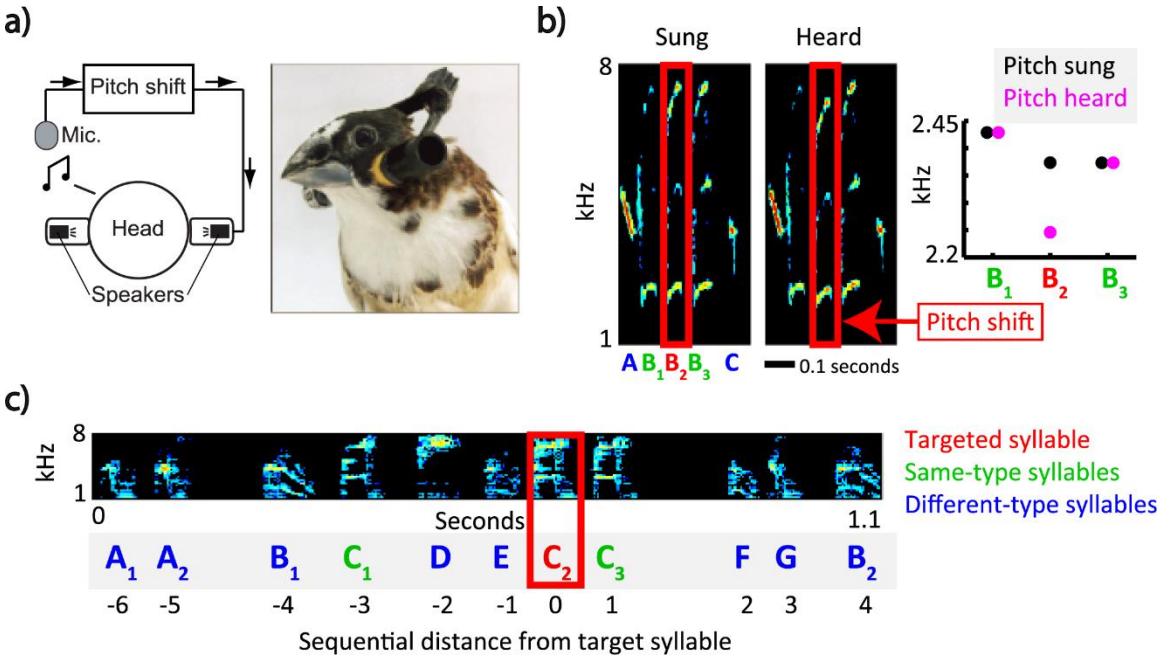

Figure 3.1. Technique for manipulating auditory feedback during individual vocal gestures. **(A)**, Experimental apparatus. Song is collected by a microphone, pitch-shifted by an online sound processor, and immediately relayed to head-mounted speakers. **(B)**, Example of pitch-shift during a five-syllable motif. The targeted syllable (B_2, red) was artificially pitch-shifted by -100 cents, whereas nearby same-type (B_1 and B_3, green) and different-type (A and C, blue) syllables were unaltered. Left spectrogram, the bird's vocal output ("sung"). Right spectrogram, the auditory feedback signal played through the headphones ("heard"). Inset at right, sung and heard pitches are the same for B_1 and B_3 but not B_2. **(C)**, Top, spectrogram of a stereotyped motif from a different bird. Bottom, syllables are color-coded by their assigned category. Only the targeted syllable (C_2, red) was pitch-shifted. All syllables in the motif were assigned a sequential distance from the target syllable.

The experiment began with a baseline period (5–7 d) of singing with headphone speakers relaying the songs online at zero pitch shift. After this, birds were exposed to 14 d (2 birds) or 20 d (4 birds) of altered auditory feedback ("shift days"). All analyses of the shift epoch are restricted to the 14 d in which all 6 birds were exposed to shifts; however, similar patterns were seen in days 15–20 in the birds undergoing longer pitch shifts (data not shown).

During the shift days, all songs were relayed online through the headphone speakers. Target syllables within a stereotyped motif were pitch-shifted upward or downward by 100 cents, whereas all other syllables remained at zero pitch shift (**Fig. 3.1**). A ±100 cents pitch shift has been shown to robustly drive learning when applied to all song syllables [7,218]. Custom-written LabView software [33] was used to detect a syllable early in the motif. After syllable detection, a square wave was sent

to an analog audio switch (Intersil, ISL54405), which switched from a zero-shift to shift channel for the desired time interval. As a result, targeted syllables were played through headphone speakers at 100 cents (3 targeted syllables) or -100 cents (5 targeted syllables). Averaged across all syllables in our analysis, the mean hit-rate (percentage of all targeted syllables correctly pitch-shifted) was 92.1% and in no case was <90% and the false-positive rate was 0.9%. Three syllables (of a total of 85) were excluded from analysis because false-positive pitch shifts occurred on >20% of those syllable iterations, making them neither target nor nontarget syllables.

Two birds had two targeted syllables. For both birds, these syllables were sung consecutively within the motif with a very small temporal gap (for example, A***BC***D). During each iteration, the targeting algorithm detected the preceding syllable (A) at a slightly different time. This caused the pitch-shift to frequently overlap the second syllable. Therefore, it was decided to lengthen the shift time period to shift both syllables. Furthermore, Bengalese finch song consists of several motifs, which are frequently sung in different order. Some motifs are nonstereotyped; in these motifs, syllables are added, omitted, or swapped. However, all targeted syllables occurred in a stereotyped motif where syllable order was always the same.

Syllable categories and sequential distance. Song syllables were divided into three groups (**Fig. 3.1c**), designated "targeted" (n = 8), "same-type" (n = 19), and "different-type" (n = 55). Targeted syllables were artificially pitch-shifted, as described above. Some of the nontargeted syllables were visually indistinguishable from targeted syllables when viewed in a spectrogram (**Fig. 3.1**, green syllables) but occurred in different sequential positions within the motif. These were considered "same-type" syllables. The rest of the pitch-quantifiable syllables were assigned to the "different-type" group (**Fig. 3.1**, blue syllables). Same-type and different-type syllables were not pitch-shifted, except during rare accidental false-positive syllable detections.

Syllable labels were assigned using their acoustic structure as well as their sequential context. For example, **Figure 3.1c** shows a spectrogram of a stereotyped motif above the labels for each syllable. In this example, syllables are labeled A–G based on their spectral structure. Additionally,

syllables are given numerical subscripts (A1, A2, etc.) to identify when a syllable is produced at different sequential positions within a motif. In the example shown, only syllable C2 is pitch-shifted (**Fig. 3.1c**, red box). Syllables C1 and C3 are therefore same-type syllables, and all other syllables are categorized as different-type, as described above. **Figure 3.1c** (bottom) also shows the sequential distance of each syllable from the shifted syllable. Syllables produced at different sequential distances from the target syllable were analyzed separately to quantify how changes to a shifted syllable generalized to nearby syllables as a function of sequential distance. Bengalese finches tend to have relatively short stereotyped motifs, so there were more data points for smaller sequential distances than for larger ones. Syllables produced outside of stereotyped motifs had variable sequential distances to the nearest target syllable and were not included in the sequential distance analysis, although they were included in all other analyses.

Pitch quantification. Song pitch changes were quantified by measuring pitch at specific times within individual syllables as previously described [7]. Although individual song syllables can be made up of multiple vocal gestures in some songbird species, the majority of Bengalese finch syllables contain only a single gesture with a reliably quantifiable pitch. Therefore, although measurements of "syllable pitch" refer to the pitch of individual vocal gestures, our analysis includes every gesture with quantifiable pitch. Each bird produced 5–8 (median 7) syllable types with quantifiable pitch. Pitch was quantified for all songs sung from 10:00 A.M. to 12:00 P.M. each day. Birds sang a median of 945 (range, 0–4328) pitch-quantifiable syllable iterations in each 2 h window. Whenever a bird did not sing within this window (3.5% of all experimental days), the bird did not contribute to pitch data for that day.

Each individual syllable iteration's measured pitch (in Hz) was converted to the fractional change from that syllable's baseline pitch (in cents) as follows:

$$C = 1200 \log_2 \frac{H}{B}$$

where *C* is the syllable's pitch change from baseline (in cents), *H* is the syllable's measured pitch (in Hz), and *B* is the mean pitch (in Hz) of all iterations of that syllable over the last three baseline days. A shift of 100 cents corresponds to one semitone, which is a ~6% change in absolute frequency.

The "mean pitch change for one syllable" is the average of individual syllable iterations over the specified time period (one day or multiple days). The mean pitch change across multiple syllables was calculated in two ways (which yielded similar results):

$$M_{syls} = \frac{M_{S1} + M_{S2} + \cdots + M_{SJ}}{J}$$

where M_{syls} = mean pitch change across multiple syllable types, M_S = mean pitch change of syllable *S*, *J* = total number of syllables used, or:

$$M_{iterations} = \frac{\sum_j \sum_d \sum_{i=1}^{N_{d,j}} S_{i,d,j}}{\sum_j \sum_d N_{d,j}}$$

where $M_{iterations}$ = mean pitch change across multiple syllables' iterations, *j* = syllables used, *d* = days used, $N_{d,j}$ = total number of iterations of syllable S_j on day *d* within the 2 h window, $S_{i,d,j}$ = the pitch change relative to baseline for individual syllable S_j iteration *i* on day *d*. A frequently-sung syllable will contribute proportionally more to $M_{iterations}$, where each syllable iteration is one data point, than M_{syls}, where each type of syllable is one data point.

Pitch contrast. To determine whether pitch changes in different-type syllables acted to restore preexisting pitch relationships between syllables, three "pitch contrasts" were calculated for each target-syllable/different-type syllable pair. We define this pitch contrast at three different times during the experiment. First, for each pair of targeted and different-type syllables within each experiment, we define the "baseline" pitch contrast C_{Baseline} as the difference (in cents) between the mean baseline pitch of a target syllable and a different-type syllable:

$$C_{\text{Baseline}} = 1200 \log_2 \frac{T_{\text{Baseline}}}{D_{\text{Baseline}}}$$

Where T_{Baseline} and D_{Baseline} are the mean pitches of the targeted and different-type syllables, respectively, before shift onset. We then define the "shift start" contrast as the pitch difference between those two syllables when the shift on the target syllable first began (as heard by the bird, i.e., with the target syllable pitch-shifted ±100 cents relative to baseline):

$$C_{\text{Shift start}} = 1200 \log_2 \frac{T_{\text{Shift start}}}{D_{\text{Shift start}}}$$

Finally, we define the "shift end" contrast as the difference during days 12–14 (as heard by the bird, i.e., with the target syllable pitch-shifted ±100 cents relative to the sung pitch on those days):

$$C_{\text{Shift end}} = 1200 \log_2 \frac{T_{\text{Shift end}}}{D_{\text{Shift end}}}$$

Thus, C_{Baseline} quantifies the preexisting pitch relationship between two syllables, $C_{\text{Shift start}}$ quantifies the suddenly changed pitch relationship when pitch-shifted auditory feedback began, and $C_{\text{Shift end}}$ quantifies the pitch relationship after the bird has responded to the perturbation by altering syllable pitches.

These contrasts were used to calculate percentage "restoration of pitch contrast" (R_C) for each syllable pair:

$$R_C = \frac{(C_{\text{Shift end}} - C_{\text{Shift start}})}{(C_{\text{Baseline}} - C_{\text{Shift start}})} * 100\%$$

Therefore, if by the end of the shift period the bird has restored the pitch contrast between syllables to its baseline value (i.e., if $C_{\text{Shift end}} = C_{\text{Baseline}}$), then R_C will equal 100%. On the other hand, if the pitch contrast at the end of the shift epoch is unchanged from the beginning of the shift epoch ($C_{\text{Shift end}} = C_{\text{Shift start}}$), then restoration will be 0%. Importantly, the restoration of pitch contrast can be achieved by changing the pitch of the targeted syllable (T_x), the pitch of different-type syllables (D_x), or both.

To determine whether different-type syllable pitch changes significantly contributed to restoring pitch contrast, for each pair of targeted and different-type syllables, percentage restoration

was calculated once when pitch changes in different-type syllable were included and once when they were excluded. We excluded the effects of different-type syllable changes by computing

$$C'_{\text{Shift end}} = 1200\ \log_2 \frac{T_{\text{Shift end}}}{D_{\text{Shift start}}}$$

which quantifies the pitch contrast at the end of the shift epoch but does not include the effects of changes in different-type syllable (because it uses $D_{\text{Shift start}}$ rather than $D_{\text{Shift end}}$). We then computed R'_C, a measure of pitch restoration that excludes the effect of changes in different-type syllables

$$R'_{\text{C}} = \frac{(C'_{\text{Shift end}} - C_{\text{Shift start}})}{(C_{\text{Baseline}} - C_{\text{Shift start}})} * 100\%$$

If different-type syllable pitch changes contribute to pitch contrast restoration, then R_C will be greater than R'_C. A pairwise comparison of these two quantities was performed on the set of target-syllable/different-type syllable pairs across birds. Finally, we quantified the fraction of total restoration provided by different-type syllables as

$$\frac{R_C - R'_C}{R_C}$$

Acoustic distance to target syllable. To determine whether there was a relationship between adaptive changes in a syllable and its similarity to the target syllable(s), an acoustic distance metric was calculated for each syllable. The algorithm is similar to a previously described metric [216]. First, three acoustic features were calculated for each syllable iteration that was sung during baseline: fundamental frequency (pitch), amplitude, and spectral entropy [216]. These three features were chosen because they capture a large fraction of the total trial-by-trial acoustic variation and are correlated with neural activity in the vocal motor system [29]. Each individual feature was then transformed to a z-score using the global mean and SD of that feature across all syllables within each bird. Next, the 3D center of mass (COM) was calculated for each syllable: the mean z-score for pitch, amplitude, and spectral entropy across syllable iterations. Finally, the acoustic distance was defined as the Euclidean distance between a syllable's COM to the bird's target syllable's

COM. For the two birds that had two target syllables, the acoustic distance is the mean distance to each target syllable. Additionally, we calculated COM distances using only one acoustic feature (pitch, amplitude, or entropy) at a time using the same procedure. In that case, the distance between two syllables was obtained by subtracting the mean z-score of those syllables' pitches (or amplitudes, or entropies).

Mean spectrograms. Mean spectrograms were computed by aligning individual syllable spectrograms and taking the natural log of the mean spectral power. The spectrograms are used for display only, and all reported analyses use acoustic data from single trials, not mean spectrograms.

3.4 Results

We investigated how a sensory error on one syllable in a sequence caused adaptive changes on that syllable (targeted syllable) and examined generalization by quantifying the concurrent pitch changes of other syllables in the song (same-type and different-type syllables). A representative experiment in which the pitch of the targeted syllable was shifted by -100 cents is shown in **Figure 3.2**.

Adaptive pitch changes in the same syllable produced in other sequential contexts

Spectrograms in **Figure 3.2a** show the targeted syllable (A_2) and surrounding syllables on the last baseline day (left) and the same sequence on the last day of a 100 cent downwards pitch shift (right). **Figure 3.2b** (magenta and blue symbols) shows the pitch of the shifted auditory feedback on the first and last shift days, respectively. In response to the downward shift, the pitch of the target syllable changed in the adaptive direction (increased) between the baseline period (**Fig. 3.2b**, white symbol) and the end of the shift period (**Fig. 3.2b**, black symbol). The spectrograms also show surrounding same-type syllables (A_1, A_3, A_4, A_5) in the motif (i.e., the same vocal gesture as the target syllable but produced in other sequential contexts). The bird changed the pitch of syllables

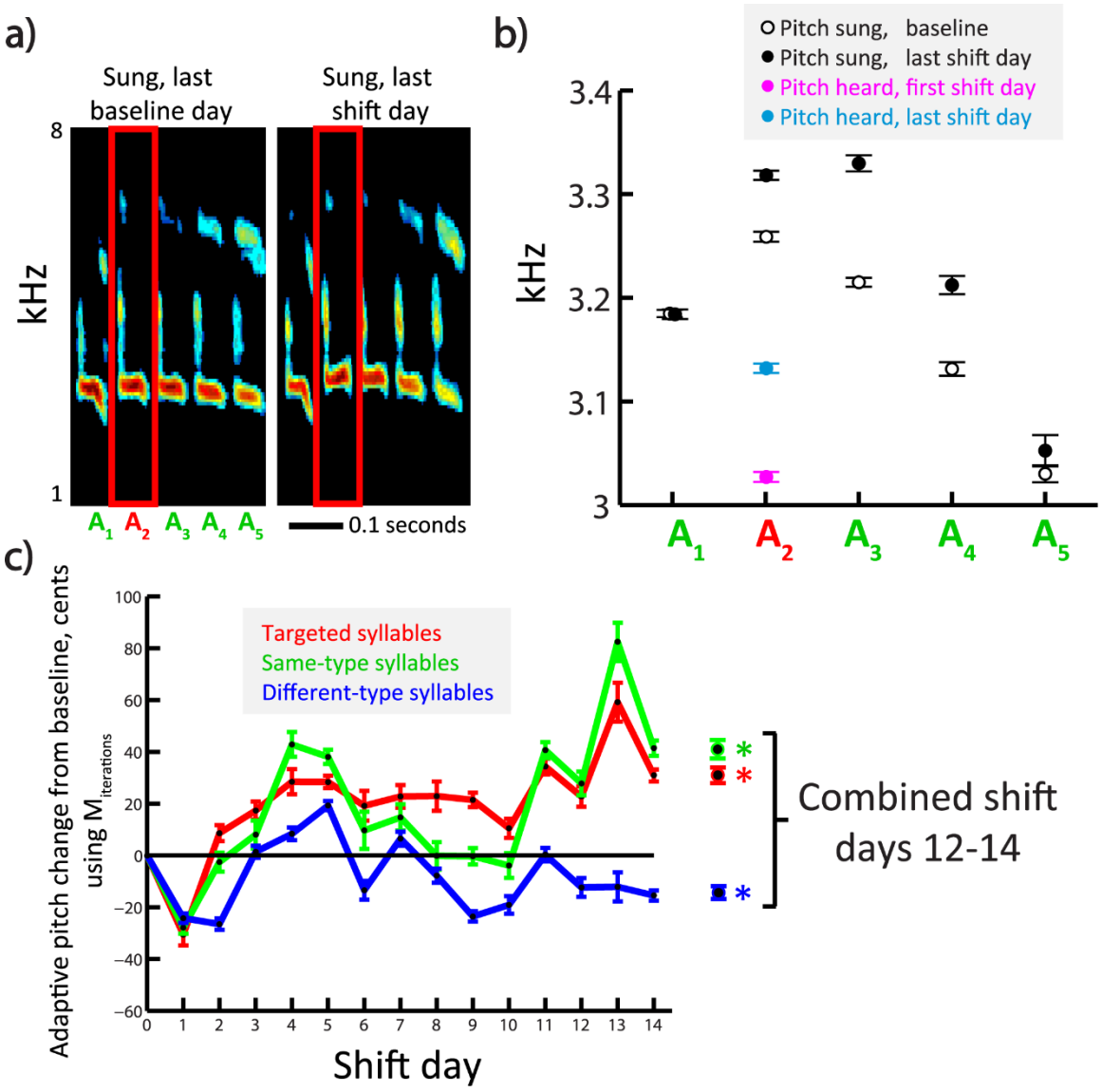

Figure 3.2. Example of pitch-shift learning on a targeted vocal gesture and generalization to other contexts. **(A)**, Mean spectrograms showing vocal pitch before (left) and after (right) a bird experienced a -100 cent (downward) pitch shift to syllable A_2. Red box represents portion of the vocal sequence to which pitch shift was applied; syllables A_1, A_3, A_4, and A_5 were not pitch-shifted. **(B)**, Mean ±SEM pitches for baseline and last shift day, same motif as in **A**. The bird increased pitch of the targeted syllable and subsequent syllables in the motif, even though the latter were not artificially pitch-shifted. The magenta and blue symbols represent the pitch heard by the bird on the first and last shift days, respectively. Syllables A_1, A_3, A_4, and A_5 were not pitch-shifted, so no colored points are shown. **(C)**, Pitch changes for the same bird during shift period. Colored lines represent mean ±SEM pitch, measured in cents relative to baseline. Each syllable iteration is one data point ($M_{iterations}$, see Section 3.3, Materials and Methods). The bird changed pitch of the targeted syllable in the adaptive direction, partially compensating for the sensory error. Same-type and different-type syllables were not artificially pitch-shifted but changed pitch in the adaptive and antiadaptive direction, respectively. *Significant pitch changes for syllables on shift days 12–14 ($p < 10^{-15}$, two-tailed t test).

produced after the targeted syllable, although they were not artificially pitch-shifted (A_3, A_4, A_5; white and black symbols, **Fig. 3.2b**). By the end of the shift period, the mean target syllable pitch had increased 30.9 cents above baseline, indicating ~30% compensation in the adaptive direction for the -100 cents shift (**Fig. 3.2c**, rightmost red symbol). The bird also changed its same-type syllable pitches in the adaptive direction over shift days 12–14 (**Fig. 3.2c**, rightmost green symbol). Surprisingly, different-type syllable pitch was changed significantly in the antiadaptive direction (**Fig. 3.2c**, rightmost blue symbol). Data from this representative experiment therefore indicate that, although only the targeted syllable was artificially pitch-shifted, pitch changed in the adaptive direction for the same vocal gesture produced in other sequential contexts and in the antiadaptive direction for different vocal gestures.

When data were combined across birds, we found an overall pattern of significant adaptive changes in target syllables. **Figure 3.3** shows pitch changes for all target syllables (red symbols). We quantified mean pitch changes two different ways (**Fig. 3.3a,b,** M_{syls}; **Fig. 3.3c,d,** $M_{iterations}$; see Section 3.3, Materials and Methods) and obtained similar results. M_{syls} uses the mean pitch of each syllable as one data point, whereas $M_{iterations}$ uses each individual syllable iteration as one data point. The calculated fraction of sensory error compensated for by the end of the shift period in **Figure 3.3a** (27.1% on shift day 14, red line) and **Figure 3.3c** (35.2% on shift day 14, red line) is similar to the 36% compensation fraction reported earlier when the entire song was shifted [7]. Thus, the birds changed pitch by a similar amount despite performing a syllable-specific learning task. Furthermore, as reported previously in experiments where the entire song was shifted [7], adaptive pitch changes on target syllables fell within the range of baseline pitch variability. The SD of baseline variation was 38.3 cents (averaged across brds), so birds changed target syllable pitch by ~1 SD.

To investigate whether error correction generalizes to the same vocalization produced in other sequential contexts ("same-type syllables"), we combined data across birds. Average pitch time courses for same-type syllables are shown in **Figure 3.3a, c** (green lines). Similar to the

example experiment shown in **Figure 3.2**, the pitch of same-type syllables changed in the adaptive direction. **Figure 3.3b, d** displays the average pitch over shift days 12–14. Same-type syllables changed significantly in the adaptive direction (green asterisks), as did target syllables (red asterisks). Thus, although the magnitude of vocal changes depended somewhat on the averaging technique used ($M_{iterations}$ vs M_{syls}), both methods show that there were adaptive pitch changes for the same vocal gestures produced in other contexts.

Antiadaptive pitch changes in different vocal gestures

We also combined data across birds to ask whether error-corrective learning on one vocal gesture generalizes to different gestures. **Figure 3.3a, c** shows that different-type syllables (blue lines) gradually separated from target and same-type syllables. Surprisingly, we found that, on average, different-type syllables significantly changed pitch in the antiadaptive direction (**Fig. 3.3b,d**; blue asterisks). That is, whereas shifted song syllables (**Fig. 3.3**, red) change their pitch in the direction opposite the applied pitch shift, different-type syllables (**Fig. 3.3**, blue) exhibit pitch changes in the same direction as the applied pitch shift. We refer to the latter as "negative generalization" in the Discussion (Section 3.5) to indicate that nonperturbed syllables are changing in the opposite, or antiadaptive, direction as shifted syllables. Compared with the adaptive pitch changes observed in same-type syllables (**Fig. 3.3b,d**; green), the overall antiadaptive pitch change found in different-type syllables is smaller in magnitude (**Fig. 3.3b,d**; blue) and somewhat more variable over the duration of the experiment (**Fig. 3.3a,c**; blue). Nevertheless, these antiadaptive changes are both statistically significant and insensitive to the choice of how changes in vocal pitch are measured ($M_{iterations}$ vs M_{syls}; see Section 3.3, Materials and Methods).

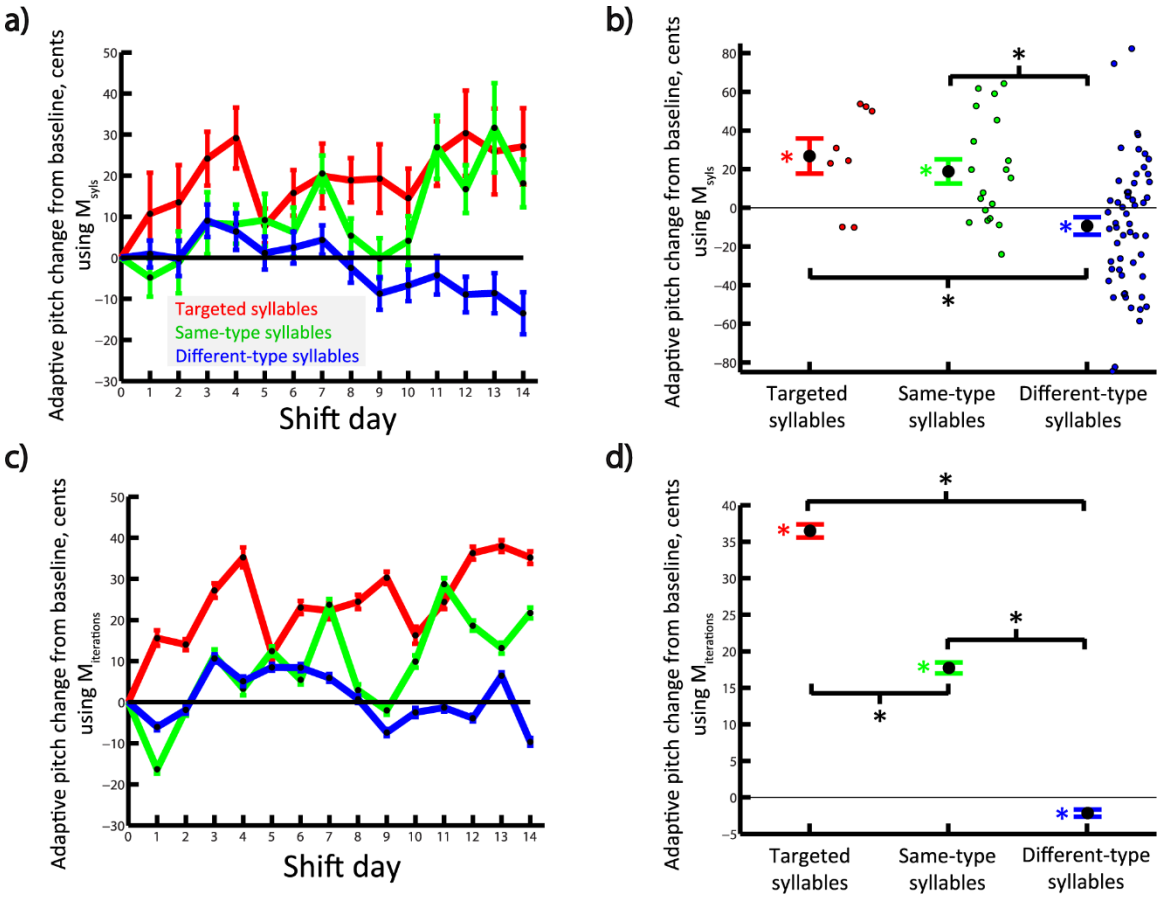

Figure 3.3. Pitch-shift learning on targeted vocal gestures generalizes to other gestures. **(A)**, Pitch changes during the first 14 shift days, combined across n=6 birds. Birds were exposed to either 100 or -100 cents shift on the targeted syllable(s), but same-type and different-type syllables were not artificially pitch-shifted. Colored lines indicate mean ±SEM pitch, measured in cents relative to baseline. Each syllable is one data point (see Section 3.3, Materials and Methods, M_{syls}). The pitches for birds exposed to 100 cents shift were multiplied by -1. Thus, positive values signify that the birds changed pitch in a direction that is opposite to the artificial pitch shift (adaptive direction). **(B)**, Mean ±SEM pitch over shift days 12–14 for each syllable category, combined across birds. Each syllable is one data point (circles). Birds changed the pitch of targeted syllables to partially compensate for the error. They also changed same-type syllable pitch in the adaptive direction and different-typ syllable pitch in the antiadaptive direction. Colored asterisks indicate significant pitch changes ($p < 0.05$, two-tailed t test). Black asterisks indicate that the indicated syllable categories have different pitch change distributions ($p < 0.05$, two-tailed two-sample t test). **(C)**, Same as **A**, except using each syllable iteration as one data point ($M_{iterations}$, see Section 3.3, Materials and Methods). **(D)**, Same as **B**, except using each syllable iteration as one data point. Target syllables and same-type syllables changed pitch in the adaptive direction, whereas different-type syllables changed in the antiadaptive direction. Asterisks are defined as in **B**.

In conjunction with the adaptive changes observed in shifted syllables, antiadaptive changes in different-type syllables act to partially restore the pitch differences between song syllables. As shown in **Figure 3.4a**, introduction of a pitch shift (**Fig. 3.4a**, "prelearning") will perturb the relative pitches of hypothetical syllables "A" and "Z" when syllable "A" is pitch-shifted.

Whereas an adaptive change in the pitch of syllable "A" (**Fig. 3.4a**, "postlearning," upward arrow) will partially restore this acoustic relationship (or "pitch contrast"), a concomitant antiadaptive change in the pitch of syllable "Z" can further restore the relative pitch.

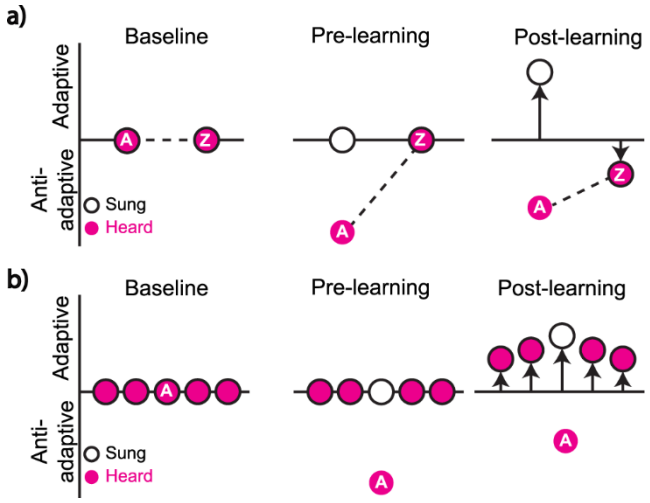

Figure 3.4. Two patterns of generalization in vocal learning. **(A)**, Antiadaptive shifts preserve pitch relationships across syllables. Schematic represents changes in the pitch sung by the bird (black) and heard through auditory feedback (magenta) of two song syllables, "A" and "Z". The dashed line indicates the relative pitch of the two syllables. Just after the onset of a downward pitch shift applied to syllable A ("Pre-learning"), the relative pitch of auditory feedback between the two syllables is altered. After error correction ("Post-learning"), syllable A exhibits an adaptive pitch change (i.e., a change in vocal pitch opposite the imposed sensory error), indicated by the upward-pointing black arrow. This pitch change does not completely correct the imposed pitch shift. However, syllable Z exhibits an "antiadaptive" pitch change (downward arrow). This contributes to partially restoring the relative pitch between auditory feedback from the two syllables (dashed line). **(B)**, Adaptive changes generalize to nearby syllables in a sequence. Here, the "credit" for a pitch error during syllable A is generalized to nearby syllables, resulting in "adaptive" pitch changes in multiple syllables (black arrows at right). Vocal plasticity in response to single-syllable pitch shifts may reflect an interaction between the patterns shown in **A** and **B**.

As described in Section 3.3, Materials and Methods, we determined whether pitch changes in different-type syllables contributed significantly to this restoration of pitch contrast by quantifying restoration for each pair of target syllables and different-type syllables. A pairwise analysis isolated the contributions of pitch changes in different-type syllables and revealed that these changes contributed significantly to pitch contrast restoration across the learning epoch ($p<0.05$, one-tailed paired-sample t test) and on average accounted for 19.6% of the total restoration (see Section 3.3, Materials and Methods), with changes in the targeted syllables contributing the

remainder of the restoration. These antiadaptive changes may therefore reflect a corrective mechanism that preserves the pitch relationships across syllables (see Section 3.5, Discussion).

The observed pattern of vocal changes is not an artifact of targeting errors

As described in Section 3.3, Materials and Methods, online targeting of pitch shifts to selected syllables was very accurate, with mean hit and false-positive rates of 92.1% and 0.9%, respectively. However, because infrequent targeting errors sometimes resulted either in pitch shifts being applied to nontargeted syllables or a lack of pitch shift to targeted vocal gestures, it was important to assess whether our findings might have resulted from these targeting errors. This is very unlikely to have been the case. First, false-positive rates did not differ significantly for same-type and different-type syllables (1.8% and 0.6%, respectively, $p = 0.09$, two-tailed two-sample t test), suggesting that the difference in pitch changes shown in **Figure 3.3** does not reflect a difference in the frequency with which pitch shifts were accidentally applied to same-type and different-type syllables. Second, we performed an alternate analysis in which we excluded the two same-type syllables with the highest false-positive rates (13% and 15%; remaining same-type syllables' false-positive rates did not exceed 2%). In this alternate analysis, the false-positive rates were nearly identical (0.4% and 0.6% for same-type and different-type syllables, respectively; $p = 0.55$), and the results of all other analyses were qualitatively identical to the original analysis. Third, if false-positive shifts caused pitch changes, we might also expect the reverse to be true, where higher false negative percentages on targeted syllables would cause smaller pitch changes. However, there was no correlation between number of false-negative shifts on target syllables and the amount they changed pitch ($p = 0.96$). Thus, although we cannot exclude the possibility that rare false-positive or false-negative pitch shifts may have affected the birds' behavior, the above evidence suggests that this alone cannot account for our results.

Vocal changes are not predicted by acoustic similarity

The above analyses compare how errors during a particular syllable affect both different syllables and the same syllable produced in different sequences. However, the bird's repertoire exists on a continuum, where some syllables are more acoustically similar to the targeted syllable than others. Many studies of generalization have found that the amount of transfer declined as movements became more dissimilar from the learned movement [34–36,42,54,55]. This has also been found in some studies of human speech, where learning transferred less as vocalizations became less similar to the training utterances [23,37,38]. We therefore asked whether the amount that birds changed pitch of different-type vocal gestures was correlated with acoustic similarity to the targeted vocal gesture.

For each different-type syllable, we calculated the acoustic distance between it and the target syllable in a 3D space consisting of pitch, amplitude, and spectral entropy, acoustic features that have previously been shown to account for a substantial portion of acoustic variability in songbirds [29]. We compared this acoustic distance with the amount the syllable pitch changed during the pitch shift period. We found no significant correlation between different-type syllable pitch changes and acoustic distance (**Fig. 3.5**). Furthermore, we performed three additional analyses in which acoustic distances were computed using only a single acoustic parameter (i.e., three separate one-dimensional analyses; see Section 3.3, Materials and Methods). The additional analyses also failed to yield any significant correlation between acoustic similarity and adaptive vocal change ($p > 0.4$ in all cases). Therefore, in contrast to several studies of human speech (see Section 3.5, Discussion), we find no significant relationship between change in pitch and acoustic similarity to the perturbed vocal gesture, suggesting that the pitch change observed in nontrained song syllables is not strongly related to their acoustic similarity to the trained gesture.

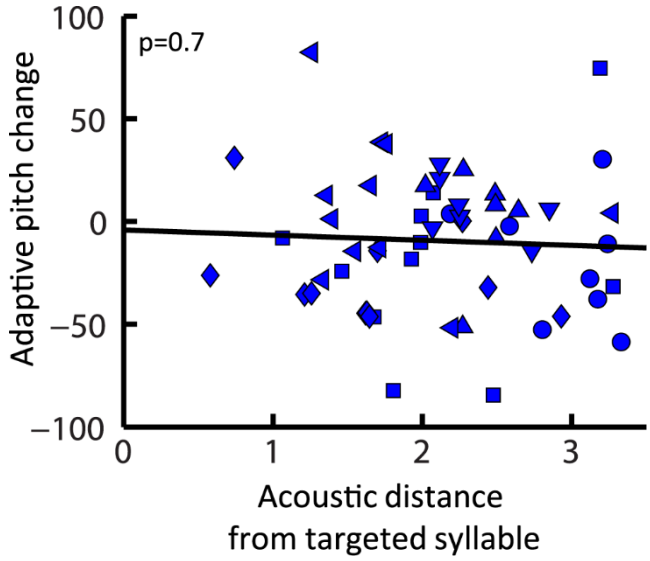

Figure 3.5. A vocal gesture's acoustic similarity to targeted gesture does not predict learning transfer. Each symbol shows the mean pitch change for one different-type syllable over shift days 12–14 as a function of its acoustic distance to the targeted syllables (see Section 3.3, Materials and Methods). Data from individual birds are shown with different symbol shapes. Two birds had two targeted syllables; thus, their syllables' acoustic distance is the mean distance to both targeted syllables (▲ and ▼). The regression is not significant ($p = 0.7$), suggesting that amount of pitch change does not vary with the degree of similarity to the trained gesture.

Sequential context affects vocal changes

After analyzing how birds changed the pitch of other vocal gestures of varying acoustical similarity, we investigated whether generalization of error correction was sequence-dependent. Specifically, we asked whether the amount of pitch change in a vocal gesture depended on how closely it was produced to the targeted vocal gesture in the motif. For example, **Figure 3.2b** shows that the first syllable sung after the target syllable (A_3) changed pitch by a greater amount than the third syllable sung after the target syllable (A_5), suggesting a correlation between sequential distance and the amount of pitch change.

Across all birds, we found that, on average, nontargeted syllables changed in the adaptive direction when they were produced in close proximity to the pitch-shifted syllable. **Figure 3.6** shows that both same-type and different-type syllables produced immediately adjacent to the targeted syllable changed pitch in the adaptive direction. Linear regression analyses revealed significant relationships between sequential distance and changes in vocal pitch in all cases (**Fig.**

3.6, blue and green lines), indicating that the amount of pitch change decreased with increasing sequential distance from the targeted syllable. This sequence-dependent pattern of adaptive vocal changes suggests that error information from one syllable is used to generate adaptive vocal changes in nearby syllables as well, as schematized in **Figure 3.4b**.

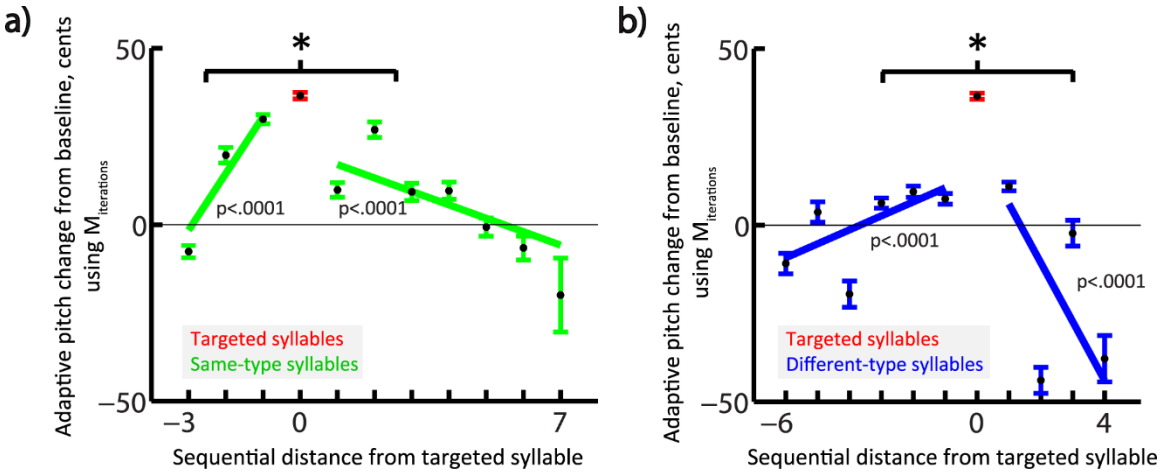

Figure 3.6. Transfer of learning across vocal gestures in a stereotyped sequence depends on sequential distance. **(A)**, Each point shows the mean ±SEM pitch changes for same-type syllables that were produced at a stereotyped distance from the nearest targeted syllable. Data are combined across n=6 birds and use syllables from shift days 12–14. Each syllable iteration is one data point (see Section 3.3, Materials and Methods, $M_{iterations}$). Adaptive pitch change lessened and turned into antiadaptive pitch change as the sequential distance increased ($p < 0.0001$ for both lines). The slopes differed for syllables produced before versus after target syllables: $*p < 10^{-10}$ (F test). Results were qualitatively similar when using M_{syls} but did not reach significance, possibly because there were too few data points at each distance. **(B)**, Same as **A**, except showing different-type syllables. There was increasing antiadaptive pitch change as sequential distance increased, and different slopes for syllables produced before versus after target syllables: $*p < 10^{-10}$ (F test). Only syllables that were produced within stereotyped sequences were included in this analysis (see Section 3.3, Materials and Methods).

The overall pattern of pitch changes shown in **Figure 3.6** may therefore reflect a combination of category-specific (same-type vs different-type) and sequence-dependent effects. That is, although on average same-type and different-type syllables changed in opposite directions (a "category-specific" effect, **Fig. 3.3b,d**), both types of syllables displayed adaptive changes in syllables immediately adjacent to the targeted syllable with smaller or negative changes at greater distances (a "sequence-dependent" effect). In the Discussion (Section 3.5), we speculate that these two effects result from two distinct processes underlying vocal adaptation.

We also asked whether experiencing vocal errors at a single vocal gesture led to asymmetrical effects on the surrounding movements. For example, **Figure 3.2b** shows an example in which significant pitch changes occur in the syllables after, but not before, the targeted syllable. We therefore tested whether the magnitude of pitch change falls off more quickly at positive and negative sequential distances by comparing the absolute slopes of the regression lines shown in **Figure 3.6a, b**. We found a significant difference in slopes (**Fig. 3.6a**, asterisk; partial F test), indicating an asymmetrical pattern: the magnitude of pitch change decreased more rapidly (in terms of sequential distance) for same-type syllables produced before the targeted syllable. When we performed the same analysis for different-type syllables, we also found a significant difference in slopes (**Fig. 3.6b**, asterisk; partial F test) but with the opposite pattern: the amount of pitch change decreased more rapidly for syllables produced after the targeted syllable.

Finally, it is possible that the apparent effect of sequence on vocal learning (**Fig. 3.6**) and the lack of an effect of acoustic similarity (**Fig. 3.5**) result from a confound between sequential and acoustic distances. For example, if vocal changes depended only on acoustic similarity, and nearby syllables were more acoustically similar to the targeted syllable than distant syllables, we could observe the same learning pattern as seen in **Figure 3.6** and erroneously conclude that learning depends on sequential context when it actually depended on acoustic distance. However, we found that syllables' sequential and acoustic distances were not correlated ($p = 0.36$ for different-type syllables, $p = 0.84$ for same-type syllables, $p = 0.32$ for combined syllables), suggesting that acoustic similarity cannot account for the patterns of vocal changes observed in **Figure 3.6**. The evidence therefore suggests that acoustic and sequential distances are largely independent in our dataset and make different contributions to the observed patterns of vocal plasticity.

3.5 Discussion

We found that songbirds use sensory errors to change the acoustics of individual vocal gestures occurring in particular sequential contexts. Songbirds also modified the pitches of unperturbed

vocal gestures, which we suggest is evidence for transfer of learning, or generalization. As hypothesized, adaptive pitch changes generalized to the same syllables produced in other sequential contexts. We also found two surprising results. First, the average transfer of learning to different vocal gestures was in the antiadaptive direction, signifying negative generalization. Second, generalization magnitude was negatively correlated with the sequential distance from the pitch-shifted syllable.

Learning to alter specific vocal gestures

Although prior studies have used negative reinforcement to show that birds can alter specific syllables [33], our results demonstrate that birds adjust individual syllables in response to naturalistic pitch perturbations (**Fig. 3.3**, red), suggesting that birds generate internal error signals specific to particular gestures. Our results parallel similar findings in humans, who alter the acoustics of single phonemes in response to manipulated auditory feedback [3,24]. Gesture-specific error correction may therefore be a general principle to help maintain learned vocal behaviors.

Learning generalizes to the same gesture in other contexts

We found that compensatory changes in a vocal gesture generalize to the same gesture produced in other contexts (**Fig. 3.3**, green). In humans, learning similarly generalizes to the same vowel in different words [3,23]. Our results show that this phenomenon occurs in songbirds during natural vocal behaviors, not only in the reduced "training utterance–test utterance" paradigms used in many human studies. This type of generalization may be advantageous because it reduces the need to relearn how to produce a vocal gesture correctly in each possible context.

Negative generalization to different gestures

Unexpectedly, learning generalized in the antiadaptive direction for different-type syllables (**Fig. 3.3**, blue). To our knowledge, negative generalization has not been reported in any sensorimotor learning studies. One study [219] involving visual rotations showed that, when subjects received limited visual feedback and reached to one target, errors to targets in the opposite direction were in the same direction as the sensory perturbation. However, these effects disappeared when more visual feedback was provided and, as the authors noted, likely reflect normal adaptation in a Cartesian reference frame, not negative generalization.

Why would negative generalization occur? Intuitively, altering different-type syllables should cause sensory error signals and a subsequent return to baseline [7]. However, our data suggest that the brain does not treat vocal gestures as isolated units, each having a specific set of desired acoustic features. Rather, we propose that the brain seeks to maintain specific acoustic relationships among vocal gestures. The observed antiadaptive pitch changes act to partially reestablish the preexisting pitch contrast between syllables (**Fig. 3.4a**). Therefore, although songbirds generate syllable-specific vocal corrections, alterations of unperturbed syllables could be used to maintain the relationships between vocal gestures.

A recent study simulating reward-based learning [63] proposes a possible computational mechanism for negative generalization. The authors showed that, when model neurons that transform sensory input into motor output respond to a wide range of sensory stimuli, negative generalization (or "destructive interference") can result. Although future work is required to assess whether the songbird brain implements such mechanisms, these modeling results suggest that negative generalization might result from auditory responses in the song system. Auditory activity is influenced by multiple syllables in a sequence [220–222], suggesting that the effects on nontargeted syllables could reflect the relatively long integration time observed in auditory responses.

Generalization is not predicted by acoustic similarity

We found that learning transfer was uncorrelated with acoustic distance from the targeted syllable (**Fig. 3.5**). This contrasts with some human speech [37,38] and limb movement [34–36,42,54,55] studies finding more generalization for gestures similar to the trained gesture. The differing results may arise because different-type syllables represent entirely different movement categories to the bird, analogous to performing reaching versus ball-throwing movements. Although some studies have found that learning generalizes across categorically different movements [50–53], others have not [34,35,42,43]. Analogously, in speech studies, the training and test utterances may not have been internally represented as separate categories.

Differences between our results and those in humans may also reflect differences in the degeneracy of speech and birdsong. Generalization studies in humans have explored vowel formant changes [3,23,37–39]. Vowel production involves precisely configuring vocal tract shape, and particular articulator configurations are thought to uniquely determine the formant frequencies in most cases [2,223,224]. In contrast, pitch control in songbirds appears to be more degenerate. Pitch is controlled by both air pressure and vocal fold tension [225–227], and different motor patterns can produce acoustically similar vocalizations [215,228]. Additionally, whereas voiced speech has one sound source, the songbird vocal organ (syrinx) contains two independently controlled sources, which might allow the same acoustic feature to be produced using either source (but see [229]). The discrepancy between our findings (**Fig. 3.5**) and those in humans might therefore arise because acoustically similar vocalizations necessarily reflect similar motor programs in humans but not in songbirds.

Importantly, our finding that acoustic similarity does not predict generalization may depend on the choice of acoustic parameters (pitch, amplitude, and spectral entropy; see Section 3.4, Results) used to measure similarity. We used these parameters because they account for a significant fraction of behavioral variation [29]. However, computing acoustic differences with more or other parameters might yield different results. Also, the degeneracy in pitch control described above may require measurements of muscle dynamics during song to obtain a more complete

picture of gesture similarity. Nevertheless, the lack of a robust relationship between generalization and similarity may reflect either a significant difference between songbirds and humans or between vocal error correction across a natural vocal repertoire and experiments using a more limited set of vocalizations.

Sequence-dependent generalization

Unexpectedly, we found that, for same-type syllables, generalization decreased with increasing sequential distance from the pitch-shifted syllable (**Fig. 3.6a**). Furthermore, although on average they exhibited antiadaptive pitch changes (**Fig. 3.3**), different-type syllables also exhibited adaptive changes in syllables adjacent to the targeted syllable and antiadaptive changes at larger distances (**Fig. 3.6b**) and therefore exhibited similar sequence-dependent differences in generalization. To our knowledge, the finding that generalization varies with sequential context is novel in both the speech and limb movement literature. Importantly, prior studies suggest that this phenomenon does not reflect biomechanical constraints preventing syllable-specific pitch changes. Songbirds can be trained to modify the pitch of individual syllables without altering temporally adjacent syllables [33] and can modulate pitch within syllables with 10 ms resolution [230]. The spread of generalization to adjacent syllables shown in **Figure 3.6** is therefore highly unlikely to reflect a motor constraint preventing songbirds from generating syllable-specific changes.

What might account for this sequence-dependent generalization? We speculate that, when a sensory error occurs during one syllable in a sequence, the "error credit assignment" [231] is not localized in time to just that syllable but is partially assigned to nearby syllables in the sequence (**Fig. 3.4b**). Because trial-by-trial variations in consecutive syllables' acoustics are typically correlated [29], if a bird makes an error on one syllable, it is likely to have made an error on the next and previous one as well. Thus, an advantageous strategy may be to extend the credit assignment function several syllables backward and forward in time from the syllable in which an error is detected. Why, then, are pitch changes not observed in syllables adjacent to those targeted by

negative reinforcement [33]? One possible explanation is that the highly salient (and artificial) negative reinforcement signals provide additional information that birds use to localize vocal changes in time.

Interactions between sequence-dependent and category-specific effects

Although they show similarly sequence-dependent patterns of generalization (**Fig. 3.6**), same-type and different-type syllables differ significantly in the average magnitude and direction of generalization (**Fig. 3.3**). We therefore speculate that our results reflect a combination of sequence-dependent and category-specific effects. That is, the changes in generalization across sequential distance in both same- and different-type syllables (regression lines in **Fig. 3.6**) may reflect a sequence-dependent effect of error credit assignment (**Fig. 3.4b**), as discussed above. At the same time, the overall antiadaptive bias in different-type syllables may reflect an additional mechanism for reestablishing acoustic relationships between syllables (**Fig. 3.4a**) that affects different-type syllables but is weaker or absent in same-type syllables (and is thus syllable-category-specific). Therefore, changes in different-type syllables (**Fig. 3.6b**) might reflect the combination of sequence-dependent (adaptive changes at small sequential distances) and category-specific (antiadaptive changes across all different-type syllables) effects. This combination of adaptive and antiadaptive effects might account for the relatively small average magnitude of changes in different-type syllables (**Fig. 3.3b**).

A key remaining question is whether generalization in same-type syllables (**Fig. 3.6a**) includes a global antiadaptive component in addition to the strongly sequence-dependent adaptive changes. The regression line shown in **Figure 3.6a** crosses the y = 0 line, suggesting that antiadaptive shifts might be present at long sequential distances, as is the case for different-type syllables (**Fig. 3.6b**). However, because our dataset contains very few examples of longer distances (and no examples of distances > 7 syllables), we do not have sufficient statistical power to

determine whether same-type syllables exhibit global antiadaptive changes in addition to local adaptive changes, as is the case for different-type syllables.

An alternate hypothesis is that, rather than resulting from the combined action of two processes (sequence-dependent error assignment and category-specific changes), the patterns in **Figure 3.6** might reflect variations in how a sequence-dependent error signal affects different motor programs. In this scenario, a sensory error during one syllable would result in a modulatory signal affecting multiple syllables in a sequence, but this signal would interact differently with the motor programs underlying same-type and different-type syllables to bias vocal changes in the adaptive and antiadaptive directions, respectively. Future studies showing how auditory errors reshape premotor activity will provide mechanistic insight into how sensory signals interact with motor changes in sequenced behaviors.

CHAPTER 4

DOPAMINERGIC CONTRIBUTIONS TO VOCAL LEARNING*

A similar version of this chapter was originally published in [232].

4.1 Abstract

Although the brain relies on auditory information to calibrate vocal behavior, the neural substrates of vocal learning remain unclear. Here we demonstrate that lesions of the DAergic inputs to a basal ganglia (BG) nucleus in a songbird species (Bengalese finches, *Lonchura striata*) greatly reduced the magnitude of vocal learning driven by disruptive auditory feedback in a negative reinforcement task. These lesions produced no measureable effects on the quality of vocal performance or the amount of song produced. Our results suggest that DAergic inputs to the BG selectively mediate reinforcement-driven vocal plasticity. In contrast, DAergic lesions produced no measurable effects on the birds' ability to restore song acoustics to baseline following the cessation of reinforcement training, suggesting that different forms of vocal plasticity may use different neural mechanisms.

4.2 Introduction

The brain relies on sensory information to guide the acquisition and maintenance of complex motor skills, including vocal behavior. Neurophysiological studies in mammals have shown that the activity of midbrain dopamine (DA) neurons reflects the difference between predicted and experienced reward, leading to the widespread hypothesis that such signals guide reinforcement learning [72,233]. However, establishing DA's role in sensorimotor learning, including vocal learning, has proved challenging in both experimental and clinical settings. Neurotoxic lesions of DA inputs to the BG often result in severe motor performance deficits [81,101], complicating efforts to isolate

* Modified from: **Hoffmann L.A.**, Saravanan V, Wood A.N., He L., Sober S.J. (2016). Dopaminergic Contributions to Vocal Learning. *Journal of Neuroscience*, 36:2176–2189

DA's specific contributions to motor learning. Moreover, because the mammalian striatum mediates a wide range of behaviors, DAergic inputs likely affect cognitive and behavioral processes other than those being assayed experimentally. Additionally, Parkinson's disease (PD), which includes dysfunction of the DAergic system, is associated with vocal performance and plasticity deficits [14,84]. However, because PD involves pathologies that extend beyond a simple loss of DAergic neurons [85], it is difficult to use clinical studies to pinpoint DA's role in vocal behavior.

Songbirds provide a well-defined neural circuit in which to investigate DA's role in vocal learning. As in a number of forms of mammalian behavioral plasticity [89,95], the BG are crucial for vocal plasticity in songbirds. Area X (**Fig. 4.1a,b**), the song system's BG component, is a nucleus in the anterior forebrain pathway (AFP), a BG- thalamocortical loop long implicated in vocal learning [134,156,157]. Area X is necessary for song learning but not performance. Its destruction abolishes normal song learning in juveniles and degrades the adaptive modification (but not performance) of song in adults [104,156–158]. However, it remains unclear how auditory error signals are conveyed to Area X [234,235]. In mammals, DAergic inputs to the BG convey error-related signals, suggesting that DAergic afferents to Area X might guide vocal learning in songbirds [104,106,130,151,209,236]. However, to our knowledge, no studies have directly addressed how DA contributes to vocal learning. We therefore reasoned that selectively lesioning DAergic inputs to Area X would allow us to isolate DA's contribution to learning without inducing performance deficits.

We used the neurotoxin 6-hydroxydopamine (6-OHDA) to reduce DAergic innervation within Area X. In mammalian systems, 6-OHDA injections are commonly used to selectively eliminate DAergic fibers and cell bodies [237]. The DAergic cells innervating Area X originate in the VTA and SNc and are spatially intermingled with DAergic neurons that project to other parts of the striatum [148], precluding injection directly into the VTA/SNc. Instead, we directly microinjected 6-OHDA into Area X to reduce DAergic innervation of Area X, but not surrounding striatum, and quantified the resulting effects on song performance and vocal learning (**Fig. 4.1c**).

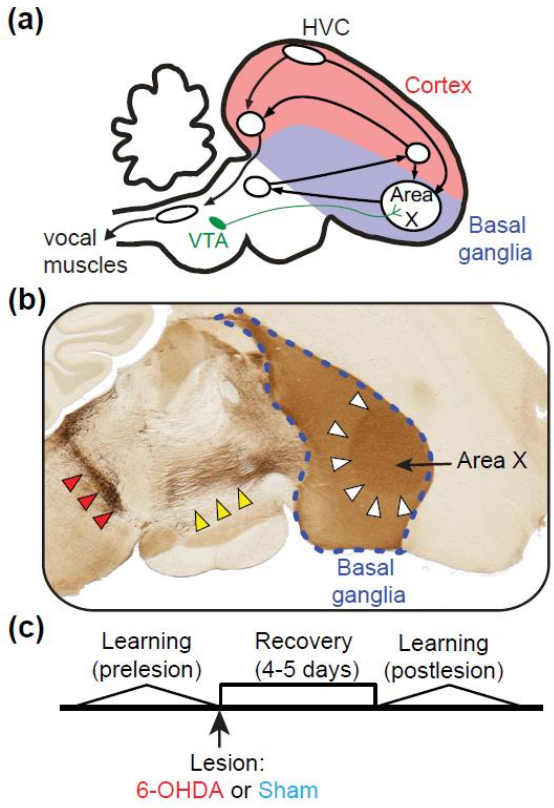

Figure 4.1. A song-specific BG nucleus receives strong DAergic input. **(A)**, The song system includes Area X, a BG nucleus critical for vocal learning. **(B)**, A parasagittal section stained for TH shows heavy label within the BG (blue dotted line) with especially strong label in Area X (borders of X indicated by white triangles). TH stain also shows DAergic cell bodies in the VTA/SNc (red triangles) and their ascending axons (yellow triangles). **(C)**, Experimental design (see Section 4.3, Materials and Methods).

4.3 Materials and Methods

All subjects were adult (>100-d-old) male Bengalese finches (*Lonchura striata var. domestica*). All procedures were approved by Emory University's Institutional Animal Care and Use Committee.

Vocal learning paradigm and behavioral analysis

Adaptive changes in the pitch (fundamental frequency) of targeted syllables were driven using a disruptive auditory stimulus as described previously [33]. Briefly, when the pitch of a particular "targeted" syllable was above (or below) a particular threshold, a blast of white noise (WN) was

played through the speakers, a contingency previously shown to induce birds to lower (or raise) vocal pitch to avoid WN playback. During reinforcement, a randomly selected subset of target syllables (10%) were selected as "catch trials" during which WN was not played back, allowing quantification of holistic syllable features, such as sound amplitude. The frequency threshold for WN was determined using the target syllable's pitch distribution from songs produced the morning of the first WN day (>25 song bouts). To drive pitch down (or up), the targeting software was set to trigger a 40–50 ms WN blast whenever target syllable pitch was above the 10th percentile (or below the 90th percentile) of this distribution.

All behavioral experiments began with a 3 d baseline period in which no WN playbacks occurred. Postlesion baseline occurred during postsurgery days 4–6 or 5–7. In prelesion experiments, birds were exposed to WN training for 3 d. In postlesion experiments, training continued for at least 3 d plus up to 3 additional days to ensure that birds had sung at least 90% as many songs as during the prelesion WN regimen, allowing comparison of learning between prelesion WN day 3 and the approximately trial-matched postlesion WN day. This extra training means that the WN day immediately preceding washout day 1 is not necessarily WN day 3. Although across experiments lesions did not significantly affect the amount of song production on average (see Section 4.4, Results), comparing trial-matched prelesion and postlesion days allows us to control for the effect of different amounts of vocal practice on the amount of learning in individual animals. Notably, as described in Section 4.4, Results, all findings were qualitatively identical if prelesion and postlesion learning was compared on the same chronological day (WN day 3) rather than the trial-matched day. Each bird's postlesion trial-matched day was the day where (by the end of the day) birds had sung the closest number of songs under the WN regime as they had after prelesion day 3. Across birds postsham or postlesion, WN training ended after days 3, 4, 4, 5 (for shams) and 2, 2, 3, 3, 6 (for 6-OHDA), and for each trial-matched day the total number of songs was within 10% of the number produced after prelesion day 3. Daily targeting sensitivity (hit rate) had a median value of 92% across all experiments (range, 58%–99%). Daily targeting

precision (1 – false-positive rate) had a median value of 93% across all experiments (range, 51%–100%). Across experiments neither sensitivity nor precision was significantly different between the prelesion and postlesion epochs (Kolmogorov– Smirnov tests, $p > 0.25$). All singing was undirected (i.e., in the absence of a female bird) throughout the WN experiments.

After the last WN day, we withdrew reinforcement and recorded song for 3 additional days to monitor spontaneous pitch restoration back to baseline, which typically occurs after several days [33,137]. Throughout this paper, we refer to this time period as "washout" and the birds' process of returning vocal acoustics to their baseline values as "restoration." Washout occurred between 11 and 18 d after surgery, depending on the bird.

Although all singing was undirected (i.e., no female bird was present) during baseline, WN training, and washout, we collected female-directed songs from 4 birds (three pre- and post-6-OHDA lesion, one presham) to assess the effect of 6-OHDA lesion on social context-dependent changes in pitch variability [123]. We obtained directed songs 1–4 d after washout was concluded in both prelesion and postlesion conditions. Interleaved directed and undirected songs were collected as described previously [123]. We obtained 1207 directed (919 undirected) syllable iterations across 11 prelesion syllables and 707 directed (688 undirected) iterations across 8 postlesion syllables and analyzed an equal number of interleaved undirected songs per bird/condition (>30 syllable iterations per syllable and condition).

Custom-written MATLAB software (The MathWorks) was used for data analysis. Pitch changes were quantified in units of semitones as follows:

$$s = 12 * \log_2(h / b)$$

where s is the pitch change (in semitones) of the syllable, h is the pitch (in Hertz) of the syllable, and b is the average baseline pitch (in Hertz) of the syllable. On each baseline, WN day, and washout day, we quantified the pitch, amplitude, and spectral entropy of the targeted syllable in 100 song bouts spaced evenly throughout the day (or all songs when birds sang <100 songs on a given day), as described previously [29]. To assess lesion-related changes in the quantity of song

produced, for each bird we quantified the ratio of the mean number of song bouts per day after 6-OHDA or sham lesion to the mean number produced per day before lesion. We then tested whether the distribution of ratios from 6-OHDA-injected animals differed from both unity and the distribution of ratios from the sham-injected group using one- and two-sample Kolmogorov-Smirnov tests, respectively. These tests allow us to quantify whether neurotoxin injection had a consistent effect on the amount of song production relative to both preinjection behavior and any effects of sham injections.

To assess changes in vocal pitch during the washout period (i.e., after the cessation of WN training), we fit an exponential decay model to the pitch data as follows:

$$p(t) = p_{initial} e^{-\frac{t}{\tau}} + p_{final}(1 - e^{-\frac{t}{\tau}})$$

where p_{initial} was set to the mean pitch on the final day of WN training, and fit parameters were τ and p_{final}, corresponding to the time constant of pitch restoration during washout and the asymptote of the exponential fit (final value of pitch if restoration were to reach equilibrium), respectively. We note that this exponential model is a generalization of a model we have used previously to quantify the time course of learning when songbirds experience real-time errors in the pitch of auditory feedback delivered via miniature headphones [218]; in that earlier model, p_{initial} was zero, because changes in vocal pitch were quantified relative to baseline error of zero.

6-OHDA and sham lesions

Subjects were randomly assigned to either the sham or 6-OHDA lesion group. Before injections, birds were anesthetized with ketamine, midazolam, and isoflurane, mounted in a stereotax at a 20° beak angle relative to the table surface, and small craniotomies were made above Area X. Lesioned birds received bilateral injections of 11.8 mg 6-OHDA-HBr/ml (i.e., 8 mg freebase 6-OHDA/ml) and 2 mg ascorbic acid/ml (stabilizer) in a 0.9% NaCl solution into Area X using a Drummond Scientific Nanoject II auto-nanoliter injector. During each injection, the pipet was lowered into the

brain along a plane perpendicular to the table surface. We injected 13.8 nl at each location and waited 30 s before raising the pipet. For sham lesions, only vehicle (2 mg ascorbic acid /ml in 0.9% NaCl) was injected per the procedure described above. All birds recovered from surgery within a few hours and usually sang the next day.

We varied injection coordinates and volumes slightly between birds and hemispheres to optimize injection parameters. For detailed parameters for each bird, see **Tables 1 and 2**. Total injection volume in each hemisphere ranged from 124.2 to 179.4 nl for all hemispheres, except one (234.6 nl). Necrotic damage within Area X was observed in only one hemisphere of one bird (the right hemisphere of Bird 3, which was the hemisphere receiving the largest total injection volume of 234.6 nl). This necrotic damage affected 8% of the total volume of Area X in the affected hemisphere. As our results are unaffected by removing Bird 3 from our dataset, we have included it in our analysis. As described below in Histology, we also performed a number of other analyses to investigate whether 6-OHDA injections killed neurons in Area X in cases where no necrosis was apparent.

To cover the greatest possible volume of Area X while still injecting low volumes, we placed injections (13.8 nl each) on a 3x3, 3x4, or 4x4 grid. Each grid was located at a single dorsal-ventral (DV) coordinate between 3.1 and 3.4 mm and individual injections were evenly spaced anterior–posterior (AP) and medial-lateral (ML) coordinates between 5.1 and 6.3 mm and 0.9 –2.2 mm, respectively. All AP and ML coordinates were relative to the posterior edge of a Y-shaped sinus visible beneath the inner skull layer, whereas DV coordinates were relative to the exposed brain surface. In three birds (and right hemisphere of a fourth), there was an additional injection outside of the main grid intended to hit the most medial portion of Area X, where its pear shape comes to a dorsal and posterior point at coordinates DV = 2.6 mm, AP = 4.8 mm, and ML = 0.8–0.9 mm.

Histology

Each bird was perfused 14–23 d after 6-OHDA or sham lesion. Dissected brains were fixed overnight at 4°C in 4% formaldehyde, sunk in 30% sucrose for 1–4 d, and sliced in 40 µm sections on a microtome. We performed chromogenic tyrosine hydroxylase (TH) stains on odd-numbered sections (to assess loss of Area X catecholaminergic fiber innervation) and either Nissl stains (7 birds) or fluorescent NeuN (neuronal nuclei protein) and fluorescent TH stains (2 birds; one sham, one 6-OHDA) on even-numbered sections (to assess postlesion necrosis).

In two additional birds, we performed unilateral 6-OHDA lesions (one bird in left and one in right hemisphere) and perfused 11 d after surgery. We performed chromogenic TH and fluorescent NeuN stains on alternating sections to compare Area X cell counts in sham- and 6-OHDA-lesioned hemispheres together with the two bilaterally lesioned NeuN-stained birds mentioned above. All hemispheres in these birds used the same injection coordinates and volumes as Bird 4 in **Table 1**. These birds were housed singly after surgery (no other birds were present), and no behavioral data were collected from them.

For chromogenic TH immunohistochemistry, all steps used 0.2 M PB (phosphate buffer solution; 23 g sodium phosphate (dibasic) + 5.25 g sodium phosphate (monobasic) per 1 L deionized H_2O) as the solvent unless otherwise indicated. Between each of the following steps, tissue was rinsed three times for 10 min in 0.2 M PB. Tissue was first incubated in 0.3% H_2O_2 for 30 min and 1% $NaBH_4$ for 20 min. It was then incubated at room temperature overnight in a solution containing primary antibody against TH (Millipore MAB318; 1:4000), 0.3% Triton X-100, and 5% normal horse serum. Tissue was then incubated in biotinylated anti-mouse secondary antibody (Vector Laboratories horse anti-mouse; 1:200 0.3% Triton X-100) for 1 h, followed by 1 h in avidin-biotin-complex (ABC) solution (Vector Laboratories Vectastain ABC kit; 1% horseradish peroxidase (HRP) conjugated streptavidin, 1% biotin, 0.3% Triton X-100, and 20 mg NaCl/ ml). ABC solution was left to react for 30 min before use. Finally, tissue was exposed to

diaminobenzidine (DAB) solution for exactly 5 min. Per tray, DAB solution contained two DAB tablets (Amresco E733; 5 mg DAB per tablet) in 20 ml of purified water.

For fluorescent immunohistochemistry, tissue was incubated in 1% $NaBH_4$ for 20 min, then blocked in 5% normal horse serum and 0.5% Triton X-100. Tissue was incubated for 48 h at 4°C in primary antibodies against TH (Millipore MAB318; 1:2000) and NeuN conjugated to AlexaFluor488 (Millipore ABN78A4; 1:2000) in 1% normal horse serum and 0.5% Triton X-100. Tissue was then rinsed and incubated in biotinylated anti-mouse secondary (Vector Labs BA-2000; 1:200 + 0.5% Triton X-100) for 1 h at room temperature, rinsed, and incubated in streptavidin-AMCA (SA-5008; 5 µg/ml + 0.5% Triton X-100) for 1 h at room temperature. Sections were mounted and coverslipped with Fluoro Gel with 1,4-diazabicyclooctane. Similar to chromogenic immunohistochemistry, 0.2 M PB was used as a solvent, and tissue was rinsed three times for 10 min after each step, except for blocking.

Image Analysis

Lesion size and location. We quantified both the fraction of Area X that exhibited reduced TH label and the extent to which the lesions affected different subregions of Area X by measuring lesion-induced changes in the density of TH label. Images were acquired on a slide scanner (Meyer Instruments PathScan Enabler IV; 24 bit color, 7200 dpi, "sharpen more" filter, brightness, and contrast level 50). A custom-written ImageJ (version 1.47) macro was used to manually outline Area X as a region of interest (ROI) on each TH-stained section.

As shown in **Figure 4.2b**, in each image an optical density (OD) threshold was established and then used to binarize the image so that each pixel within Area X was categorized as belonging to either the "lesioned" (indicated by a lighter TH stain in that area) or "nonlesioned" subregion of Area X. We use the terms "lesioned" and "nonlesioned" to differentiate subregions of Area X in 6-OHDA-injected birds that do or do not exhibit a loss of TH label (i.e., these terms do not refer to 6-OHDA injected vs sham-lesioned animals). Because the level of background staining varied

Table 1. Injection parameters for 6-OHDA lesioned birds[a]

Bird ID	Hemisphere	6-OHDA concentration (mg/ml)	Injected volume (nl)	Total 6-OHDA injected (μg)	AP coordinates (mm)	ML coordinates (mm)	DV coordinates (mm)	Days killed after surgery
Bird 1	Left	8	179.4	1.435	5.1, 5.5, 5.9, 6.3 (4.8 for Med_X)	0.9, 1.55, 2.2 (0.9 for Med_X)	3.18 (2.6 for Med_X)	18
Bird 1	Right	8	179.4	1.435	5.1, 5.5, 5.9, 6.3 (4.8 for Med_X)	0.9, 1.55, 2.2 (0.9 for Med_X)	3.18 (2.6 for Med_X)	18
Bird 2	Left	8	124.2	0.994	5.3, 5.8, 6.3	1.0, 1.6, 2.2	3.1	14
Bird 2	Right	8	124.2	0.994	5.3, 5.8, 6.3	1.0, 1.53, 2.05	3.4	14
Bird 3	Left	8	179.4	1.435	5.1, 5.5, 5.9, 6.3 (4.8 for Med_X)	0.9, 1.55, 2.2 (0.8 for Med_X)	3.18 (2.6 for Med_X)	21
Bird 3	Right	8	234.6	1.877	5.1, 5.5, 5.9, 6.3 (4.8 for Med_X)	0.9, 1.33, 1.77, 2.2 (0.8 for Med_X)	3.18 (2.6 for Med_X)	21
Bird 4[b]	Left	8	179.4	1.435	5.1, 5.5, 5.9, 6.3 (4.8 for Med_X)	0.9, 1.55, 2.2 (0.8 for Med_X)	3.18 (2.6 for Med_X)	22
Bird 4[b]	Right	8	179.4	1.435	5.1, 5.5, 5.9, 6.3 (4.8 for Med_X)	0.9, 1.55, 2.2 (0.8 for Med_X)	3.18 (2.6 for Med_X)	22
Bird 5	Left	8	124.2	0.994	5.1, 5.7, 6.3	0.9, 1.55, 2.2	3.18	14
Bird 5	Right	8	138	1.104	5.1, 5.7, 6.3 (4.8 for Med_X)	0.9, 1.55, 2.2 (0.8 for Med_X)	3.18 (2.6 for Med_X)	14

[a]AP and ML coordinates are on a grid such that each AP coordinate is paired with each ML coordinate in three or four rows. AP and ML coordinates are relative to Y_0, and ML coordinates are offset to the left or right of Y_0 depending on the hemisphere. DV coordinates are relative to the exposed brain surface. "Med_X" indicates a single extra injection that was intended (but not conclusively proven) to hit the medial-most portion of area X, where its pear shape comes to a dorsal and posterior point.

[b]In two additional birds, we performed unilateral 6-OHDA lesions and TH/NeuN stains to compare area X cell counts in sham- and 6-OHDA-lesioned hemispheres (see Materials and Methods). In these birds, we used identical injection coordinates and volumes as Bird 4.

Table 2. Injection parameters for sham-lesioned birds[a]

Bird ID	Hemisphere	Injection parameters	Days killed after surgery
Bird 6	Left	Identical to Bird 5 but no 6-OHDA	17
Bird 6	Right	Identical to Bird 5 but no 6-OHDA	17
Bird 7	Left	Identical to Bird 2 but no 6-OHDA	18
Bird 7	Right	Identical to Bird 2 but no 6-OHDA	18
Bird 8	Left	Identical to Bird 1 but no 6-OHDA	27
Bird 8	Right	Identical to Bird 1 but no 6-OHDA	27
Bird 9	Left	Identical to Bird 3 but no 6-OHDA	23
Bird 9	Right	Identical to Bird 3 but no 6-OHDA	23

[a]Each sham-lesioned bird's injection parameters were precisely matched to those of a 6-OHDA bird for consistency. "no 6-OHDA" indicates that birds were injected with saline and ascorbic acid (instead of 6-OHDA, saline, and ascorbic acid).

somewhat across sections, the OD threshold was set manually. We then used the binarized images to quantify the fraction of Area X in that image that had been lesioned as follows:

$$\alpha_i = \frac{N_i^{\text{lesioned}}}{N_i^{\text{lesioned}} + N_i^{\text{non-lesioned}}}$$

Where α_i is the fraction of Area X affected by the lesion in histological section *i*. Terms N_i^{lesioned} and $N_i^{\text{non-lesioned}}$ represent the number of lesioned and non-lesioned pixels in the image, respectively.

To assess the total fraction of X that received lesions in a given bird (α_{Total}), we quantified the following:

$$\alpha_{\text{Total}} = \frac{\sum_{i=1}^{k} N_i^{\text{lesioned}}}{\sum_{i=1}^{k} (N_i^{\text{lesioned}} + N_i^{\text{non-lesioned}})}$$

where the lesioned and non-lesioned pixels are summed across the k sections of Area X. This measure is summed across the two hemispheres, resulting in a single value of α_{Total} for each bird

which was then compared to each bird's learning behavior (see Relationship between lesion size/location and behavioral data). Additionally, we quantified the fraction of lesion in subregions of Area X. To do so, we divided images of Area X into dorsal, ventral, anterior, posterior, lateral, and medial subregions, as shown in **Figure 4.2b**. Thus, each of the six subregions comprised half of Area X (e.g. the dorsal subregions included measurements from the dorsal half of Area X in each section). We then calculated the fraction of each subregion that was lesioned (α_{dorsal}, $\alpha_{ventral}$, etc.) using the procedure described above.

Alternate analysis of OD. In addition to the above analysis of lesion size and location, we performed an alternate analysis that did not rely on manually establishing an OD threshold. A custom-written ImageJ macro was used to manually outline Area X as an ROI on each TH-stained section and place 0.5-mm-diameter ROI circles on representative areas of cortex (just dorsal to Area X) and non-X-striatum (just posterior to Area X near the dorsal border of the striatum). In some cases (e.g., **Fig. 4.2a**, right) loss of TH label extended slightly outside of the border of Area X; the "non-X-striatum" ROI was positioned to exclude such areas. OD was quantified by converting the image to 8-bit grayscale and then measuring the average pixel value in each ROI.

To assess the effects of 6-OHDA injection into Area X, we quantified [$OD_{Area\ X}$ / $OD_{Striatum}$], the ratio of OD in the Area X ROI to the non-X-striatum ROI. This ratio was calculated separately in each TH-stained section to account for cross-section and cross-animal variations in stain density. We also performed an alternate analysis in which the OD of the cortex ROI was treated as background signal, and OD ratio was computed as [($OD_{Area\ X} - OD_{cortex}$) / ($OD_{Striatum} - OD_{cortex}$)] within each stained section. This alternate technique yielded nearly identical results as the primary analysis. Quantifying the distribution of OD ratios in sham-lesioned animals (which is typically >1 because Area X receives denser catecholaminergic input than the surrounding striatum) [238] allowed us to determine the 95% confidence interval of this metric in sham-lesioned brains. Any section

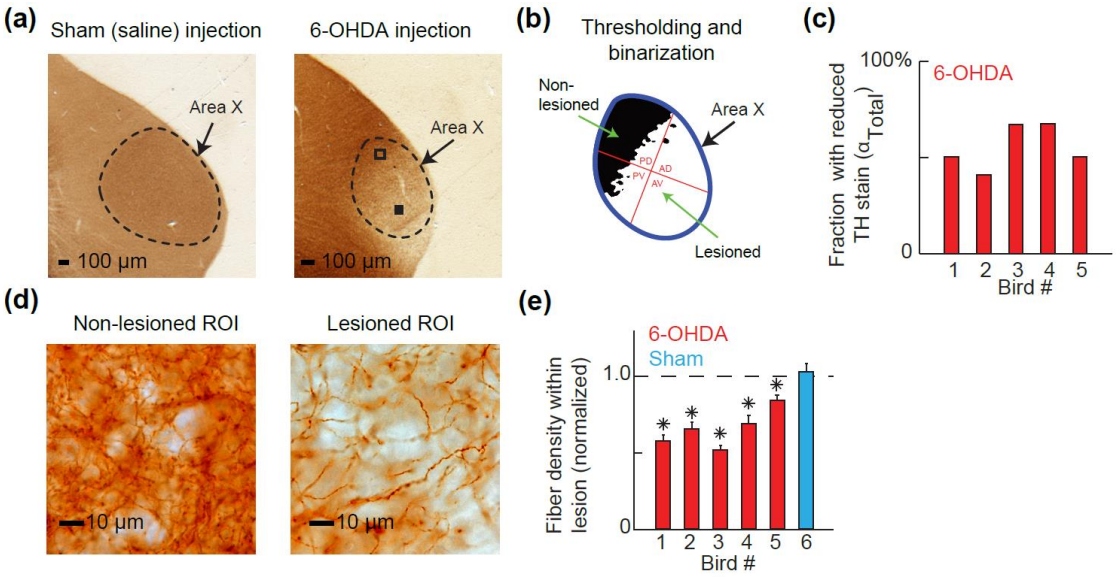

Figure 4.2. Lesions of DAergic inputs to Area X. **(A)**, Comparison of TH stain in sham (left) and 6-OHDA-lesioned (right) brains shows a reduction in the OD of stain in 6-OHDA-injected animals. **(B)**, To measure the loss of DAergic inputs, we used an OD threshold to divide images of Area X into "lesioned" (white) and "nonlesioned" (black) subregions. Additionally, to quantify the location of lesions, we divided Area X into dorsal, ventral, anterior, and posterior subregions. Red lines and letters indicate subregions that are both posterior and dorsal (PD), anterior and dorsal (AD), posterior and ventral (PV), and anterior and ventral (AV). Because all sections were cut parasagittally, medial and lateral subregions were designated by categorizing each section as belonging to either the medial or lateral half of Area X. **(C)**, Using the binarization shown in **B**, we quantified the fraction of Area X in which TH stain was reduced (α_{Total}; see Section 4.3, Materials and Methods). **(D)**, We also quantified the density of TH-positive fibers both within and outside the lesioned subregion of Area X ("lesioned ROI" and "nonlesioned ROI," respectively) in individual histological sections. Examples of lesioned and nonlesioned ROIs are shown as filled and empty squares in **A**, respectively. **(E)**, Within each section, we normalized the fiber density in the lesioned ROI by the density in the nonlesioned ROI from the same image. Histogram and error bars indicate the mean ±SEM of this measure across five 6-OHDA-injected birds and one sham. *$p < 0.05$ (two-sided Kolmogorov–Smirnov tests). We obtained the same result when raw (un-normalized) fiber density measures were used.

from a 6-OHDA-injected animal with an OD ratio beyond the 95% interval therefore exhibits a significant reduction in TH staining density with $p < 0.05$.

Neuron counts. We quantified the number of surviving neurons following 6-OHDA (and sham) lesions in Area X as well as in VTA/SNc, which sends a massive DAergic projection to the striatum, and in the locus coeruleus (LC), which may send a weak noradrenergic projection to Area X (but see [168,239]). We quantified the number of neurons in Area X by imaging 4–10 sections from each of the four NeuN-stained brains (see Histology) at 40x magnification (0.75 zoom) using a Leica SP8 multiphoton microscope. We excluded 3 of the 29 images due to an imaging artifact.

ImageJ was used to convert images to 8-bit grayscale, threshold based on pixel intensity to create a binary image, reduce noise (Remove Outliers in ImageJ), and separate touching cell bodies (Watershed in ImageJ). Cell bodies were counted using the Analyze Particles plug-in. Identical acquisition and processing parameters were used for all images.

To assess whether the number of NeuN-stained cells in Area X differed between experimental conditions (6-OHDA vs sham), we performed a multilinear regression analysis with birds and lesion condition as factors. Including each bird as a factor in the model increased our power by controlling for any between-bird differences. We combined data across NeuN-stained birds (one bilateral sham, one bilateral 6-OHDA, two unilateral 6-OHDA as described in Histology) and fit a standard multiple linear regression model [240] as follows:

$$y_{ij} = \beta_0 + \beta_1 * b2_{ij} + \beta_2 * b3_{ij} + \beta_3 * b4_{ij} + \beta_4 * C_{ij} + \varepsilon_{ij}$$

where y_{ij} = cell counts for bird i and image j, C_{ij} is an indicator variable to represent experimental condition (C_{ij} = 1 if image ij is from a 6-OHDA hemisphere, 0 if from a sham hemisphere), b2-b4 are indicator variables to represent bird-specific effects ($b2_{ij}$ = 1 if image ij is from bird 2, 0 otherwise), β values are regression coefficients, and ε is the residual error, assumed to be normally distributed. The term β_4*C represents the condition-specific effect after controlling for bird-specific effects ($\beta_0 + \beta_1 b_2 + \beta_2 b_3 + \beta_3 b_4$). Because indicator variables are 1 or 0 depending on the bird, the term β_0 represents the effect of Bird 1. To determine whether 6-OHDA-lesioned hemispheres had fewer cells in Area X than sham-lesioned hemispheres, we performed a partial F test on whether β_4 is significantly different from zero after including the other factors.

To quantify neuron numbers in VTA/SNc and LC in each WN trained bird, chromogenically TH-stained sections were imaged at 10x on an Olympus IX51 Widefield microscope with a Hamamatsu Orca ER CCD camera (for VTA/SNc) or an Axioplan widefield microscope with an Optronics camera (for LC). Ten sections containing VTA/SNc and two containing LC were imaged for each subject. Because sections were cut parasagittally, we did not

attempt to identify the border between VTA and SNc. The most medial sections of VTA and the most lateral sections of SNc were not imaged because these regions contain few Area X-projecting neurons [148]. Image acquisition parameters were held constant across subjects. In cases where the region being imaged was too large to fit into a single field of view, multiple images were taken and stitched together using the ImageJ Pairwise Stitching plug-in [241].

VTA/SNc and LC cell counts were performed using the ImageJ Cell Counter plug-in by four raters who were blinded to bird identity and treatment condition. Rater bias was quantified by having all raters count cells in the same histological sections and comparing mean counts across raters. The mean count from each individual was used to linearly scale all counts from that rater, with all correction terms having an absolute value of ≤13%. Cell count results were qualitatively identical even if this correction term was not applied. As described in Section 4.4, Results, cell counts from all birds revealed no significant difference in either VTA/SNc or LC. However, a *post hoc* power analysis revealed that we would be unlikely to detect such change given the very small size of our neurotoxin injections, given that Area X comprises ~10% of the total volume of the BG [242] and that our lesions affected only part of Area X. To perform the power analysis, we made two extremely conservative assumptions to put an upper bound on the number of catecholaminergic neurons that project to Area X. First, we can assume that Area X received 10% of the catecholaminergic input (the actual fraction is likely much lower given that both VTA and LC send inputs to the forebrain in addition to the striatum). Second, we can assume that 6-OHDA injections will kill 100% of neurons that project to the affected region of the striatum (the actual fraction of neurons killed is likely significantly lower than this). Therefore, given that our lesions affected ~50% of Area X, we would expect that our lesions would kill at most 5% of catecholaminergic neurons projecting to Area X (50% * 10%), and likely much less.

We therefore performed a power analysis to quantify whether we would be likely to be able to detect a 5% change in neuron number. Across repeated measurements of the same TH-stained section, our cell counts had an SD of σ_{section} =10% relative to the mean. We assessed the

total number of TH^+ cells in the VTA by summing cell counts across n_{sections}=10 histological sections. Assuming that cell counts of different sections represent independent measurements, we therefore expect that the total cell count for each bird has a SD of the following:

$$\sigma_{\text{Bird}} = \sqrt{n_{\text{sections}}\sigma^2_{\text{section}}} = 32\% \text{ (relative to the mean)}$$

We then quantified the power of an analysis to detect a 5% difference in the number of TH^+ neurons with a SD of 32% and a total of 5 measurements (5 birds per group). This analysis yielded a power of 0.07, indicating that we would only have a 7% chance of detecting such a difference. Our failure to detect a significant change in TH^+ cell body number (see Section 4.4, Results) is therefore unsurprising given the very small size of our neurotoxin injections within the BG.

Analysis of fiber density. For TH fiber density analysis in Area X, sections were imaged at 63x using a Zeiss Axioplan 2 Widefield microscope with an AxioCam HRc Color Camera. Lesioned and nonlesioned portions of Area X within a single section were selected based on previously captured images (see Lesion size and location). Image acquisition parameters varied slightly between sections but were held constant for lesion-nonlesioned pairs within a single section.

Mammalian studies frequently induce unilateral lesions (e.g., injecting 6-OHDA into the striatum on one side and vehicle into the other side), allowing the experimenter to normalize the fiber density in the lesioned hemisphere to that in the opposite hemisphere to compensate for stochastic variations in TH stain intensity (i.e., animal-by-animal variation that is unrelated to the experimental condition). Because all birds used in our behavioral experiments received bilateral lesions of DAergic inputs to Area X, we were unable to take this approach. Instead, we normalized the fiber density within the lesioned subregion of Area X to the fiber density within a nonlesioned subregion in the same histological section, as described below. However, as described in the main text of this chapter, we obtained qualitatively identical results when we did not perform this within-section density normalization.

Images were analyzed using ImageJ, with identical image-processing steps applied to every section. In each brain, we chose 10 tissue sections (five from each hemisphere) that contained both lesioned and nonlesioned subregions of Area X. We then captured two images from each section, one from the lesioned and one from the nonlesioned subregion, and converted all images to 8-bit grayscale. To isolate TH-positive fibers, images were then bandpassed (FFT Bandpass Filter in ImageJ) to emphasize features with high spatial frequency (i.e., labeled axons) and then thresholded based on pixel intensity to create a binary image in which black pixels represented TH-stained fibers. After removing outlier pixels (Remove Outliers in ImageJ), we then measured the density of TH-positive fibers by quantifying number of black pixels as a fraction of total pixels in the image. Fiber density from each lesioned subregion was then normalized to the density of the nonlesioned subregion in the same images. To assess the level of variation in this measure in a sham-lesioned bird, in one sham bird we randomly selected 5 of 10 ROIs to serve as the "lesioned" subregions.

High performance liquid chromatography (HPLC)

In a separate set of adult (>100-d-old) male Bengalese finches (n = 6), we performed unilateral 6-OHDA lesions and used HPLC to compare Area X DA and norepinephrine (NE) levels in lesioned and sham-lesioned hemispheres. Each bird received a 6-OHDA lesion in Area X in one hemisphere and a sham lesion in the other hemisphere using the same procedure described in 6-OHDA and sham lesions. All hemispheres across birds used the same injection coordinates and volumes as Bird 4 in **Table 1**. We alternated which hemisphere was injected with 6-OHDA, so half the birds received lesions in the left and half in the right hemisphere. The birds were housed singly after surgery (no other birds were present), and we did not collect any behavioral data from these animals.

Fourteen days after surgery, we decapitated each bird, rapidly harvested the brains, flash-froze them in powdered dry ice 2–4 min after decapitation, and stored them at -80°C. Frozen brains

were sliced into 300 µm parasagittal sections in a -12°C cryostat, placed on slides, briefly wet-thawed to room temperature (<20 s) to allow tissue to settle on the slide and placed on dry ice. In each hemisphere, we made 1-mm diameter, 300-µm-thick circular tissue punches of Area X in two sections using a previously described technique [243], placed both punches in a tube while still frozen and stored the sample at -80°C until tissue was analyzed for monoamine content. Area X was identified by observing the frozen and briefly wet-thawed sections with the naked eye and through a dissecting microscope using a bright light and dark surface to enhance contrast.

NE and DA concentrations were determined by HPLC with coulometric detection using established methods [244]. Each sample was processed individually (one sample per hemisphere). Briefly, samples were first homogenized in 0.1 N $HClO_4$ solution (containing 0.01% sodium metabisulfite and 25 ng/ml internal standard 3,4-dihydroxybenzylamine HBr), and centrifuged at 13,000 x g for 15 min at 4°C. Supernatant fraction aliquots were injected into an Ultrasphere 5 µm ODS column, 250x4.6 mm (Hichrom) and separated with a mobile phase containing 0.1 M sodium phosphate, 0.1 mM EDTA (ethylenediaminetetraacetic acid), 0.35 mM sodium octyl sulfate, and 7% (v/v) acetonitrile, pH 3.2. DA and NE amounts (ng/sample) were then quantified by comparison with internal standards, with a standard curve generated with 0.1–5 ng for each analyte. Protein (mg/sample) was determined using the Lowry protein assay with a standard curve generated with 0–95 µg bovine serum albumin (BSA) [245].

Relationship between lesion size/location and behavioral data

We used a stepwise regression procedure [240] to ask whether the magnitude and/or location of the loss of DAergic inputs to Area X was predictive of the observed changes in learning behavior. To do this, we calculated the change in the absolute magnitude of learning due to 6-OHDA lesion as $\Delta_{\text{Absolute}} = \mu_{\text{post}} - \mu_{\text{pre}}$, where μ_{pre} and μ_{post} are the magnitude of pitch change before and after lesion, respectively, on last prelesion WN day and trial-matched postlesion day. We then asked

which of seven measurements of lesion size and location (α_{Total}, α_{dorsal}, α_{ventral}, α_{anterior}, $\alpha_{\text{posterior}}$, α_{lateral}, α_{medial}) were significantly predictive of Δ_{Absolute}. Stepwise regression analysis provides a systematic method for testing which predictor terms should be included in a multilinear model by beginning with an initial model and testing changes in the model's predictive power that result from including or excluding individual predictor terms. We therefore applied this procedure to ask which, if any, of the seven candidate predictors should be included in a multilinear model that predicts Δ_{Absolute}. This analysis concludes when neither including nor excluding any additional terms significantly improves the model ($p<0.05$ after Bonferroni correction). In an alternate analysis, we used the same seven candidate predictors to produce a model of Δ_{Relative}, which quantifies the fractional reduction ("percent decrease in learning") in learning behavior after lesion:

$$\Delta_{\text{Relative}} = \left(1 - \frac{\mu_{\text{post}}}{\mu_{\text{pre}}}\right) * \ 100\%$$

In one 6-OHDA-lesioned bird, in the postlesion experiment, the bird made a small pitch change in the antiadaptive direction (i.e. μ_{post} was negative). In this case, Δ_{Relative} was set to 100%.

4.4 Results

We injected 6-OHDA into Area X of adult male Bengalese finches, measured the ensuing effects on song performance and vocal learning, and quantified the lesion-induced depletion of Area X's DAergic input. Following previous studies in mammals, we quantified DAergic innervation using an immunohistochemical stain for TH, the rate-limiting enzyme in the DA synthesis pathway (**Fig. 4.1b**). As shown in **Figure 4.2a**, 6-OHDA injections substantially reduced TH label within Area X. To quantify the volume of Area X affected by the lesion, we manually set an OD threshold for each image (see Section 4.3, Materials and Methods; and **Fig. 4.2b**) and counted the fraction of pixels in which TH density fell below the threshold. As shown in **Figure 4.2c**, by this metric TH stain was reduced in 46%–68% of Area X across birds, indicating that our lesions affected

approximately half of the volume of the nucleus. Furthermore, to obtain a more direct measure of the lesions' effects on DAergic innervations, we analyzed tissue at high magnification to quantify the prevalence of TH-positive axons within Area X (**Fig. 4.2d**). We found that 6-OHDA injections reduced TH-positive fiber density to 51%–84% of the normal value within the lesioned subregions of Area X (**Fig. 4.2e**).

In the analyses shown in **Figure 4.2a–c**, we manually set an OD threshold to delineate the lesioned and nonlesioned subregions of Area X (see Section 4.3, Materials and Methods). To verify that these results were not an artifact of this procedure, we also performed an alternate analysis of lesion volume that did not rely on manual thresholding. As shown in **Figure 4.3**, this alternate analysis similarly found that 6-OHDA injections led to significant reductions in TH stain in approximately half of Area X.

In addition to optical imaging of TH-stained sections, we also quantified the extent to which 6-OHDA injections reduced DA concentrations within Area X using HPLC. In a separate cohort of Bengalese finches (n = 6), we injected one hemisphere with 6-OHDA and performed a sham lesion on the other hemisphere. This design allowed us to control for interindividual differences in neurotransmitter levels. As shown in **Figure 4.4a**, left, 6-OHDA lesions reduced the concentration of DA by an average of 47.1% (range 9.3%–74.1%, mean concentration 206.1 and 390.5 ng DA/mg protein in lesioned and sham hemispheres respectively).

6-OHDA is toxic to both DAergic and noradrenergic neurons, and TH staining labels both types of neurons. It was therefore important to consider the possibility that any observed effects of 6-OHDA injections on both behavior and TH stain density might reflect changes in noradrenergic input as well as (or instead of) changes in DA. However, we think that this possibility is extremely unlikely. Catecholaminergic innervation of Area X has previously been shown to be overwhelmingly DAergic [112,168,239].

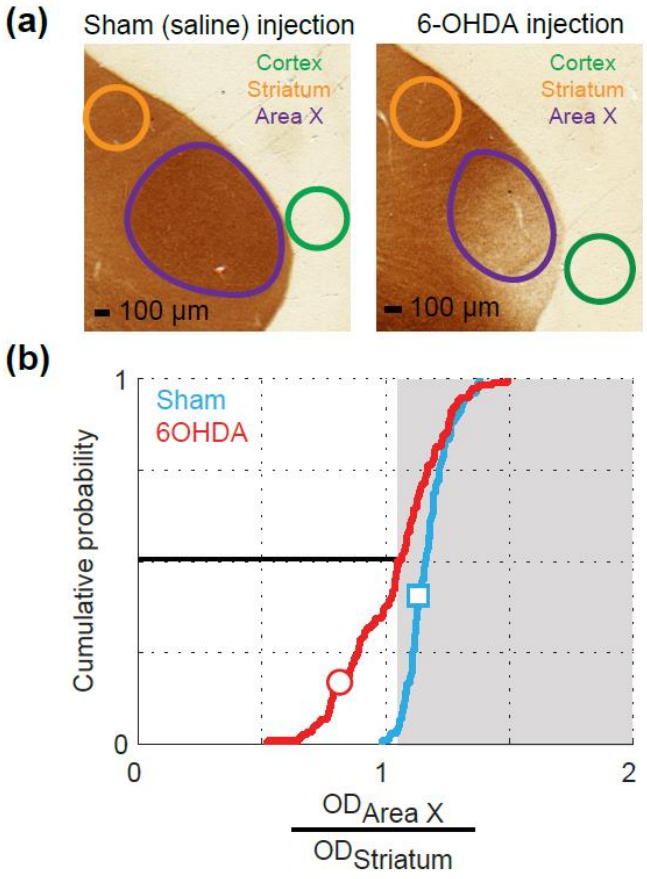

Figure 4.3. Alternate method of quantifying loss of TH label. In our primary analysis of lesion size (see Section 4.3, Materials and Methods; **Fig. 4.2b**), we manually set an OD threshold to quantify the fraction of Area X in which TH stain was reduced in each histological section. Here we present an alternate analysis (see Alternate analysis of OD) that does not rely on a within-image threshold but rather simply measured the mean OD across all of Area X in each section. **(A)**, Comparison of TH stain in sham (left) and 6-OHDA-lesioned (right) brains, showing the same sections as in **Figure 4.2a**. To measure the loss of DAergic inputs, in each histological section, we quantified the OD of TH stain across all of Area X (purple) and in the adjacent striatum (orange). **(B)**, Analysis of the ratio of OD in Area X to that in striatum. In nearly all sections from sham-lesioned birds, TH stain is darker in Area X than in surrounding striatum (OD ratio > 1). In 6-OHDA-injected birds (red trace), 50% of sections (horizontal black line) of Area X had an OD ratio below the 95th percentile of the sham distribution (gray region). In **B**, red and blue symbols represent measurements taken from the left and right panels shown in **A**, respectively.

Studies of noradrenergic inputs to Area X have reported that such inputs are either absent [239] or extremely weak [168], and NE concentration within Area X has been reported to be < 3% of that of DA [112]. Consistent with these prior findings, NE concentrations assessed by HPLC were < 2% as great as DA concentrations in sham hemispheres (**Fig. 4.4a**, right; mean 1.2%, range 0.5%–1.6%, mean concentration 4.9 and 4.3 ng NE/mg protein in lesioned and sham hemispheres,

respectively), and furthermore were not significantly affected by 6-OHDA injections (**Fig. 4.4b**). Therefore, loss of noradrenergic inputs to Area X is very unlikely to have affected our results.

Importantly, staining for the neuron-specific nuclear protein NeuN revealed that 6-OHDA injections did not reduce the number of neuronal somata within Area X relative to sham injections (**Fig. 4.5**), suggesting that 6-OHDA injections reduced DAergic inputs without killing neuronal cell bodies in the BG. Additionally, we examined lesion-induced loss of DAergic neurons by counting TH-positive cell bodies in midbrain nuclei VTA/SNc and assessed lesion-related changes in noradrenergic neurons by counting TH-positive cells in the LC. Cell counts revealed no significant difference in either area (2655 ± 427 mean ± SD for VTA/SNc in sham birds; 2598 ± 369 for VTA/SNc in lesioned birds; 193 ± 40 for LC shams; 201 ± 48 for LC lesions; $p > 0.8$ in all cases, Kolmogorov–Smirnov test). However, a *post hoc* power analysis (see Section 4.3, Materials and Methods) revealed that we would be highly unlikely to detect the loss of TH-positive neurons resulting from our injections of 6-OHDA given the fact that Area X comprises only ~10% of the total volume of the BG [242] and that our lesions affected only part of Area X. Therefore, because of the very small volume of tissue injected with neurotoxin, the loss of TH-positive cell bodies in VTA/SNc known to follow 6-OHDA injections was well below our threshold for detectability.

Bilateral depletions of Area X's DAergic innervation did not affect the amount or quality of song production. As shown in **Figure 4.6a**, 6-OHDA injections had no significant effect on the number of songs produced per day, and the small changes in song number observed after neurotoxin injections were not significantly different from those that followed sham injections ($p > 0.05$, one- and two-sample Kolmogorov–Smirnov tests, respectively). Additionally, there were no detectable differences in the acoustic structure of song syllables. The gross spectral structure of song was unaffected by the lesions, as shown in example songs from the same bird before and after lesion (**Fig. 4.6b**). Quantitative acoustic analysis revealed that 6-OHDA injections caused no consistent changes in either the mean or variance of syllable pitch (**Fig. 4.6c**), sound amplitude, or spectral entropy ($p > 0.25$, Kolmogorov–Smirnov tests).

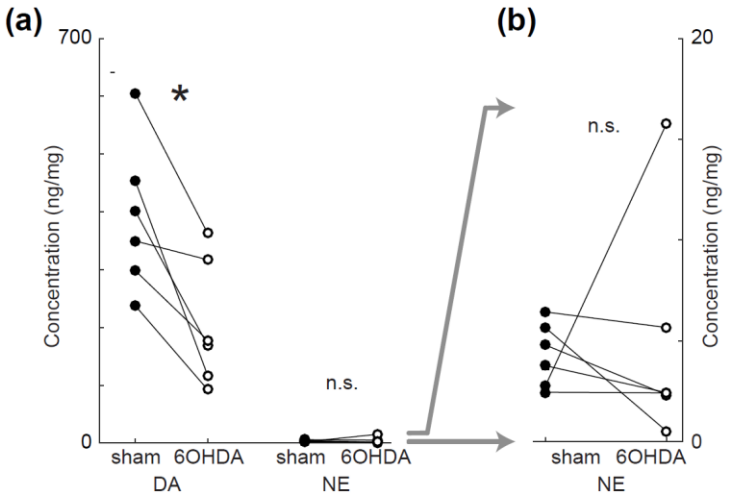

Figure 4.4. Concentrations of DA and NE in 6-OHDA- and sham-lesioned tissue. As described in Section 4.3, Materials and Methods, we used HPLC to directly measure the concentration of DA and NE in birds that received 6-OHDA lesions of Area X in one hemisphere and sham lesions in the other hemisphere. **(A)**, In sham-lesioned hemispheres (filled symbols), the concentration of NE was extremely small relative to that of DA, with NE concentrations on average 1.2% as great as that of DA (range 0.5%–1.6%). Injections of 6-OHDA significantly reduced the concentration of DA (*$p < 0.05$, one-sample Kolmogorov–Smirnov test on normalized DA concentrations in the lesioned hemisphere) but did not significantly affect concentrations of NE. ($p > 0.8$; one-sample Kolmogorov–Smirnov test on normalized NE concentrations in the lesioned hemisphere). **(B)**, Expanded view of NE data; note the difference in vertical scale between **A** and **B**. n.s., Not significant.

Because increased DA within Area X during female-directed song is associated with reductions in acoustic variability [124,126,127,246], depleting DA with 6-OHDA injections might cause vocal variability to increase in directed song even if it does not affect the variability of undirected song (**Fig. 4.6c**). Alternatively, because PD is associated with reductions in vocal variability [14], 6-OHDA lesions might cause vocal variability to decrease. Accordingly, we collected prelesion and postlesion directed song from 4 birds (see Section 4.3, Materials and Methods) and analyzed pitch variability. Consistent with prior results [30,123,247], we found a lower pitch SD in prelesion directed versus undirected song ($p < 0.05$, Wilcoxon signed-rank test; prelesion directed SD: mean 0.36 semitones, range 0.17–0.64 semitones; prelesion undirected: 0.47, 0.23– 0.98). Interestingly, we did not find differences in either prelesion versus postlesion directed pitch SD or prelesion versus postlesion undirected pitch SD ($p > 0.05$, Wilcoxon signed-rank tests). Nor did we find a difference in postlesion directed versus undirected pitch SD ($p > 0.05$, Wilcoxon signed-rank test). The ~50%

reduction in DA induced by 6-OHDA lesions (**Figs. 4.2, 4.4**) therefore appeared to have no significant effect on acoustic variability in either female-directed or undirected song.

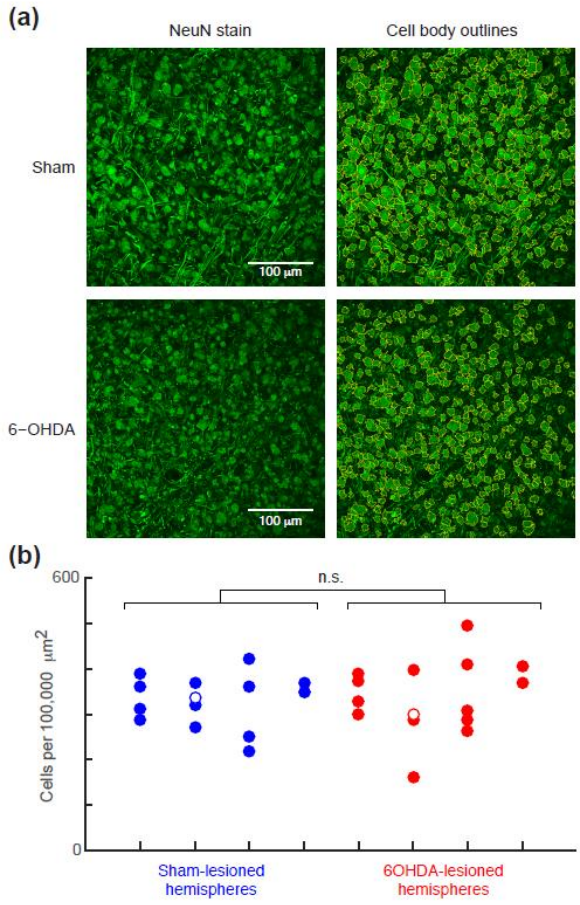

Figure 4.5. 6-OHDA injections do not lead to neuron loss within Area X. **(A)**, Representative NeuN-stained images from birds that received sham (top) and 6-OHDA (bottom) lesions. In each section, we counted the number of neuronal cell bodies (right column; see Section 4.3, Materials and Methods). **(B)**, Area X images were taken from two bilaterally and two unilaterally lesioned birds (each 369x369 µm). Blue and red circles represent the number of cell bodies in individual sections. Open circles represent the values for the example sham and 6-OHDA lesions shown in **A**. All images from 6-OHDA-injected hemispheres were taken from within subregions of Area X that exhibited significant loss of TH staining. We did not detect a significant difference in the number of cell bodies in Area X in 6-OHDA versus sham conditions ($p > 0.7$, partial F test; see Section 4.3, Materials and Methods). This suggests that, while lesions decreased DAergic inputs to Area X (**Figs. 4.2, 4.3, 4.4**), 6-OHDA injections did not kill neurons with cell bodies within Area X. n.s., Not significant.

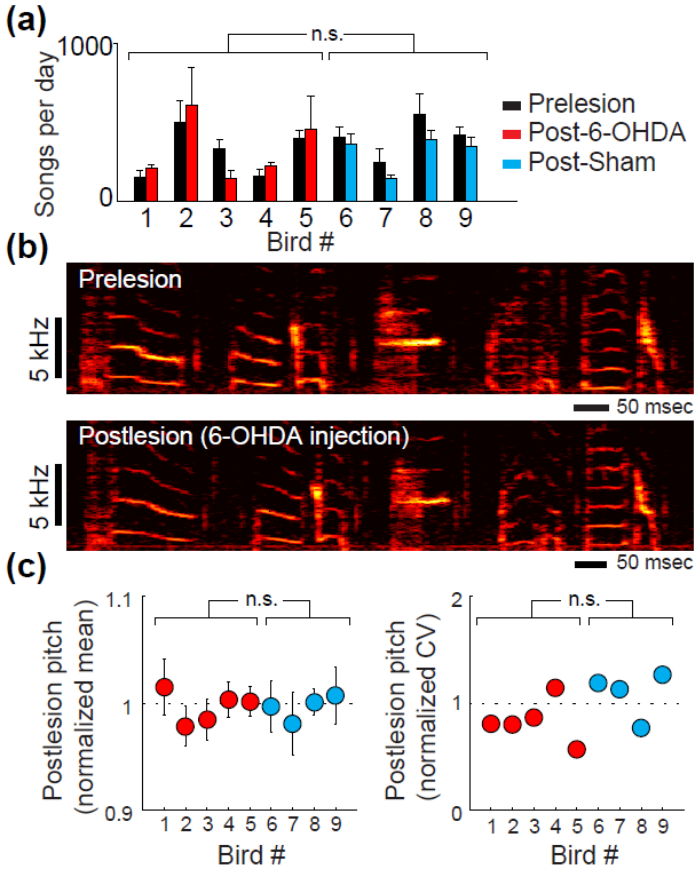

Figure 4.6. Removal of DA inputs to Area X does not degrade song quantity or quality. **(A)**, The number of song bouts produced per day did not significantly differ in 6-OHDA-injected versus sham-lesioned animals (see Section 4.4, Results). **(B)**, Spectrograms represent the acoustic power (color scale) at different frequencies as a function of time for two representative samples of a bird's song before (top) and 5 d after (bottom) bilateral 6-OHDA injections into Area X. **(C)**, Across animals, there were no consistent differences in the mean (left) or variability (CV; right) of the pitch of the song syllables targeted with WN when the postlesion data were normalized by their prelesion values ($p > 0.5$, Kolmogorov–Smirnov tests) in birds receiving 6-OHDA injections (red) or sham lesions (blue). n.s., Not significant.

However, we caution that these results are based on a relatively small dataset of directed song that is likely underpowered to detect subtle differences. Bengalese finches produce directed song much less readily than do zebra finches. Although we were able to collect some directed song (from 11 syllables prelesion and 8 syllables postlesion, with a mean of 110 and 88 iterations per syllable, respectively), attempting to collect more female-directed song would have significantly impeded our examination of 6-OHDA's effect on learning because introducing female songbirds acutely reduces the total amount of song production. Importantly, we note that a recent study of the

effects of 6-OHDA lesions of Area X in zebra finches collected a much larger amount of female-directed song and reports significant variability changes after 6-OHDA lesions in Area X [129].

In each bird, we compared vocal learning before and after either 6-OHDA or sham (saline) injections into Area X (**Fig. 4.1c**). We evoked learning by providing disruptive auditory feedback (WN blasts) conditional on the sung pitch of a particular syllable [33]. In response to this reinforcement training, birds modify the pitch of the targeted syllable to avoid WN, as shown in a representative prelesion experiment (**Fig. 4.7a**, black line, **b**). Following 6-OHDA injections, learning was greatly reduced in this bird (**Fig. 4.7a**, red line, **c**). Averaged across all subjects, the rate of learning decreased by >50% following 6-OHDA injections (**Fig. 4.7d**), whereas no reduction was seen following sham surgeries (**Fig. 4.7e**).

In addition to directly comparing the time course of learning across the first 3 d of WN (**Fig. 4.7a–f**), we also quantified learning on trial-matched prelesion and postlesion days (see Section 4.3, Materials and Methods) and similarly found reduced learning in 6-OHDA-lesioned (**Fig. 4.7g**) but not sham-lesioned birds (**Fig. 4.7h**). This analysis addresses a confound that could arise if we interpreted learning solely on a chronological basis (**Fig. 4.7a–f**). Because of normal variation in singing rate, birds sang a somewhat different number of songs by postlesion day 3 than by prelesion day 3. Hence, if a particular bird learned less by postlesion day 3 (compared with prelesion day 3), it could occur because that bird experienced substantially fewer learning trials, not because of DA lesion. Likewise, if a bird learned the same amount by postlesion day 3, it could occur because that bird experienced substantially more trials, masking a DA-dependent learning deficit. Therefore, it is crucial to compare prelearning/postlearning both chronologically (**Fig. 4.7a-f**) and using a postlesion day where birds had a similar number of trials (within 10%) as in the prelesion experiment (**Fig. 4.7g–i**). Additionally, because difference between p values does not always correspond to a difference between effects [248], we directly compared the (post – pre) learning changes between conditions and found significantly reduced learning in 6-OHDA birds

(**Fig. 4.7i**). To our knowledge, these results provide the first direct evidence that vocal learning in songbirds depends strongly on DAergic input to the BG.

As described in Section 4.3, Materials and Methods, animals were randomly assigned to either the 6-OHDA lesion or sham group. Notably, two of the birds randomly assigned to the lesion group exhibited stronger prelesion learning than did their counterparts in the presham group (compare black symbols showing "prelesion" and "pre-sham" learning values in **Fig. 4.7g** and **Fig. 4.7h**, respectively). As a result, the prelesion learning data combined across subjects (**Fig. 4.7d**, black trace) exhibited noticeably greater learning than the presham data (**Fig. 4.7e**, black trace). To assess whether the apparent effects of 6-OHDA on learning could have arisen from a difference in prelesion/presham learning ability, we repeated the analysis in **Figure 4.7d** after excluding the two animals that exhibited the greatest prelesion learning. As shown in **Figure 4.7f**, this reanalysis yields comparable prelesion/presham learning (compare black traces in **Fig. 4.7e and 4.7f**) and, similar to the full dataset from lesioned animals, reveals a significant drop in learning ability following 6-OHDA injection, demonstrating that the 6-OHDA-dependent reduction in learning shown in **Figure 4.7d, e** was not an artifact of a difference in learning ability in the two subject groups before lesion or sham injections.

We used a stepwise regression procedure to quantify whether the size or location of the loss of DAergic input within Area X predicted the magnitude of behavioral effects shown in **Figure 4.7g**. We found that none of the candidate predictor values, which included the total fraction of Area X in which TH stain was reduced (α_{Total}) as well as the fraction within six different subregions of Area X (anterior, posterior, medial, lateral, dorsal and ventral), were significantly correlated with either the absolute or relative change in vocal plasticity (Δ_{Absolute} or Δ_{Relative}; see Section 4.3, Materials and Methods), either as individual predictors or in any combination. However, it should be noted that our datase contains a somewhat limited range of lesion sizes (**Fig. 4.2c**), potentially limiting our ability to identify such effects. Notably, anatomical studies have shown a topographic

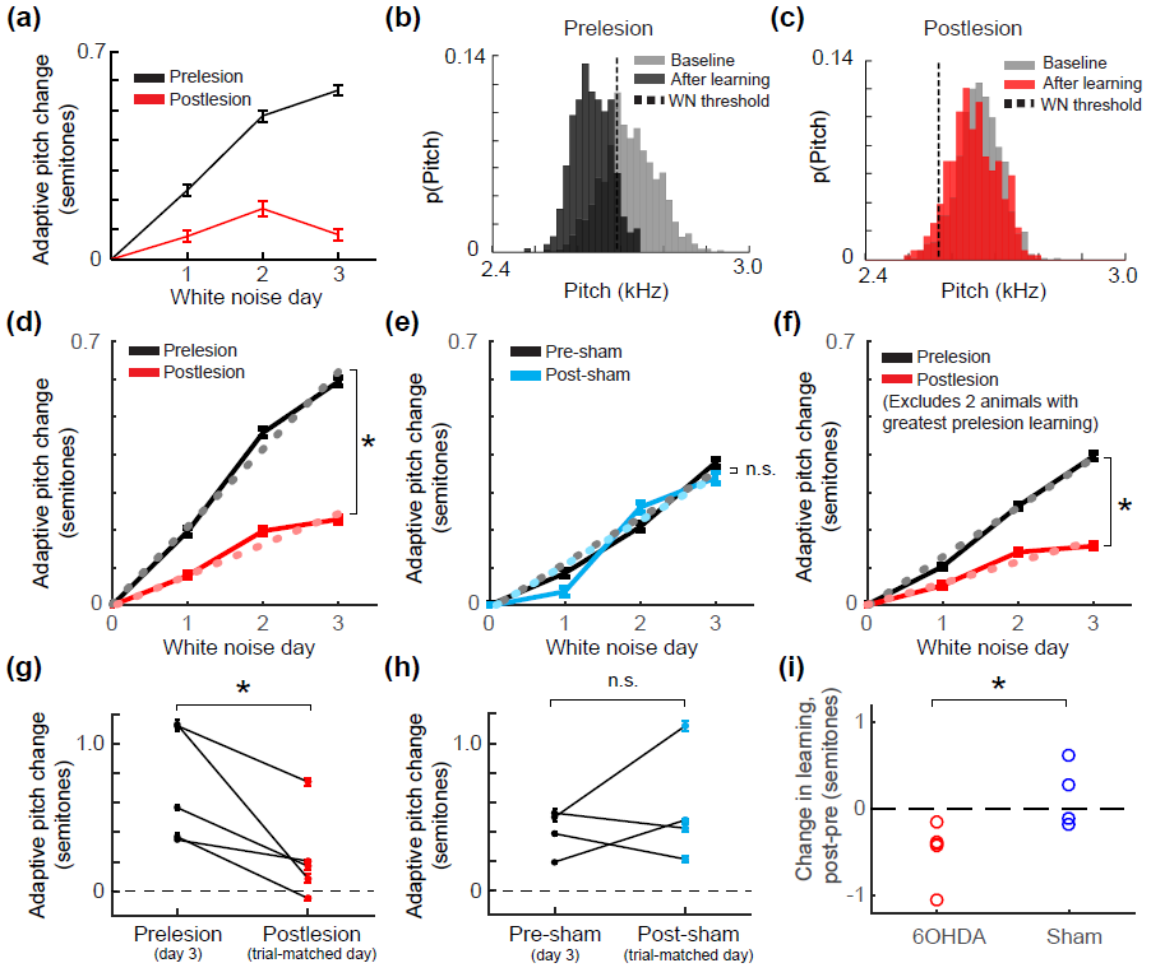

Figure 4.7. Removal of DA inputs to Area X impairs reinforcement-driven vocal learning. **(A)**, In an example experiment, a bird received 3 d of training in which higher-pitched renditions of a syllable were punished by a disruptive auditory stimulus (see Section 4.3, Materials and Methods). Black and red traces represent the pitch of the targeted syllable (mean ±SEM) before and after 6-OHDA injections, respectively, and illustrate a substantial reduction in learning magnitude following lesion. Pitch changes in the adaptive direction (downwards) are plotted as positive values. **(B), (C),** Prelesion (**B**) and postlesion (**C**) pitch distributions for the experiment shown in **A**. Gray bars represent the 3 d baseline pitch distribution. Dashed lines indicate the threshold for WN playback (i.e., any pitches sung above that threshold received WN). In every experiment, learning was driven in the same syllable and in the same direction prelesion and postlesion. **(D)**, Group data for lesioned (6-OHDA-injected) animals. Solid lines indicate the pitch of the targeted syllable as in **A**, except that here data are combined across n = 5 lesioned animals. Dotted lines indicate linear regression to pitch data. *p < 0.0001, significantly different slopes (F test). **(E)**, Group data for n = 4 sham-lesioned animals, plotting and testing conventions as in **D**. Slopes of pitch as a function of time are not significantly different (p = 0.48, F test). **(F)** Alternate analysis of data from 6-OHDA-lesioned animals, excluding the two subjects who showed the greatest prelesion learning (see Section 4.4, Results and **G**). Plotting and testing conventions as in **D**; pitch slopes are significantly different (*p < 0.0001, F test). **(G)**, Adaptive pitch change on the last WN day in the prelesion experiment (relative to baseline) versus adaptive pitch change on a trial-matched WN day in the postlesion experiment (not necessarily day 3; see Section 4.3, Materials and Methods). *p < 0.05, significant difference in prelesion and postlesion learning magnitude (one-sided Wilcoxon signed-rank test). **(H)**, Adaptive pitch change on the last WN day for sham-lesioned animals (conventions as in **G**). **(I)**, Direct comparison between sham and 6-OHDA learning changes. *p < 0.05 (two-sample t test). n.s., Not significant.

mapping between different subregions of Area X and downstream components of the song system [145], suggesting that different portions of Area X might be dedicated to the modification of particular vocal parameters, such as pitch [104,145]. Although our analysis did not produce positive evidence for such specificity, the spread of 6-OHDA within Area X prevented us from fully assessing this idea by precisely confining lesions to particular subregions of the nucleus.

Following training, we turned off WN playbacks and continued to monitor vocal acoustics for at least 3 d (see Section 4.3, Materials and Methods). In contrast to the large deficits in learning observed during operant conditioning (**Fig. 4.7**), 6-OHDA lesions did not appear to impair spontaneous pitch restoration after learning. Both before and after lesion, the pitch of song changed monotonically toward the baseline (pretraining) value (**Fig. 4.8a**). Furthermore, quantifying the time constant of restoration demonstrated that pitch actually recovered significantly faster after 6-OHDA lesion than prelesion ($\tau_{\text{prelesion}}$ = 2.15 d, $\tau_{\text{postlesion}}$ = 0.87 d; **Fig. 4.8b**). However, the faster time constant of restoration postlesion does not necessarily reflect enhanced learning after 6-OHDA lesions. Rather, the observed difference in time constant may reflect the well-established phenomenon [218,249] that learning speed increases when the experienced sensory error is smaller relative to baseline. Indeed, in postlesion experiments, birds began restoration with a smaller error because learning was impaired (compare the last WN day for prelesion and postlesion experiments in **Fig. 4.8a**). The fit parameter p_{final}, which estimates the eventual equilibrium state of learning, was close to zero in both cases (p_{final} = -0.04 semitones prelesion, p_{final} = 0.05 semitones postlesion), suggesting that both prelesion and postlesion animals would have returned pitch to near the baseline value had washout been allowed to run for longer than the three post-WN washout days shown in **Figure 4.8a**.

To control for the fact that learning speed depends on sensory error magnitude, we further examined the effects of DA lesion on pitch restoration by comparing postlesion restoration (**Fig. 4.8**, red traces) with data from specially selected subsets of experiments performed in the non-6-OHDA-lesioned condition. Specifically, we created these subsampled datasets by progressively

eliminating the nonlesioned animals with the greatest learning on the last WN day until the remaining nonlesioned animals showed nearly identical vocal errors on the final WN day as did the DA-lesioned population. **Figure 4.8c** shows a version of this analysis in which we compared all post-6-OHDA animals (red, n = 5 experiments) with data selected from prelesion, presham, and postsham animals so that the selected nonlesioned dataset ("Non-6-OHDA (selected)," n = 6 experiments; **Fig. 4.8c**, blue trace) had approximately the same initial error as the postlesion data (**Fig. 4.8c**, red trace). In an alternate version of this analysis (**Fig. 4.8e**), we selected the nonlesioned datasets only from postsham animals ("Postsham (selected)," n = 2 experiments). In both cases, these alternate analyses (**Fig. 4.8d,f**) yielded qualitatively the same results as those shown in the initial analysis (**Fig. 4.8b**), with significantly faster learning after 6-OHDA lesion (**Fig. 4.8d,f**, asterisks) and p_{final} values very close to zero (p_{final} = 0.004 and 0.1 semitones for the nonlesioned data shown in **Fig. 4.8d** and **Fig. 4.8f**, respectively). Thus, although analysis of our relatively short washout period does not allow us to make strong conclusions regarding the effects of DA lesions on spontaneous error correction, our analyses clearly indicate that restoration back to pitch baseline is not impaired by reduction of DAergic inputs to Area X, as is learning guided by WN, and indeed may be facilitated by 6-OHDA lesions (see Section 4.5, Discussion).

4.5 Discussion

Our experiments show that 6-OHDA injections into the songbird BG nucleus Area X caused significant loss of DA inputs without causing detectable loss of neurons within Area X. These DAergic lesions caused significant vocal learning deficits when pitch changes were driven by WN reinforcement but did not result in measurable changes in song performance, song variability, or pitch restoration to baseline after WN was discontinued. These results suggest DAergic inputs to the BG are critical for guiding vocal learning, at least when learning is driven by external reinforcement signals.

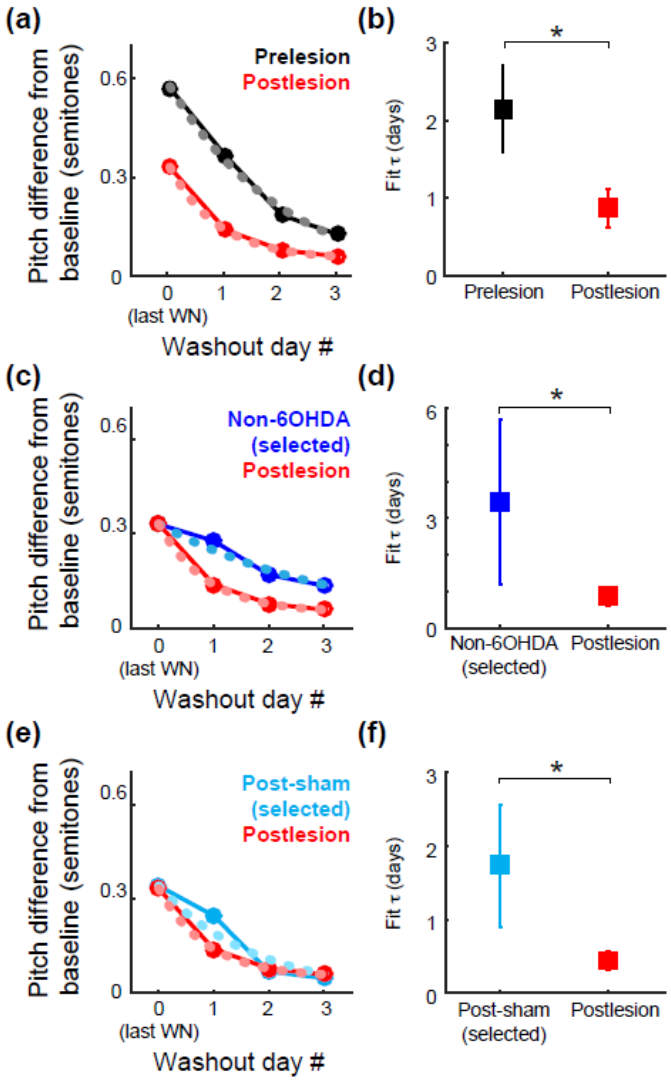

Figure 4.8. Removal of DA inputs to Area X does not impair pitch restoration. **(A)**, Combined data across five 6-OHDA-lesioned birds during the restoration period, after WN was discontinued. Washout day 0 is the last day of WN (not necessarily day 3; see Section 4.3, Materials and Methods). Black and red represent prelesion and postlesion experiments, respectively. Prelesion and postlesion restoration data were fit with an exponential decay model (dashed lines; see Section 4.3, Materials and Methods). Birds restored pitch toward baseline in both prelesion and postlesion experiments. After 6-OHDA lesions, birds began with a lower absolute pitch difference from baseline because of postlesion learning deficits (**Fig. 4.7d**). **(B)**, Fitted time constant τ for prelesion and postlesion learning. Lower τ indicates faster return to baseline. In postlesion experiments, birds restored pitch significantly faster than in prelesion experiments (*$p < 0.05$, permutation test). Error bars indicate 95% confidence intervals. **(C)**, **(D)**, Same analysis as in **A**, **B**, but selecting nonlesioned datasets so as to approximately equalize the initial error (i.e., to approximately equalize error on the last WN day). Here nonlesioned datasets are selected from prelesion, presham, and postsham subjects (see Section 4.3, Materials and Methods). **(E)**, **(F)**, Same analysis as in **C**, **D**, but with nonlesioned datasets drawn only from postsham subjects. Note different vertical scale in **D** compared with that in **B**, **F**. **A**, **C**, **E**, ±SEM error bars are obscured by the plotted circles.

Although we took pains to precisely target 6-OHDA injections to Area X, and indeed loss of TH stain was mostly confined to this nucleus, in some cases we observed loss of label in the striatum immediately surrounding Area X (**Fig. 4.3a**). Importantly, the "shell" region immediately surrounding Area X is hypothesized to be part of a circuit parallel to the classical song system shown in **Figure 4.1a**. Although cortical components of this parallel system appear to contribute to vocal learning [148,250,251], the involvement of Area X_{shell} in learning remain to be directly tested. Because some spillover of 6-OHDA is inevitable, we cannot exclude the possibility that some of the observed effects on vocal learning reflect loss of DAergic input to the shell surrounding Area X. However, we consider this possibility unlikely given that the loss of label outside of Area X affected a very small fraction of the surrounding striatum.

Because female-directed song has lower acoustic variability and is associated with increased DA in Area X [124,126,127,246], we expected to see increased vocal variability after 6-OHDA lesions. However, we did not observe a significant change in pitch variability in either direction following 6-OHDA injections for undirected (**Fig. 4.6c**) or directed song, consistent with another study finding no changes in syllable structure after unilateral 6-OHDA lesions in VTA/SNc [252]. The lack of an effect of lesions on social context-dependent variability may reflect the incomplete nature of our lesions, which spared a substantial number of DA terminals within Area X. Alternatively, it is possible that neuromodulatory factors in addition to DA or neural circuits other than Area X also contribute to context-dependent changes in variability and were able to compensate for lesion-induced changes.

Notably, a recent study analyzed vocal variability after 6-OHDA lesions of DAergic input to Area X in zebra finches [129]. Contrary to our hypothesis, this study found significant reductions in undirected (but not female-directed) song variability, similar to the decreases in vocal variability observed in PD [14]. Our conflicting results may be attributed to two factors beyond the obvious difference in the species being studied. First, as noted in Section 4.4, Results, we had a relatively small sample size of interleaved directed/undirected songs, lowering our statistical power to detect

subtle differences in variability. Second, our average 6-OHDA dosage was slightly higher (1.3 μg; **Table 1**), and we quantified variability at later time periods (13–22 d after lesion for directed song analysis compared with 4–5 d after lesion in [129]), raising the possibility of a complex relationship between the extent of DA depletion, time course of compensation, and changes in vocal variability. The effects of DA depletion on vocal variability in Bengalese finches therefore remain to be clarified by future studies.

Although 6-OHDA lesions caused vocal learning deficits during WN training (**Fig. 4.7**), restoration to baseline pitch was not impaired during the washout phase (**Fig. 4.8**), suggesting that DA might play different roles in distinct forms of vocal learning. Wholesale lesions or inactivation of Area X or LMAN (the output nucleus of the AFP) severely degrade both WN-driven pitch learning and spontaneous restoration back to baseline [109,114,137,158]. Our data indicating that only the former process depends on DAergic inputs to Area X suggest that the BG might mediate these two forms of vocal plasticity in distinct ways. Interestingly, lesions in caudal medial nidopallium, proposed as a candidate site for template song memory, disrupt restoration but spare noise-avoidance learning [253], the opposite pattern we observed following DAergic lesions to Area X. These observations support the idea that "vocal plasticity" can be divided into different subtypes, each driven by distinct yet interacting neural processes.

Despite the above considerations, however, our data suggesting that restoration is less impeded by DA loss than is noise-driven learning should be treated with a great deal of caution. First, our 6-OHDA injections only partially ablated DA within Area X, and the robust restoration observed after lesion might reflect residual DA function. Second, because washout experiments necessarily occurred after WN training, it is possible that some form of compensatory plasticity occurred in the few days that elapsed between the onset of postlesion WN training and the beginning of the washout period. Third, it is important to emphasize that the return to baseline is not necessarily auditory-guided and could in theory be mediated by a bird's matching proprioceptive feedback to the baseline motor command. Finally, as shown in **Figure 4.8a, c, e**, we

did not collect washout data for sufficient time for syllable acoustic to fully return to baseline either prelesion or postlesion. Therefore, although the speed of restoration appears unimpeded by 6-OHDA lesions, the endpoint of restoration following DA depletion remains to be measured directly. Intriguingly, the analyses shown in **Figure 4.8** suggest that pitch restoration may actually progress more quickly following DA lesions, even when selecting subsets of the data so as to equalize the initial error size (**Fig. 4.8c–f**). Although the caveats detailed above prevent us from drawing strong conclusions about DA's role in vocal learning other than that driven by WN, future studies could ask whether DA is necessary for error-corrective learning by providing a correctable auditory perturbation to baseline song without explicit external reinforcement [7,208].

Prior studies have identified potential mechanisms by which DAergic inputs to Area X might mediate vocal learning. The nuclei of DAergic neurons that project to Area X reside in the VTA/SNc complex, which in turn receives input from forebrain neurons that respond to perturbations of auditory feedback during singing [121], providing a candidate pathway by which sensory error signals might influence DA release within the BG. Furthermore, DAergic signaling plays a crucial role in mediating plasticity at corticostriatal synapses in both mammals and songbirds [67,119,130], suggesting that DA might mediate vocal learning by modulating changes in synaptic strength between cortical area HVC and spiny neurons in Area X [104]. Although our results strongly suggest that DAergic projections from VTA/SNc guide vocal plasticity, future studies (including recording from DA neurons that project to Area X) are needed to investigate the nature of the signals conveyed by these projections.

Our lesions only partially eliminated DAergic inputs to Area X, in contrast to studies in mammals in which injections of neurotoxins into the medial forebrain bundle produces near-complete ipsilateral loss of DAergic input throughout the striatum [254]. Specifically, our lesions reduced TH stain in approximately half of Area X (**Fig. 4.2c**), and within the affected regions eliminated ~15%–50% of catecholaminergic axons (**Fig. 4.2e**), comparable with the fiber loss observed following intrastriatal 6-OHDA injections in mammals [255]. HPLC results similarly

showed DA concentration dropping 47% on average (**Fig. 4.4a**). Because even these relatively modest reductions in DAergic innervation produced learning deficits, our results demonstrate that vocal learning is sensitive to disruptions of DAergic input to the BG and suggest that DA plays a crucial role in the processing of sensorimotor errors.

CHAPTER 5

DOPAMINE-DEPENDENT FEATURES OF BASAL GANGLIA NEURAL ACTIVITY

5.1 Introduction

In this pilot study, we examined how partial loss of Area X's DAergic input affected its neural activity in urethane-anesthetized birds. It provided preliminary data for future studies of Area X neural activity during DA-dependent learning and future studies comparing the effect of DA lesions in songbirds to other model systems and human PD. To summarize, we performed unilateral 6-OHDA lesions of Area X and quantified how pallidal mean firing rate and LFP beta power (13-30 Hz) were affected by 6-OHDA lesions and song playbacks. ***For convenience and easier comparison with the beta band in mammals (including humans)*** [189,256–258]***, we will refer to the 13-30 Hz frequency range as the "beta band"*** despite not observing an actual band of power modulation at these frequencies (see Section 5.3).

Conceptually, the purpose of this Study was twofold. First, we wanted to help establish the songbird as a scientifically useful new model of BG DA in motor learning. To do this it is important to quantify BG neural activity changes after loss of DA and compare to changes seen in other model systems after DA depletion and in PD. Second, since we showed in Study 2 (Chapter 4) that Area X DA is required for vocal learning, we wanted to begin investigating the neural mechanisms causing learning deficits. Area X activity changes after loss of DA could be important clues as to why DA depletion caused the deficits. Thus, in this Study we searched for DA-dependent neural activity.

We chose to start the search for DA-dependent activity by examining mean firing rates and LFP beta power. In a pilot study, it makes sense to first examine basic neural firing properties, and mean firing rates are a fundamental yardstick of neural activity. More importantly, Area X neurons

are known to exhibit firing rate increases to acoustic stimuli under anesthesia [173,174,177], particularly in response to playbacks of the bird's own song (BOS). This could indicate cortico-BG synaptic connectivity tuned towards BOS-specific acoustic features (such as pitch) that could help Area X guide adaptive learning and sensorimotor error correction in awake birds. We hypothesized loss of DA would lead to abnormal plasticity and a loss of this tuning, which we predicted would manifest as a lack of BOS responsiveness. Thus, a loss of BOS selectivity in the DA-depleted state (measured by analyzing mean firing rates in response to playbacks) would provide circumstantial evidence that the Area X microcircuit might be undergoing abnormal plasticity – in other words, the synaptic weights would no longer be optimized for processing BOS-related information. This could contribute to the learning deficits. We also analyzed LFP beta power. As discussed below, pathological beta band oscillations are one of the most prominent features observed in DA-depleted states. We hypothesized that if DA-depleted Area X also had these oscillations, it might indicate pathological synchronization in the Area X microcircuit, particularly among pallidal neurons, which in turn could lead to Area X's inability to properly guide learning. Thus, although loss of DA could affect neural activity in many ways other than mean firing rate and LFP beta power, those features were a worthwhile starting point.

We first investigated how auditory stimuli affected the mean firing rates of sham- and 6-OHDA-lesioned Area X pallidal neurons. These neurons are similar to those in mammalian GPe and GPi (see Section 1.4) [142,144]. As in other song system nuclei, Area X neurons are responsive to auditory input under anesthesia (although not in awake or singing birds [104]). Zebra finch (*Taeniopygia guttata*) and Bengalese finch pallidal neurons increase firing rate selectively when hearing playbacks of BOS, compared to acoustically similar stimuli such as reversed BOS (REV) [174,177]. This is driven by excitatory projections from HVC and LMAN (**Fig. 1.2a,b**) which have BOS selectivity under urethane anesthesia [259]. DA neurons in X-projecting VTA/SNc also have BOS selectivity but this is driven by Area X via its inhibitory pallidal projection to VP (**Fig. 1.2c**), which leads to disinhibition of DA neurons [260]. During song, this disinhibition could gate auditory-

guided LTP, resulting in Area X firing changes that alter downstream neural activity and lead to adaptive song changes [260].

We hypothesized that DA-related learning deficits (see Chapter 4) occur because Area X does not receive sufficient DA prediction error signals to help guide learning. Loss of DA neuromodulation could have led to abnormal plasticity at corticostriatal synapses (i.e. the DA-mediated LTP of HVC/LMAN input to Area X MSNs [119]), which in turn may have caused abnormal plasticity at pallidal synapses. We predicted this would manifest as a lack of pallidal BOS-selectivity in the anesthetized state. Losing BOS-selectivity might indicate inappropriate weakening of synaptic connections that are critical for helping Area X guide learning in awake birds and show that DA-depleted Area X no longer has normal functional connectivity with the rest of the song system.

Next, we examined how loss of Area X's DA input affected the LFP power spectrum and compared to PD and mammalian models of DA depletion. We focused on analyzing power in a 13-30 Hz frequency range, which corresponds to the beta band in other model systems [257,258], because excessive beta band oscillations and resulting bradykinesia are a prominent feature in PD [189,256]. PD beta oscillations are most commonly associated with the STN [190], but while songbirds have an STN [171] it is not considered part of the song system because it does not project to or receive inputs from song system nuclei [27,131,148]. However, strong beta oscillations have also been seen in mammalian GPe, GPi and striatum under DA depletion [185–189]. The mammalian striatum and pallidum are the closest analogues to Area X because it contains striatal and pallidal cell types [143,144] linked via direct and indirect pathways [141] (**Fig. 1.2**). We predicted loss of DA in Area X would also lead to increased LFP power in the 13-30 Hz range as in mammalian BG.

To extend our knowledge of LFP oscillations in songbirds we investigated how Area X LFP power changed during playbacks of auditory stimuli in sham- and 6-OHDA-lesioned hemispheres. In general, LFP oscillations could have several functional roles, including but not limited to motor readiness, efficient rate coding, gain of sensory input, gating communication

between brain regions, encoding prediction errors and allowing neurons to communicate information depending on where they fire during LFP phase [179–181]. The only other study of Area X LFP found increased high-gamma oscillations (80-160 Hz) in sleeping birds and that Area X spikes were phase-locked to the gamma rhythm [184]. Area X's phasic reactivation during sleep could help the AFP consolidate learning in downstream motor nuclei [184]. However, a large knowledge gap remains in terms of characterizing LFP oscillations in Area X, how they are affected by loss of DA and their possible functions in vocal learning. By quantifying LFP responses to auditory input, our Study took an important step towards investigating the functions of oscillatory population activity in the BG during vocal learning.

5.2 Materials and Methods

We performed sham and 6-OHDA lesions in Area X of adult male Bengalese finches, played back auditory stimuli during anesthesia, measured auditory responses of Area X pallidal neurons and quantified LFP beta band power in 6-OHDA versus sham hemispheres. All subjects were adult (>100-d-old) male Bengalese finches (*Lonchura striata var. domestica*). All procedures were approved by Emory University's Institutional Animal Care and Use Committee.

6-OHDA lesions. We performed sham and 6-OHDA lesions in Area X using the same surgical procedure described in Section 4.3. One bird received only a sham lesion in one hemisphere. This bird was included in group data (all sham vs. all 6-OHDA hemispheres). The other birds received 6-OHDA lesions of Area X in one hemisphere (8 mg freebase 6-OHDA / ml and 2 mg ascorbic acid / ml as stabilizer in 0.9% NaCl solution) and sham lesions in the other hemisphere (2 mg ascorbic acid / ml in 0.9% NaCl solution). Injection coordinates for all birds were the same as for Bird 3, left hemisphere in **Table 1**. We alternated the 6-OHDA-lesioned hemisphere between birds.

Playback stimuli. We collected several examples of each bird's own song (BOS) < 15 days before 6-OHDA lesions. We selected a 3-6 second song segment as the BOS playback stimulus to

assess how 6-OHDA lesions affected Area X neural responses, particularly the BOS-selective increase in firing rate [174,177]. As a control we also created reversed BOS (REV) which maintains all acoustic features but does not evoke the same firing rate changes [174,177]. Another stimulus was 3 or 6 seconds of silence (SIL) to control for purely auditory responses. Note that any baseline data used for normalization consists of 4-6 second silent pauses between stimuli, not the SIL stimulus. To suppress acoustical transients, we silenced gaps between syllables and added a 10 ms linear ramp to the sound waveform before syllable onsets and after syllable offsets. Onsets and offsets were determined by setting an amplitude threshold.

We created three additional stimuli in MATLAB: BOS shifted up or down one semitone with a phase vocoder [261] (BOSup / BOSdown) and BOS with several syllables interrupted by 50-ms WN blasts (BOSwn). These mimicked the bird's auditory experience during pitch shift [7,208] and WN experiments [232]. Although we did not analyze responses to these stimuli in this chapter, this is a possible future direction of research (see Section 6.4).

We saved 40 trials of each stimulus in a .wav file. We presented the stimuli in 40 blocks. Each block presented each stimulus once (BOS, BOSup, BOSdown, BOSwn, REV and SIL) but in a random order. Stimuli were separated by 4-6 second silent pauses.

Prior to surgery we calibrated stimulus amplitude to a range of 75-85 dB SPL, which corresponds to the high end of what birds hear during song [262]. We first recorded a pure tone at a known volume (94 dB) using a miniature microphone inserted into a calibrated speaker (Cal73 by BK Precision). Then we placed the microphone at the future location of the bird's head on the stereotax and recorded all six stimuli. As described previously [262] we computed dB SPL using the RMS voltage of the 94 dB tone and average RMS of several representative syllables. Once amplitude was calibrated we used the same speaker volume settings during surgery.

Acute electrophysiology. Intrastriatal 6-OHDA injections cause progressive loss of DA innervation over several days [263,264], so we performed acute electrophysiology experiments 7-11 days after lesions. At the start of the procedure birds were anesthetized with a single intraperitoneal

injection of 5 µL of 20% urethane / g body weight. Although playbacks began several hours after injection, no booster shots were necessary to maintain anesthesia. After injection, we placed birds in the stereotax and fixed the anterior part of their skulls to a metal post with cyanoacrylate and dental cement.

We recorded neural firing and LFP with a linear array of 16 electrodes, with 21.7 µm separation between electrodes (Neuronexus A1x16-5mm-25-177-A16). Birds were headfixed in a stereotax at a 20° beak angle relative to the table surface. Optimal targeting coordinates for Area X were 5.3-5.7 mm anterior and 1.55 mm lateral of Y_0 and 2.8-3.0 mm ventral of the brain surface. This is near the center of the 6-OHDA injection grid. AP coordinates were difficult to optimize, as AP 5.5 mm resulted in electrodes being in center, anterior or posterior Area X depending on the bird. We connected electrodes to an Intan RHD2000 evaluation board with an Omnetics 1315 connector and Intan RHD2132 amplifier board. We used a sampling rate of 20 kHz, bandpass filter of 1-10,000 Hz and subtracted 1 Hz DC offset. Power-line noise and its harmonics (60, 120, 180 Hz) were removed in postprocessing. Although arrays can be cleaned by soaking in contact lens solution, we found neural spikes were better isolated when we used a new array for each surgery.

Once we identified a well-isolated single unit at an appropriate depth, we began a playback recording using Logitech S-120 speakers placed in front of the bird's head (30-45 min for 40 trials). During recordings, we removed ear bars to prevent muffling and isolated the bird in a sound-attenuating chamber. To synchronize playbacks with neural activity, we also recorded audio on two Intan analog input channels. One channel received input from a miniature microphone inside the chamber, while the backup received a direct copy of the signal going to the speakers. We alternated electrode penetrations between left and right hemisphere Area X and obtained 5-8 playback recordings per bird.

After all playbacks were completed, we made small electrolytic lesions (EL) (20 or 40 µA for 20 secs, A-M Systems 2100 pulse stimulator) in each hemisphere, running current through one or two electrodes for histological verification of electrode position. We found the 20 µA current

produced smaller lesions which were better suited for reconstructing electrode positions. We made lesions in pairs along the penetration track of a playback, with one lesion 2-3 mm dorsal of the other. Immediately after surgery birds were perfused and we placed their brains in 3.7% formaldehyde overnight. After sinking brains in 30% sucrose, we performed TH or Nissl stains on alternating 40 µm parasagittal sections as described in Section 4.3.

Histological verification of electrode position. To confirm the array was in Area X during recordings, we acquired images of each section on a slide scanner (Meyer Instruments PathScan Enabler IV). The boundaries of Area X were clearly visible in most sections. For each bird, we computed how much tissue shrank during processing by measuring the distance between the center of the dorsal and ventral ELs. For example, if one lesion was 2.0 mm dorsal of the other *in vivo*, but the measured distance was 1.6 mm in the images of the sections, the tissue shrank by a factor of 1.25. Importantly, TH-stained tissue shrank slightly more than Nissl-stained tissue (average shrink factors were 1.26 and 1.19, respectively). Because the exact center of ELs is somewhat subjective, we performed an additional confirmation step to verify shrink factors were correct. We measured the ratio of the distance between anatomical landmarks in several adjacent TH and Nissl sections. We confirmed the ratio [TH distance between landmarks / Nissl distance between same landmarks] was nearly equal to the ratio [TH distance between ELs / Nissl distance between ELs] from which shrink factor was derived. Because the brain gets slightly larger or smaller across sections we averaged this ratio across the medial and lateral adjacent sections.

Next, in PowerPoint, we overlaid lines on one section to determine the likely location and angle of the 16-electrode array during each recording, as shown in **Fig. 5.1.** This required precise manual alignment to the visible penetration track and ELs, followed by using the known lesion & recording coordinates and tissue shrink factor to draw the array at specific dorsal/ventral (up/down penetration track) and anterior/posterior (right angles to penetration track) distances relative to the ELs. When ELs or penetration tracks were not clearly visible on a single section, we overlaid two sections at the same angle. During surgeries, we attempted to keep all playbacks and the ELs at the

same ML coordinate (1.55) so their locations would be in the same two or three histological sections. We performed the same procedure on 2-4 adjacent sections and only included data for analysis when we were certain the electrodes were well within Area X in examined sections.

6-OHDA lesion size and location. After obtaining electrode position as described above, we confirmed that the electrodes were located within a region of lighter TH stain, which indicated we were recording from 6-OHDA-lesioned locations in Area X.

Artifact removal: Some recordings had artifacts due to the bird briefly shaking its body, which happens occasionally even in deeply anesthetized songbirds. These artifacts occurred infrequently (e.g. only during one or two minutes of a 40-minute recording) and lasted about a second per artifact. Time intervals containing artifacts were marked as ineligible for analysis for both spike and LFP data using MATLAB.

Spike sorting. We preprocessed raw waveforms by subtracting the mean amplitude from each channel to eliminate DC offset, followed by subtracting the common median across channels [265] and bandpass filtering (300 – 10,000 Hz, 3rd-order Butterworth). We spike sorted units with KlustaKwik in "Masked Expectation Maximization" clustering mode [266,267] using a spike detection threshold of 4-6 robust standard deviations above noise. The SpikeDetekt portion of the KlustaKwik suite calculated robust s.d.s as median(absolute-value voltage of several randomly chosen 1-second data chunks)/0.6745 to reduce contamination by spikes [266]. After initial spike sorting we merged, split or discarded KlustaKwik's clusters with the help of KlustaViewa [266] and detailed notes taken during surgery. Next, we used custom-written MATLAB code to decide which units to keep for analysis. We discarded any units which had >0.25% interspike intervals <1 ms (minimum refractory period), units whose peak amplitude distributions were close to the spike detection threshold and units whose firing rate was extremely unstable (indicating sudden changes in spike isolation such as the brain shifting). Some units had high peak amplitudes during a specific time interval but lost isolation gradually; we kept only trials from the well-isolated time intervals.

Finally, for each unit we plotted several minutes of data overlaid with the KlustaKwik spike times to confirm qualitatively that spikes were almost always assigned to the correct unit.

Neural spiking analysis. After spike sorting, we defined units with average firing rate >25 spikes/sec as "pallidal" and the other units as "non-pallidal", as done previously for urethane-anesthetized birds [127]. Pallidal units can be subdivided into GPe-like and GPi-like categories by examining bursting properties [144] but both types can increase firing rate selectively for BOS [174,176,177]. Since the purpose of this analysis was to broadly examine BOS selectivity in sham- versus 6-OHDA-lesioned Area X, examining differences between pallidal subtypes was left for future work. Non-pallidal units are probably striatal interneurons, since striatal MSNs are only known to fire during song [142,143]. Because we obtained a low number of interneurons (n=5) they are not analyzed here. The final analysis used n=14 Area X pallidal units (**Table 3)**. Average spontaneous firing rate across pallidal units was 67.4 spikes/sec (range 27.0 – 104.6 spikes/sec), which is similar to pallidal firing rates reported previously in urethane-anesthetized Bengalese finches [172]. That study reported 89.2 and 48.1 spikes/sec for "fast" and "moderate" firing pallidal units, which averages to 68.7 spikes/sec if we assume equal representation.

For each unit, the response to an individual 3-6 second stimulus trial was computed as follows. First, firing rate during the stimulus was computed as [# spikes throughout stimulus / stimulus duration]. This firing rate was normalized in two ways, either as 1) z-score relative to the mean & s.d. of baseline firing rates across all the 4-6 silent pauses between stimuli for that unit, or as 2) firing rate change, in spikes/sec, relative to the 4-6 second pause immediately preceding that stimulus trial. Method 2 is described as "response strength" (RS) in prior Area X studies [173,175]. Responses were averaged across trials to obtain each unit's mean response, which then contributed one datapoint to the group data. For example, for the dark gray bar of **Figure 5.3b**, the mean ±s.e.m. was computed across ten datapoints, one for each pallidal unit in the sham-lesioned hemispheres. The error bars in the rest of **Fig. 5.3** were computed similarly (not including the colored rectangles, which indicate mean ±s.e.m. across trials for each individual unit).

To subtract REV responses from BOS responses in **Figures 5.3b,d**, we first normalized responses for each individual stimulus trial using one of the two methods described above. We subtracted each normalized REV trial from the nearest normalized BOS trial. We discarded any cases where a BOS trial did not have an eligible matching REV trial or vice versa, such as if there was a movement artifact. This resulted in a vector of normalized response differences for each unit ($BOS_{trial\ 1} - REV_{trial\ 1}$, $BOS_{trial\ 2} - REV_{trial\ 2}$, ...). These were averaged across trials to obtain each unit's mean response difference, which then contributed one datapoint to the group data.

Alignment to playback stimuli. Data was aligned automatically to playback stimuli by finding peaks in the cross-correlation between smoothed and rectified stimulus waveforms and audio recorded during surgery. Occasionally, the playback program (VLC Media Player) briefly speeded up or slowed down, but this was easily detectable and those trials were deleted. Due to slight differences in computer clock timing between Intan hardware and the playback computer, playbacks became misaligned by a few ms towards the end of the 30-45-minute recording. Thus, it was also necessary to introduce a constant correction factor. Alignments were verified manually for each individual trial by overlaying the stimulus waveform with the aligned surgery audio and confirming visually that the smoothed waveform amplitudes matched precisely in time.

LFP analysis. We chose an arbitrary channel from each recording site and preprocessed raw waveforms by subtracting the mean amplitude from each channel to eliminate DC offset, followed by lowpass filtering (3^{rd}-order Butterworth, 300 Hz cutoff). We removed 60 Hz power line noise and its harmonics (120, 180 and 240 Hz) by passing data through 8^{th}-order Butterworth bandstop filters (filtering out 59-61 Hz, 119-121 Hz, etc.). All filtering was done in forward-reverse mode using MATLAB's filtfilt function. **Fig. 5.4a** shows example 1-second LFPs after these preprocessing steps.

After preprocessing we computed LFP spectra with the multitaper method using Chronux version 2.12 [268,269]. For each 3-6 second trial, we computed several power spectra with ±1 Hz bandwidth (W) in non-overlapping 1-second time windows (T), choosing 2*TW – 1 = one taper

[268]. Those spectra were averaged to obtain a single mean spectrum across the trial. The LFP power spectrum for an individual BOS trial therefore measured oscillations occurring throughout the BOS stimulus, not necessarily during any specific syllables. Each trial's spectrum was then normalized to percent of total power within a 4-300 Hz band. We did not normalize to total power below 4 Hz because the chosen frequency resolution of ±1 Hz is not optimal for measuring power at the lowest frequencies. This normalization corrects for varying total power between recording locations and permits us to observe proportion of power dedicated to the beta band for each stimulus. In some cases, (see figure captions) we additionally normalized the spectra from each trial by subtracting the spectrum during the 4-6 second silent pause immediately preceding the trial. The spectra during those pauses were computed in the same way, including conversion to percent of total power prior to subtraction.

After normalization, we obtained one mean power spectrum for each stimulus per hemisphere (**Table 3**) by averaging spectra across all recorded trials of the stimulus in that hemisphere (not including trials deleted due to artifacts etc.). These were used to compute group averages across hemispheres. Although individual hemispheres could include 1-4 recording locations and up to 40 trials of each stimulus per location, each hemisphere contributed one datapoint to the group data. This means the mean ±s.e.m. error bars and shaded areas in **Fig. 5.4b,c** and **Fig. 5.5** were computed using each hemisphere's mean power spectrum as one datapoint. For example, in **Fig. 5.4b**, since there were four 6-OHDA hemispheres (**Table 3**), we obtained four mean power spectra as described above (one per hemisphere), then computed the mean ±s.e.m. across those four spectra at each frequency, thus generating the red shaded areas.

For each trial, we obtained a single number indicating power in the beta frequency band ("beta power") by summing the normalized power (percent of total power; see above) at each frequency from 13-30 Hz. We averaged across trials to obtain one datapoint per hemisphere for the group data. In some cases, (see figure captions) we additionally normalized the beta power for each

trial by subtracting the beta power during the 4-6 second silent pause immediately preceding the trial.

To confirm that LFP beta band power was not an artifact of amplifier noise, we computed several example spectra from in-brain recordings and compared them to the power spectra obtained by inserting the same electrodes in a 0.9% NaCl solution shorted to the Intan board's ground. Total un-normalized beta band power was typically ~5-20x higher for in-brain recordings compared to in-saline recordings. This indicates our birds' beta band power was comfortably higher than the noise floor.

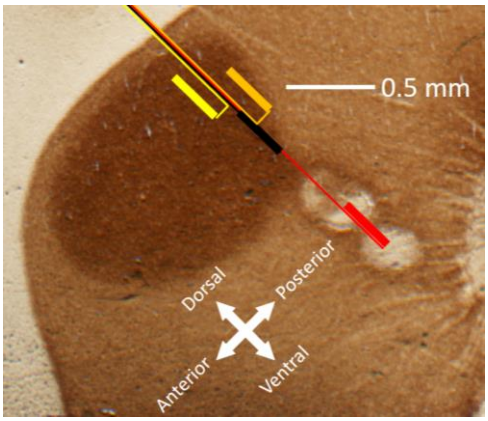

Figure 5.1. Histological verification of electrode placement in a sham-lesioned section stained for TH. Dark brown oval stain, Area X. Light brown stain, non-X striatum. Thin red line, electrode penetration track during the EL. We obtained penetration angle by manually aligning to the ELs and any visible indication of the penetration track. Thick red line, 16-channel electrode array location during the ventral EL, indicated by the two lighter-colored circles (dorsal EL not shown). Since EL current passed simultaneously through the dorsal and ventral electrodes, we centered the array in the middle. Thick black, orange, yellow lines, Approximate electrode array location during three playback recordings, relative to its location during the EL. black is 0.8 mm dorsal and 0.0 mm anterior of the ventral EL, orange is 1.0 mm dorsal and 0.1 mm posterior and yellow is 1.2 mm dorsal and 0.1 mm anterior. All are within Area X, but orange and ventral half of black are close to the border. Thus, these electrodes would be discarded from analysis. In contrast, yellow is well within Area X with room to spare in case of small measurement errors. All line lengths, including the 325-μM electrode array, were computed by converting the in vivo stereotax coordinates to distances on the images using the empirically obtained shrink factor for this bird's TH stained sections.

Table 3. Acute electrophysiology dataset size.			
Total number of birds	**Experimental condition**	**Number of pallidal units for spiking analysis**	**Number of hemispheres for LFP analysis**
5 birds	Sham-lesioned Area X	10 units (across 4 birds; one bird had 5 units)	5 hemispheres
	6-OHDA-lesioned Area X	4 units (across 3 birds)	4 hemispheres (one hemisphere rejected; failed 6-OHDA lesion)

5.3 Results

We analyzed spontaneous and playback-evoked MFR and LFP beta power in sham- and 6-OHDA-lesioned Area X. We found no significant BOS-selectivity in pallidal neurons or BOS-selective LFP beta power. We found no significant differences in spontaneous or playback-evoked activity between sham- and 6-OHDA-lesioned hemispheres. However, we observed trends towards increased pallidal firing and LFP beta power during BOS. Additionally, while there was a trend towards increased MFR/beta for BOS compared to REV, the 6-OHDA-lesioned hemispheres had nearly equal responsivity to BOS and REV (except for MFR z-scores; **Fig. 5.3a**). Thus, although these trends should be interpreted with caution, we observed weak BOS-selectivity in both sham- and 6-OHDA-lesioned Area X and nonspecific auditory responses in 6-OHDA-lesioned hemispheres. Furthermore, we found no increase in LFP beta power as occurs in mammalian models of pathological DA depletion [185–189] (but see Section 5.4, Discussion, for possible effects of anesthesia), nor evidence of large power modulations in any frequency band.

Pallidal firing rates during song playbacks in sham- and 6-OHDA-lesioned Area X

Area X pallidal units (**Table 3**) tended to increase firing rate slightly in response to auditory stimuli in both sham- and 6-OHDA-lesioned hemispheres. This is shown by two representative pallidal units (**Fig. 5.2**). **Fig. 5.2a,b** show one neuron from a sham-lesioned hemisphere, but the key difference is that **Fig. 5.2a** displays its response to BOS and **Fig. 5.2b** displays its response to REV.

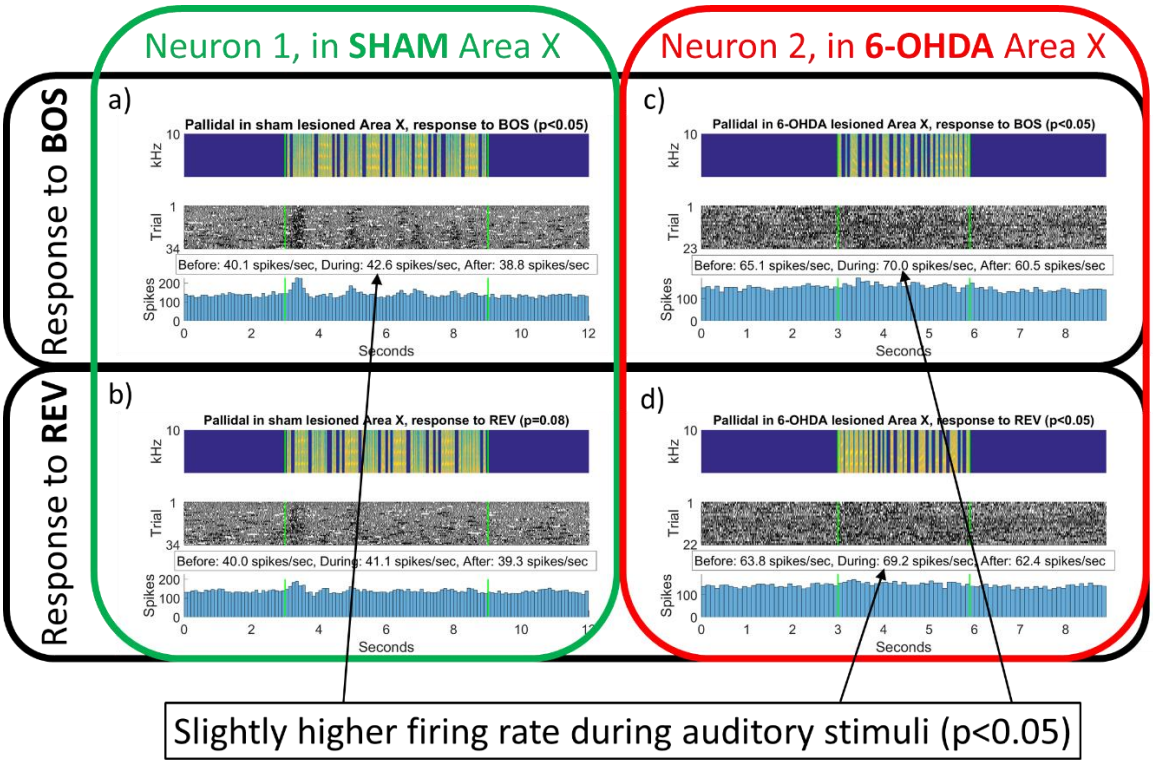

Figure 5.2. Example Area X pallidal units showing slightly higher firing rates during playback stimuli in both sham- and 6-OHDA-lesioned Area X. **(A)**, Response to BOS for a pallidal unit in a sham-lesioned hemisphere. **Top,** BOS playback spectrogram, with stimulus onset and offset marked by green lines. **Middle**, raster indicating spiking activity during 34 trials. **Bottom**, spike histogram obtained from the raster plot with 0.1 second bins. **Text box above histogram,** mean firing rate was 40.1 spikes/sec before the BOS stimulus, increased to 42.6 spikes/sec during BOS and decreased to 38.8 spikes/sec after BOS. The small firing rate increase was caused by brief rate modulations throughout the stimulus, especially at the start. **(B)**, Response to REV for the same pallidal unit shown in **A**. Firing rate increased slightly but not as much as for BOS. Firing rate increase was not significant (p=0.08). Firing rate modulations were attenuated compared to BOS. **(C)**, Response to BOS for a pallidal unit in a 6-OHDA-lesioned hemisphere showing 4.9 spikes/sec firing rate increase compared to the pre-stimulus interval. **(D)**, Response to REV for the same pallidal unit shown in **C**, showing 5.4 spikes/sec firing rate increase compared to the pre-stimulus interval. The 6-OHDA lesion did not destroy auditory responsiveness for this unit. The remaining 12 pallidal units had 12-40 eligible BOS or REV trials. **p-values in figure titles**, two-tailed paired t-tests on firing rate during stimulus versus firing rate during 3 seconds of silence preceding stimulus.

Likewise, **Fig. 5.2c,d** show a second neuron's response to BOS and REV, except this neuron was in a 6-OHDA-lesioned hemisphere. However, not all units had significantly increased firing rates in response to acoustic stimuli. In sham-lesioned Area X, 5 of 10 units increased firing rate significantly for BOS and 2 units increased firing rate for REV, compared to 3 seconds of silence immediately preceding the stimuli ($p<0.05$, paired two tailed t test; significance level not corrected for multiple comparisons). One sham pallidal unit significantly lowered firing rate by 1.7 spikes/sec

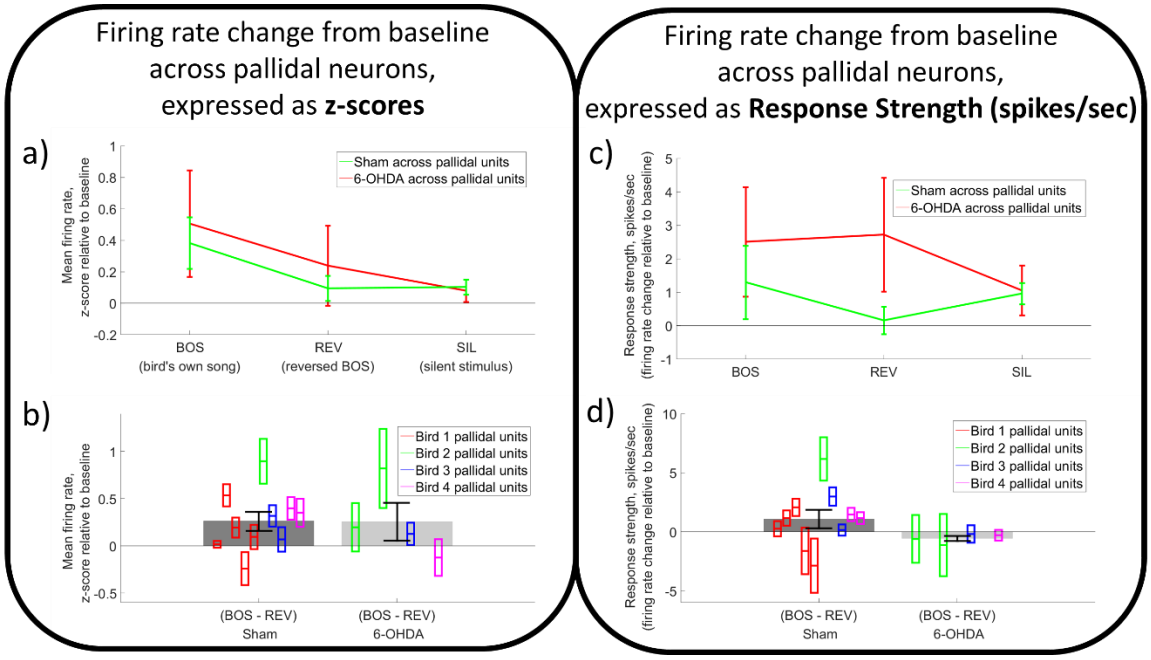

Figure 5.3. Responses to playback stimuli for Area X pallidal units do not differ between sham- and 6-OHDA-lesioned Area X. **(A)**, Mean ±s.e.m. firing rate changes during stimulus BOS and control stimuli REV and SIL across pallidal units, plotted as z-scores relative to mean and s.d. of firing rates during baseline (the 4-6 second silent pauses between stimuli). There was no significant difference between sham and 6-OHDA responses for any stimulus ($p>0.0167$, two-tailed Welch's t test with Bonferroni correction for multiple comparisons). **(B)**, Gray bars, mean ±s.e.m. difference between normalized BOS and REV responses across pallidal units. This can be interpreted as the degree of BOS selectivity compared to a control stimulus (REV) with the same spectral features. Colored rectangles, mean ±s.e.m. response difference for individual units from different birds. All responses were converted to z-scores before subtracting (see Section 5.2, Materials and Methods). Units in sham and 6-OHDA hemispheres did not differ in their BOS selectivity ($p>0.05$, two-tailed Welch's t test). **(C)**, Same as **A**, including lack of significance, except firing rate changes are plotted in spikes/sec relative to silent pauses immediately preceding stimulus trials (RS; see Section 5.2, Materials and Methods). **(D)**, same as **B**, including lack of significance, except firing rates were converted to RS before subtracting.

during REV (-1.6% relative to baseline). In 6-OHDA-lesioned Area X, 2 of 4 units increased firing rates significantly for BOS and REV.

Prior studies showed pallidal units tend to increase firing rate more for BOS than for REV [174,176]. This trend occurred in our data, but was only significant for 3 of 10 units in sham-lesioned hemispheres and 0 of 4 units in 6-OHDA-lesioned hemispheres ($p<0.05$, two tailed t test on firing rate changes for BOS vs. firing rate changes for REV; significance level not corrected for multiple comparisons). The two units shown in **Fig. 5.2** did not have significantly different responses to

BOS compared to REV, although the unit in **Fig. 5.2a,b** approached significance (p=0.08). Thus, in sham-lesioned but not 6-OHDA-lesioned hemispheres there was a weak trend towards a larger increase in firing during BOS and a smaller increase during REV.

Interestingly, the unit in **Fig. 5.2a,b** modulated its firing rate throughout the BOS stimulus, and this modulation was attenuated during REV. Firing rates remained relatively steady during silent intervals before and after the stimulus. Similar modulation patterns have been seen before in Bengalese and zebra finch pallidal neurons during BOS and REV playbacks [176,177]. In my data, only one other pallidal unit (in a sham-lesioned hemisphere) had a visible pattern of firing rate modulations during BOS stimuli. However, the prior studies discarded units that did not have a significant firing rate change in response to BOS and did not report what percent were discarded [176,177].

When averaging across pallidal units using z-scores or RS (see Section 5.2, Materials and Methods), the mean firing rate tended to increase for BOS stimuli in both sham- and 6-OHDA-lesioned hemispheres (**Fig. 5.3a,c**). However, none of the changes from baseline seen in **Fig. 5.3a,c** was significant (smallest p=0.015 across t tests, which was not significant after a Bonferroni correction for multiple comparisons). In both **Fig. 5.3a** and **Fig. 5.3c** there was no significant difference among responses to BOS, REV and SIL ($p>0.05$ for effect of playback stimulus, two-way ANOVAs). Since several prior studies reported Area X auditory responses (see below), this lack of significance is likely caused by having a small number of pallidal units (n=10 and n=4 for sham and 6-OHDA hemispheres, respectively) and a small effect size, leading to low statistical power to detect an effect. Nevertheless, our sham data trended in the expected direction of firing rate increase for BOS and less of an increase for REV. We caution, however, that there appeared to be a "response" to the SIL stimulus, which was merely 3-6 seconds of silence. The low average RS (0.1-2.7 spikes/sec) compared to the high spontaneous firing rates (average 67.4 spikes/sec) further indicate that BOS and REV responses were relatively weak.

The average pallidal responses in this Study were weaker than those reported previously in urethane-anesthetized adult zebra finches. One set of studies found Area X neurons increased firing by approximately 6.5 and 2 spikes/sec for BOS and REV, respectively [174,175,270]. Unfortunately, they combined pallidal and non-pallidal units, excluded units that did not have statistically significant responsiveness and did not state what percent of units were discarded. Two more studies reported an average pallidal RS to BOS of 9.3 and 8.4 spikes/sec, with weaker responses to REV (one study stated 3.4 spikes/sec) [127,176]. However, they also excluded non-responsive units and did not report what percent were discarded. Since our Study did not exclude units it is not surprising that our average responses were weaker. We matched our data to the previous studies by computing RS across only those pallidal units that had a statistically significant response (n=7 and n=5 units across all hemispheres responded to BOS and REV, respectively, as described at beginning of this subsection). Their mean ± s.e.m. RS to BOS and REV was 3.83 ± 1.00 and 2.78 ± 1.32 spikes/sec, respectively. When we considered only significantly-responding pallidal units in sham-lesioned hemispheres (n=5 and n=3 units responded to BOS and REV, respectively), their mean ± s.e.m. RS to BOS and REV was 3.56 ± 1.43 and 1.03 ± 1.40 spikes/sec, respectively. Thus, when we discarded non-significant units, we found greater RS to BOS and REV but the units still did not respond as strongly as in previous studies.

We directly compared BOS and REV responses by subtracting REV trials from the nearest BOS trial after normalizing responses to z-scores or RS (**Fig. 5.3b,d**). In sham- and 6-OHDA-lesioned hemispheres BOS responses tended to be larger than REV responses (except for RS in 6-OHDA-lesioned hemispheres; **Fig. 5.3d**). However, neither of the two (BOS – REV) comparisons were significant after Bonferroni correction (largest p=0.03, t tests), likely due to the small effect size and low number of units. This corroborates the findings from **Fig. 5.3a,c** that BOS generally leads to slightly higher (but not significant) pallidal firing rates than REV.

We found no significant response differences between sham and 6-OHDA hemispheres. In both **Fig. 5.3a** and **Fig. 5.3c** the sham and 6-OHDA responses were not significantly different from

each other ($p>0.05$ for effect of lesion condition, two-way ANOVAs). Likewise, there was no significant difference between $(BOS - REV)_{sham}$ and $(BOS - REV)_{6\text{-}OHDA}$ for z-scores (**Fig. 5.3b**) or RS (**Fig. 5.3d**) ($p>0.025$, t tests with Bonferroni correction). Although 6-OHDA units appeared to respond equally to BOS and REV for RS (**Fig. 5.3d**), this was not evident for z-scores (**Fig. 5.3b**) and did not significantly differ from the sham hemisphere, as we stated. Although it is clear there were no large response differences, the lack of significance is likely partially caused by the low number of 6-OHDA units (n=4).

To summarize, we found trends towards pallidal firing rate increases during BOS and less of an increase for REV, as described in several prior studies. However, these trends were not significant. We found no significant differences between sham and 6-OHDA responses to playbacks.

Spontaneous and playback-evoked LFP beta power in sham- and 6-OHDA-lesioned Area X

In contrast to sleeping birds that had high-gamma oscillations (80-160 Hz) [184], urethane-anesthetized Area X did not oscillate strongly at any particular frequency in sham- or 6-OHDA-lesioned hemispheres. To observe spontaneous LFP spectra we measured the normalized power (percent of total power) during the silent SIL stimulus (**Fig. 5.4b,c**). Across the 4-300 Hz frequency range we saw no power modulations that departed from the 1/f scaling rule [182] (**Fig. 5.4b**). Since there were no strong oscillations it was somewhat arbitrary to divide LFP spectra into frequency bands including alpha, beta and gamma (**Fig. 5.4b**). However, to compare with oscillatory bands in mammals we chose to divide spectra into frequency ranges that roughly correspond to these bands [257,258]. We caution the reader to be aware of this caveat whenever we refer to the "beta band" in our data.

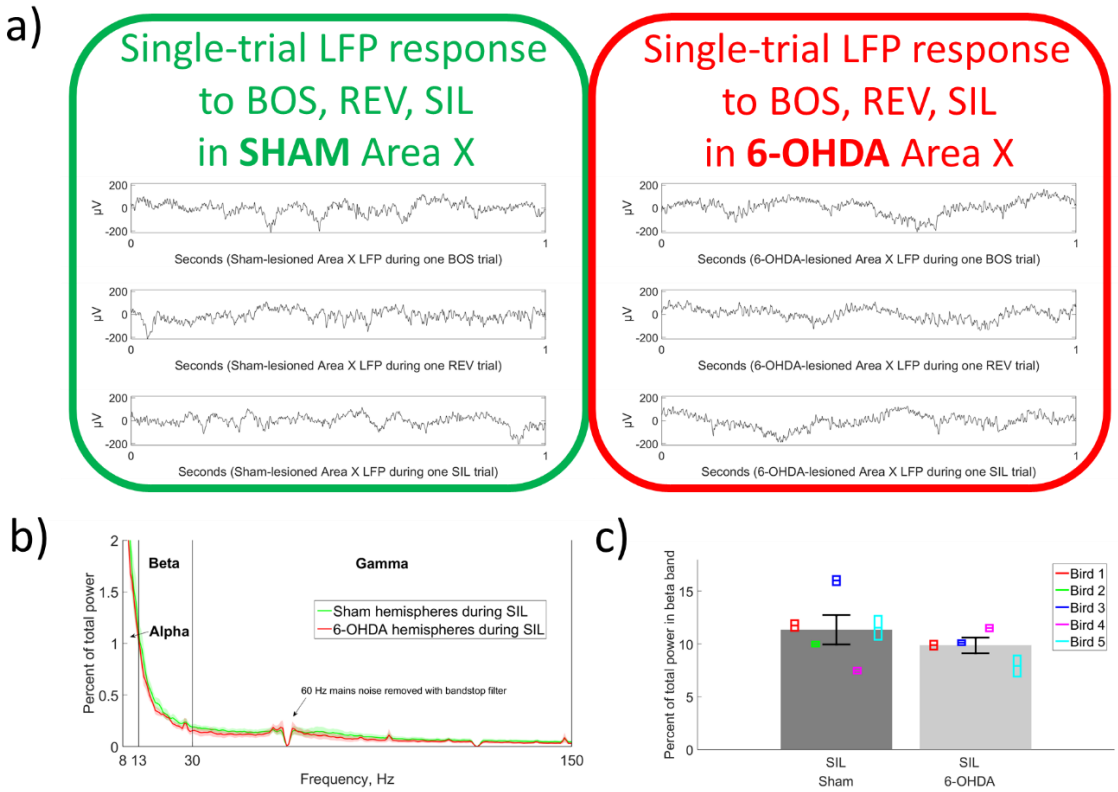

Figure 5.4. Spontaneous LFP beta power does not differ between sham- and 6-OHDA-lesioned Area X. **(A)**, Example single-trial LFPs from one bird, during the first second of the BOS, REV and SIL stimuli in sham- and 6-OHDA-lesioned Area X. Raw voltages were preprocessed as described in Section 5.2 (mean-subtraction, 300 Hz lowpass filtering and removal of 60 Hz power line noise and its harmonics). As in other birds (not shown), there are no immediately obvious differences in LFP oscillations among stimuli or between sham- and 6-OHDA-lesioned hemispheres. **(B)**, Mean ±s.e.m. spectral power in the alpha, beta and gamma bands during the silent SIL stimulus (i.e. spontaneous LFP), normalized as percent of total power across 4-300 Hz. Each hemisphere contributes one spectrum to the average. LFP power magnitude is inversely related to frequency f, obeying the classic 1/f scaling rule [182]. **(C)**, Gray bars, mean ±s.e.m. beta power (see Section 5.2, Materials and Methods) across sham- and 6-OHDA-lesioned hemispheres during the SIL stimulus. Colored rectangles, mean ±s.e.m. beta power for individual hemispheres across trials. Total proportion of beta power does not differ significantly between sham- and 6-OHDA-lesioned hemispheres ($p>0.05$, t test).

Spontaneous LFP spectra in sham- and 6-OHDA-lesioned hemispheres were nearly indistinguishable across the alpha, beta and gamma bands (**Fig. 5.4b**). Importantly, proportional beta power did not differ between sham- and 6-OHDA-lesioned hemispheres (**Fig. 5.4c**), in marked contrast to the strong beta oscillations seen in mammalian GPe, GPi and striatum after DA depletion [185–189]. These findings were not entirely surprising because 6-OHDA lesions in Bengalese finches only deplete DA by ~50% (see Study 2; Chapter 4), while mammalian models and human PD

patients often have much higher levels of DA loss. Also, beta oscillations in PD correlate with motor performance deficits, specifically bradykinesia and rigidity [189,256] but Bengalese finches do not have gross vocal performance deficits after 6-OHDA lesions (see Study 2; Chapter 4).

Next we investigated how LFP beta power was modulated by the BOS and REV playback stimuli. Analyzing LFP differences between sham and 6-OHDA hemispheres could lead to future hypotheses about LFP functionality in songbirds. For example, the suppression of beta band activity in the BG is thought to represent readiness to perform motor actions [179]. Although a full analysis would require examining multiple bands, we focused on the beta band as a proof of concept. Since there were no differences in spontaneous beta activity (**Fig. 5.4b,c**), we wanted to further explore whether there were any differences during sound playback in beta oscillations between sham- and 6-OHDA-lesioned Area X. Finally, although this falls under the scope of future work it may be notable that many song syllables are roughly the same duration as the periods of beta band oscillations (33-77 ms).

In sham-lesioned hemispheres there was a trend towards higher beta power in response to BOS and a smaller increase in response to REV (**Fig. 5.5**). In the normalized and baseline-subtracted spectra (**Fig. 5.5a,b**) there was generally a positive beta modulation (higher percent of total power in beta band) during BOS and REV except at the highest and lowest beta frequencies. We examined whether this power modulation was BOS-selective by subtracting REV from BOS spectra (see Section 5.2, Materials and Methods). For sham hemispheres, the subtracted spectra (**Fig. 5.5c, green**) generally showed increased power modulation for BOS compared to the control stimulus REV, although this effect was more variable in the lower half of the beta range. These trends were also seen when summing power across the beta band (**Fig. 5.5d-f**), but importantly none were significantly different from baseline ($p>0.008$, t tests with Bonferroni correction for 6 comparisons among **Fig. 5.5d-f**). This may indicate beta power is not modulated during song stimuli and has no relationship with BOS-selective auditory processing in Area X. But the low number of datapoints (n=5 sham hemispheres) likely reduced power to detect small effect sizes.

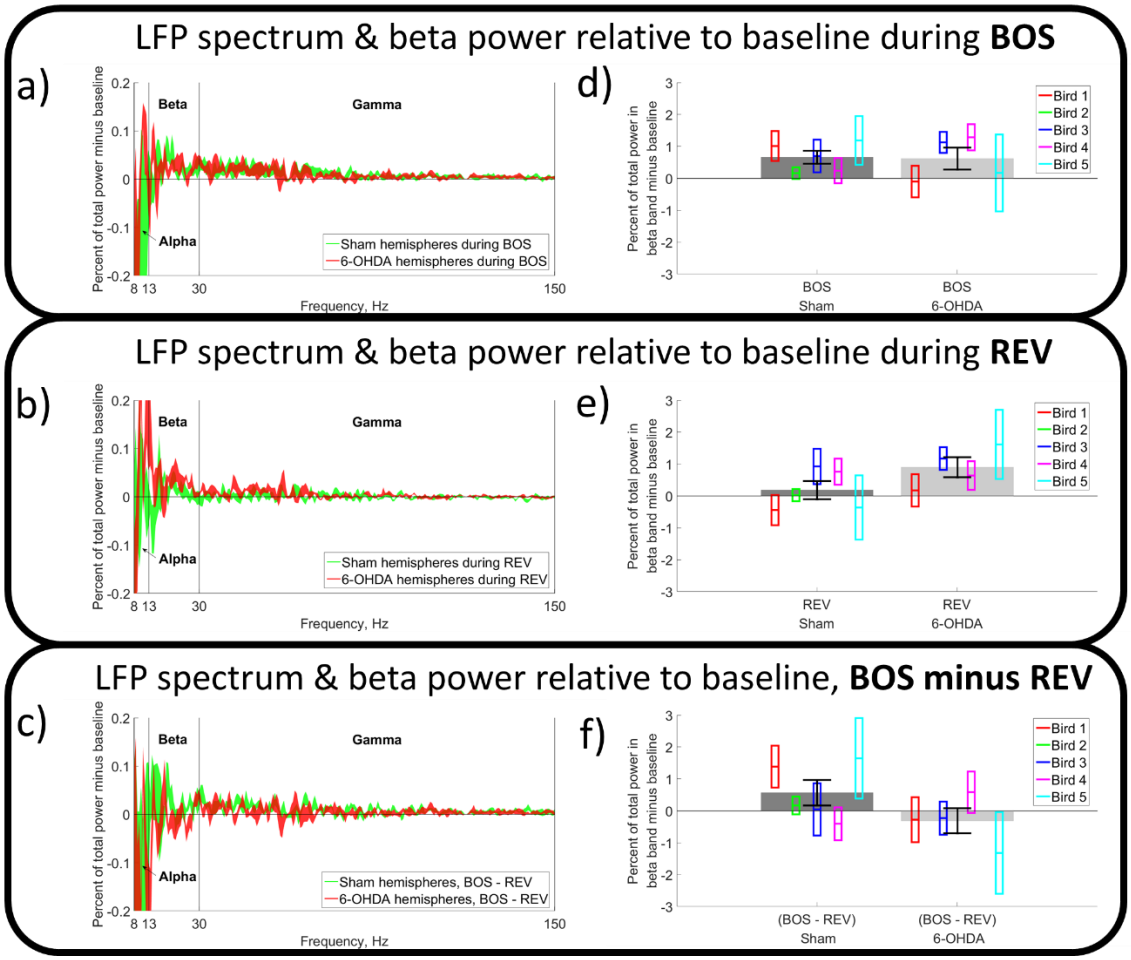

Figure 5.5. There is a trend towards slightly increased beta power during playback stimuli in sham- and 6-OHDA-lesioned Area X. **(A)**, Shaded areas, ±s.e.m. of spectral power in the alpha, beta and gamma bands during the BOS stimulus. Spectra were first normalized as percent of total power across 4-300 Hz, then we subtracted the power during baseline (4-6 second pause preceding each trial; see Section 5.2, Materials and Methods). This should be interpreted as degree of power modulation during BOS. A positive value at frequency f indicates that the proportion of total power dedicated to that frequency increased during BOS compared to pre-trial baseline power and vice versa. The percent of total power dedicated to the beta band tended to increase in both sham- and 6-OHDA-lesioned Area X except at the lowest beta frequencies. **(B)**, same as **A** except measuring power modulation during REV. **(C)**, Same as **A**, except measuring the difference between BOS and REV power modulation. Overall, sham-lesioned Area X tends to have a larger beta increase for BOS than for REV, indicated by positive values at most beta frequencies. In contrast, 6-OHDA-lesioned Area X does not have consistent difference in beta modulation for BOS vs. REV. **(D)**, Gray bars, mean ±s.e.m. baseline-normalized beta power across sham- and 6-OHDA-lesioned hemispheres during the BOS stimulus (see Section 5.2, Materials and Methods). Colored rectangles, mean ±s.e.m. baseline-normalized beta power for individual hemispheres across trials. There is a trend towards increased beta power during BOS for both sham- and 6-OHDA-lesioned hemispheres, but beta modulation did not differ significantly between sham and 6-OHDA conditions ($p>0.05$, t test). **(E)**, same as **D**, including lack of significance, except measuring beta power modulation during REV. **(F)**, Same as **D**, including lack of significance, except measuring the difference between BOS and REV beta power modulation. As in **C**, there is a slight trend towards higher beta power during BOS compared to REV in sham hemispheres.

When comparing sham and 6-OHDA spectra (**Fig. 5.5a-c**), there was no immediately obvious difference between beta band modulations. Likewise, there was no significant difference between sham and 6-OHDA hemispheres when measuring modulations across the entire beta band (**Fig. 5.5d-f**). This indicates that sham- and 6-OHDA-lesioned Area X LFPs do not differ in their BOS-selectivity and indeed may not have any BOS-selectivity, as discussed above. The lack of significance may be partially due to the low number of datapoints (n=5 sham and n=4 6-OHDA hemispheres). There is an interesting trend where the beta power is modulated almost equally for BOS and REV in 6-OHDA-lesioned hemispheres (**Fig. 5.5f**). While not significant, it is reminiscent of the trend in **Fig. 5.3d** where the pallidal RS was similar for BOS and REV in 6-OHDA-lesioned hemispheres. Although additional data is needed, the equivalent BOS and REV responses may indicate BOS-selective auditory processing is impaired in 6-OHDA-lesioned Area X.

To summarize, we found no large LFP power modulations in any frequency band and no difference in spontaneous LFP beta power between sham- and 6-OHDA-lesioned Area X. We found no significant playback-evoked beta band modulations and no significant differences in beta modulation between sham and 6-OHDA hemispheres.

5.4 Discussion

Contrary to our two main predictions (see Section 2.3), pallidal firing rates did not become less responsive to BOS playbacks after 6-OHDA lesions. Nor did we observe any differences in LFP beta power between sham- and 6-OHDA-lesioned Area X. There could be many reasons why we did not observe positive results, including the comparatively small size of our dataset and choice to analyze just two features. For group comparisons, we made each unit (or each hemisphere) one datapoint, perhaps decreasing our statistical power unnecessarily. In future analysis, it would be advisable to use statistical procedures to take advantage of the multiple trials for each unit/hemisphere. However, because this Study was intended as an initial comparison between sham- and 6-OHDA-lesioned conditions it was most important to determine whether there were

large activity changes. Thus, we believe the statistical methods used here are adequate despite some reduction of power. In future work it would be advisable to collect data from several more units and hemispheres regardless of the statistics used. Finally, by restricting our analysis we could have missed important differences in other features of neural activity such as pathological bursting and oscillatory spiking [211,212]. This can be addressed in future work.

Although we used the same anesthetic drug (urethane), BOS-selectivity was not as strong as in prior studies [127,173–177]. This can have several explanations. As described in Section 5.3, prior studies often discarded units that did not have significant auditory selectivity whereas we analyzed all pallidal units. This only partially explains our units' weak responses because when we measured RS after excluding non-significant units the BOS and REV selectivity was still lower than in prior studies. Although studies have found significant BOS responses in Bengalese finches [177] or no difference between Bengalese and zebra finch firing [174] the remaining ones used zebra finches. Thus, a species difference could account for the weaker responses. Some studies calculated a "selectivity index" or a d' metric to measure significant responses [127,175–177,271–274], while we used either z-scores or RS. In future work we could examine responses using those metrics. Finally, all our recordings were made several hours after initial anesthesia induction and the latest occurred roughly 11 hours into the surgery. Although we do not know the exact timescale of the other studies' recordings, this factor may have led to decreased BOS responses. Indeed, one study noted auditory responses were not observed in all birds and found some units were initially responsive but this disappeared later in the recording [174].

The lack of 6-OHDA-related LFP beta oscillations could also be due to the brain state caused by urethane anesthesia. Area X LFPs are likely brain-state-dependent because the strong gamma oscillations observed during sleep [184] were absent in our sham-lesioned hemispheres (**Fig. 5.4b**). Interestingly, 6-OHDA-lesioned and urethane-anesthetized rats had no pathological beta oscillations in cortex, STN or globus pallidus except during global activation states caused by toe pinches (control rats did not increase beta power during activation states) [187,275]. We thought this

might not confound our Study because we used only urethane. Those rats were also given ketamine/xylazine, which blunts neural activity and auditory responsiveness in birds [276]. However, given our results, perhaps our Study did not observe significant beta power increases because the auditory stimuli were too weak to elicit global activation as in the rat studies. Although no prior study has measured songbird LFPs under urethane anesthesia, LFP oscillations are known to occur during other brain states. In singing zebra finches, gamma power (90-150 Hz) increased in the auditory nucleus interfacialis of the nidopallium [277] and 25-35 Hz power increased in HVC [278], which projects to Area X. In auditory forebrain nuclei of isoflurane-anesthetized zebra finches, broadband LFP power (0.1-350 Hz) changed in response to playbacks of contact calls [279]. Future studies could record Area X LFPs after toe pinches, under isoflurane anesthesia and in awake birds to determine if pathological beta oscillations emerge during other brain states.

Besides the issues discussed above, there could be functional reasons why we observed no differences in MFR and beta power between sham- and 6-OHDA-lesioned Area X. The small activity changes parallel the moderate behavioral changes after 6-OHDA lesion, such as decreases in vocal variability [129] and impaired but not eliminated vocal learning (see Study 2; Chapter 4). Furthermore, 6-OHDA lesions only deplete DA by ~50% (see Study 2; Chapter 4), which is much lower than in most mammalian models, and we waited 7-11 days before recording. The degree of DA depletion and short timescale may not be enough to cause emergence of pathological activity even though it is sufficient for learning deficits. Speculatively (and if we assume urethane anesthesia did not account for it), perhaps we did not observe PD-like beta power increases because they are related to motor performance deficits but vocal performance is mostly unaffected in songbirds after 6-OHDA lesions [129]. Future studies could test whether larger degrees of DA depletion, longer timescales and different brain states lead to pathological activity changes.

Although it was not significant, the trend towards nonspecific auditory responses in 6-OHDA-lesioned hemispheres merits further investigation. A prior study also found decreased BOS-selectivity in pallidal neurons when DA levels were manipulated acutely [127]. Speculatively, lack of

BOS-selectivity under anesthesia could indicate synapses related to BOS-specific processing are weakened after 6-OHDA lesion. This could impair learning in awake birds because synaptic plasticity mechanisms are no longer strongly tuned towards BOS and the song template.

To conclude, while this pilot study did not uncover significant neural correlates of DA depletion, it was an important first step towards future studies of Area X, DA and vocal learning.

CHAPTER 6

CONCLUSIONS AND FUTURE DIRECTIONS

6.1 Conclusions

This dissertation found novel rules of generalization in error-corrective vocal learning, showed that intact DA in the BG nucleus Area X is necessary for negative-reinforcement-driven vocal learning and took the first steps towards understanding DA's effects on Area X neural activity. These results have advanced our knowledge of the neural mechanisms of vocal plasticity and will have significant impact on the field of vocal learning as well as motor learning in general.

In Study 1 (Chapter 3) we determined that adaptive error-correction on one vocal gesture generalized across the rest of the vocal repertoire in specific patterns that depended on gestures' category and position in a sequence (see Study 1 Results, Section 3.4). We likely provided the first characterization of how error-corrective learning generalizes across sequences of naturally produced skilled motor behaviors. We have added new information to the motor learning field because it is not well understood how motor learning spreads throughout the complex repertoire of natural movements. We accomplished this by perturbing one vocal gesture during a series of naturally produced vocalizations and observing how compensatory adaptation transferred to other vocalizations in the sequence. Our finding that learning generalized to the same gesture in other contexts paralleled results in humans, where learning to change frequency in one utterance can transfer to others [3,23]. Other findings were novel and surprising, especially that learning generalized anti-adaptively to different syllables and that there was more generalization for syllables produced near to the target syllable within the motif (see Study 1 Results, Section 3.4). Thus, although our original hypothesis was supported (learning transfers to the same gesture produced in other contexts), we also found surprising rules of generalization.

Study 1 (Chapter 3) was one of the first investigations of how adaptive error correction, driven by internal criteria instead of external reinforcement, generalizes across a sequence of vocal gestures. This Study was limited in that we only tested error-corrective pitch learning in songbirds, so we do not know whether error correction on other acoustic features (such as amplitude or timing) have the same generalization rules. Nevertheless, our results (i.e. sequence-dependent and anti-adaptive generalization) are previously unknown features of error-corrective learning during natural movement sequences. They could reflect learning strategies such as maintaining acoustic relationships between different gestures and sharing credit for errors among nearby gestures in a sequence (see **Fig. 3.4**). More studies are needed to investigate whether these rules apply to other motor behaviors (including humans performing natural movement sequences) and to test for more evidence of the proposed learning strategies. Pending further studies, we speculate that these rules could be a characteristic feature of sensorimotor adaptation during naturally produced movement sequences. This would be a much-needed insight on how skilled motor behaviors are learned and adaptively maintained and stimulate new experiments to examine how this generalization is implemented in neural circuits. The findings could also be beneficial for developing new speech therapies, particularly the observation that altering one vocal gesture can lead to specific patterns of changes in other gestures.

In Study 2 (Chapter 4) we determined that DA in Area X is necessary for pitch learning driven by negative reinforcement. This result provided important evidence that DA in the BG is necessary for skilled motor learning in natural behaviors. Furthermore, our work helped establish songbirds as a useful new model of BG DA in complex motor learning because by using songbirds we can avoid several confounds found in other model systems (see Chapter 1). We accomplished this by combining an established WN learning technique [33] with a new method for depleting DAergic innervation in the song system's BG nucleus Area X. We observed reduced vocal learning magnitude in DA-lesioned birds, confirming our hypothesis that DA input to Area X is necessary for learning to change pitch. This provided the first direct evidence that DAergic input to Area X

guides vocal learning, as predicted by a reinforcement learning model where DAergic RPE signals indicate "good" or "bad" syllable pitches, which leads to adaptive plasticity in Area X and downstream motor nuclei [104–106]. We found intact DAergic input to Area X was not necessary for restoring baseline pitch after learning, even though Area X itself is necessary for this process [158]. This suggests DA might play different roles in distinct forms of vocal plasticity. While there is no directly comparable study in humans, PD patients showed altered error correction (reduced or increased compensation) for pitch/formant perturbations [83,84,280,281], suggesting a DA role in human vocal learning as well.

Study 2 (Chapter 4) opened the door to future investigations of DA's role in error-corrective adaptation and generalization in vocal and non-vocal motor behaviors. Although we did not test whether DA is necessary for error-corrective adaptation or generalization, the results are an important demonstration of DA's importance for vocal learning, and they provided insight on its role in other types of motor learning as well. There is a substantial body of literature on DA in reward/punishment learning [74–76], particularly mesolimbic DA signaling during Pavlovian or operant conditioning, such as learning to press one of two levers to receive a reward. However, much less work has been done on its role in altering the performance of skilled motor behaviors, such as learning to walk on a spinning rotarod or learning to make precise forelimb reaching movements to obtain food pellets [95,99]. Study 2 results (Section 4.4) supported the idea that the BG uses reward/punishment signals to tutor downstream motor circuits [151] because of Area X's many similarities to mammalian BG [138] (see also Section 1.4).

In Study 3 (Chapter 5) we performed a pilot analysis and found no DA-dependent features of Area X neural activity, suggesting that partial DA depletion may not cause gross changes to neural activity despite leading to learning deficits (see Study 2, Chapter 4). Although our results have less impact than the other two Studies, it was important to perform an initial exploration of the neural mechanisms underlying DA-dependent vocal learning by searching for DA-dependent neural activity in Area X. We achieved this via acute electrophysiology recordings in 6-OHDA-

lesioned Area X in anesthetized birds and extracting spontaneous and playback-evoked spiking and LFP. We analyzed two features of neural activity: mean firing rates of pallidal neurons and LFP beta power. Contrary to our predictions (see Section 2.3) we found no significant differences between sham- and 6-OHDA-lesioned Area X for playback-evoked pallidal firing rates or LFP beta power. Although mammalian BG nuclei have increased beta oscillations after DA depletion [185–190] there was no increase in beta power in 6-OHDA-lesioned hemispheres, perhaps due to the urethane-induced brain state. We partially replicated prior studies showing BOS-selective pallidal firing rate increases [174,176] although they were not significant across units. Our lack of significant results may be partially due to a low number of units and hemispheres, small effect size, restricting analysis to two features and recording in anesthetized (non-singing) birds. Nevertheless, the current evidence suggests that 6-OHDA lesions did not affect gross properties of pallidal firing or LFP. While this contradicts our hypothesis that there would be higher beta power and less of a BOS-selective response after lesion, we found trends meriting further investigation (see Study 3 Discussion, Section 5.4).

Our Study 3 (Chapter 5) findings are the first steps towards a complete characterization of DA-dependent neural activity in Area X and lay the groundwork for studying Area X activity during vocal learning. By performing the first recordings of Area X neurons and LFP in a chronic DA-depleted state we obtained valuable preliminary data for studies of DA-dependent Area X activity during learning. Additionally, we began the process of comparing activity in the DA-depleted songbird BG to activity in other animal models. Understanding species differences and why they occur could provide valuable insights on DA function in future studies. While this pilot study did not yield a complete dataset or as many findings as Studies 1 and 2 (Chapters 3 and 4), it established a beachhead for future neurophysiology studies of DA-dependent vocal learning.

6.2 Future directions beyond Study 1

In Study 1 (Chapter 3) we characterized how learning generalizes across the entire natural range of vocalizations in response to errors on vocal gestures produced in a specific sequential context. We found several interesting properties, including negative generalization to different vocal gestures and that generalization decreased with increasing sequential distance. Although this filled some knowledge gaps about how learning generalizes across a stereotyped motor sequence, there are several promising options for future research on generalization, including whether the same patterns occur for all types of internally guided vocal learning, how it is implemented in neural circuits and the role of DA in regulating generalization.

Future studies could examine whether learning generalizes in a similar way when manipulating vocal features other than pitch, such as amplitude. Like humans, birds increase amplitude when there is ambient noise (Lombard effect) and decrease amplitude when their own voice seems too loud (Fletcher effect) [282,283]. However, it is unknown whether either effect generalizes across gestures in a vocal sequence. If learning generalizes in a similar way for multiple acoustic features it would suggest the rules we observed are a fundamental principle of vocal generalization.

Although increasing evidence suggests that DA guides motor learning [93,95,99,101], including Study 2 (Chapter 4), it is not understood how DA affects generalization of learning for natural motor behaviors. Most prior work focused on generalization of responses across different cues during cue-response-reward learning paradigms (such as pressing a key in response to visual cues that look similar to a reward-predicting cue) [284,285] instead of generalization during skilled motor learning (such as how learning to change one's walking style generalizes to other limb movements). Study 1 (Chapter 3) has narrowed this gap and increased our knowledge of how generalization happens during natural motor behaviors. However, a key remaining gap addressed by neither Study 1 nor Study 2 (Chapters 3 and 4) is the role of DA in generalization. Studies of motor learning in PD have been mixed; various aspects of learning (including acquisition, long-term retention and

learning speed) were either intact or impaired depending on the task, sensory cues and disease stage [194,201]. Unfortunately, studies of DA and motor skill learning are often confounded by motor performance deficits that occur in the absence of DA [81,237]. Additionally, animal models with DA deficits often assess motor learning using highly artificial tasks learned later in life (including serial reaction time tasks) [88] rather than natural behaviors acquired during development. While useful in many contexts, data from such non-natural tasks do not reflect impairments in the ability to modify long-established motor skills.

Therefore, future studies could investigate the role of DA in generalization using the songbird model. As shown in Study 1 (Chapter 3), the single-syllable pitch-shift technique is an excellent way to study how sensorimotor learning generalizes across motor gestures. As shown in Study 2 (Chapter 4), partial loss of DA does not affect vocal performance and reduces but does not eliminate learning. Therefore, a logical next step would be to drive single-syllable pitch learning with headphones in birds with DA lesions, and examine effects on generalization. This would clearly show whether DA is necessary for generalization in complex vocal sequences, and pave the way for experiments investigating whether generalization is DA-dependent in other types of motor sequences.

We could study the BG's generalization-related activity by monitoring Area X's neural firing on a population level during single-syllable pitch-shift learning, which Study 1 (Chapter 3) showed causes generalization. This could be compared to neural activity during reinforcement-driven WN learning, which does not cause generalization [33]. We predict that neural firing in Area X will change throughout learning as predicted by the "exploration-exploitation" framework, where the BG first promotes variability and later consolidates the learned behavior in downstream motor regions [30,136,286]. See Section 6.4 for a discussion of predicted firing changes. We expect these changes to directly scale with the motor output changes for both learned and generalized behavior. This would match the proposed neural tuning curve model of how generalization could be implemented, where learning generalizes because neurons fire for the trained movement as well as

similar movements [54,62]. There should be no significant change in firing for syllables where learning does not generalize, as compared to a control experiment without pitch shifts or WN. This would help us determine which firing changes are related to simple error correction (on the perturbed syllables), and which result in complex generalization patterns (on the non-perturbed syllables).

If similar generalization patterns are found across species and motor modalities, it would suggest there are universal rules of generalization for stereotyped motor sequences. To determine this, we could examine patterns of generalization for sequences of motor gestures in humans. For example, we could use a movable platform [287] to perturb posture as humans perform one step in a dance. Or we could do a force-field perturbation as subjects write one particular letter in a sentence [288]. We could also repeat the same vocal learning paradigm in humans speaking naturally, instead of a small set of training and transfer utterances. If so, we predict three things: compensation for errors will generalize to similar gestures produced elsewhere in the sequence, generalization will decrease with increasing sequential distance and there will be measurable changes to non-similar gestures (even though there was no perturbation for those gestures).

Behavioral studies in humans given DA-manipulating drugs such as amphetamines [289] could also help elucidate DA's role in generalization. Patients with PD have impaired or spared learning and generalization depending on the task or disease stage [290–296] but results can be affected by motor performance deficits [14] different disease subtypes (including tremor-dominant versus postural instability and gait difficulty dominant PD) [297] and non-DAergic pathology such as damage to lower brainstem structures [85,298]. These confounds can mask DA's specific role. To my knowledge it has not been tested how DA manipulation affects generalization across a wide movement repertoire in humans. One such experiment could be measuring motor kinematics as experienced dancers learn to alter one dance step in a stereotyped sequence to observe how learning generalizes across kinematically similar and different movements and nearby movements in the sequence.

6.3 Future directions beyond Study 2

Study 2 (Chapter 4) established that DAergic input to Area X is necessary for pitch learning driven by negative reinforcement. This supports a reinforcement learning model where DAergic RPE signals cause synaptic changes in BG neurons to bias downstream motor pathways towards rewarded (or away from punished) actions [104,105]. Although showing that DA is necessary for learning is a key first step, the results of this Study open the door to further exploration of how DA helps guide motor learning.

Future studies could ask whether DA is necessary for vocal learning driven by rewards or punishments other than an aversive acoustic stimulus. Area X activity may not be exclusively related to auditory information because Area X neuron firing rates become more variable when Bengalese finches are trained to peck a key to obtain food [178]. Thus, one could attempt to drive pitch learning using electric shocks or food rewards instead of auditory stimuli. Assuming these experiments cause learning in healthy birds, we predict reduced learning when Area X DA is reduced. This would show that DA guides spectral-feature learning (already known to depend on Area X [158]) by integrating a broad variety of sensory feedback mechanisms, not just acoustic feedback. This would match proposed models in mammals, where DA neurons integrate many types of sensory input into a single RPE or incentive salience signal. Alternatively, lack of learning (or lack of DA dependence) would show the song system (or Area X's DAergic input) is highly specialized for acoustic feedback.

The experiments proposed above are all external rewards/punishments, as is WN. However, natural song learning is driven by intrinsic error signals encoding a subjective sense of song quality. Birds learn and maintain song using error correction in order to match an internal template [7,299]. It is hypothesized that auditory feedback of BOS matching or deviating from the template causes DAergic RPE signals just as external rewards or punishments would [104–106]. Such signals were recently observed in the songbird VTA in response to distorted auditory feedback during song (delayed snippets of song syllables or broadband WN). DA neurons projecting to Area

X phasically decreased firing after distorted feedback and increased firing when distorted feedback was unexpectedly removed, consistent with RPEs arising from worse-than-predicted and better-than-predicted outcomes [115]. Future work could use the headphones pitch-shift technique as in Study 1 (Chapter 3) and prior work [7,208] to determine whether error-corrective learning also depends on DA. This would be an important contribution to the scant literature on how DA is involved in self-guided maintenance of complex motor skills.

The Study 2 experiments (Chapter 4) affected all DA signaling, but it is important to understand how the two major classes of DA receptors (D_1 and D_2) are involved in learning. As in mammalian striatum, D_1 activation increases excitability in Area X MSNs and D_2 activation decreases excitability [116]. Although Area X contains simple direct and indirect pathways similar to mammalian BG [141] (**Fig. 1.2a,b**), songbird MSNs are not as segregated: half of them contain both D_1 and D_2 receptors [118]. It is currently unknown [131] whether MSNs projecting in Area X's direct and indirect pathways have higher levels of D_1 or D_2 receptors, respectively, as we would predict based on mammalian BG MSNs [211]. D_1 activation is necessary for modulating fine spectral features of birdsong depending on social context (i.e. reducing variability when singing to a female) [126], LTP onto Area X MSNs [119] and D_1 signaling may be necessary for normal song learning [300]. Future work could drive pitch learning while chronically infusing D_1 or D_2 receptor agonists/antagonists according to a previously established protocol [127]. D_1 and D_2 receptors probably act in concert to guide reinforcement learning [104,301], so we would expect disrupting either receptor to cause some learning deficit.

An interesting extension of Study 2 (Chapter 4) would be to determine whether learning deficits become more severe with greater loss of DA. 6-OHDA injections in Area X cause a roughly 50% loss of DA in our work and others' [129]. Although this causes clear learning deficits, we might see larger deficits if we attempted to eliminate as much DA as possible. From a technical perspective, this could improve the signal-to-noise ratio in future experiments and yield a more robust model of DA and motor learning. In rodents, injecting 6-OHDA in medial forebrain bundle

causes >95% loss of DA input to striatum [302,303], but songbirds do not have a corresponding structure. One option is to inject MPP^+ (N-Methyl-4-phenylpyridine) into Area X, which would spare DA and motor performance in non-song circuits. MPP^+ is the neurotoxic metabolite of MPTP (1-methyl-4-phenyl-1,2,3,6-tetrahydropyridine) and causes DA neuron death [304]. While 6-OHDA causes a more progressive degradation over several days in songbirds, MPP^+ causes DA cell loss to peak within 12 hours [305]. It is therefore worse at mimicking the slow progress of PD than 6-OHDA [306], but remains useful for studying DA and learning. A caveat is that intrastriatal MPP^+ injections in rats cause only 40% DA loss [307]. However, MPP^+ effects vary across species and strains [308], so it is possible that injections in songbirds will yield greater loss. If MPP^+ does not reduce DA levels more than 6-OHDA, other approaches could be attempted such as chronic administration of DA receptor blockers [127], neurotoxic chemicals such as rotenone [82], viral lesions [300] or transgenic methods recently developed in songbirds [309].

Another future experiment would examine whether 6-OHDA-related learning deficits are reduced by administering L-DOPA. This would help establish songbirds as a model of motor learning deficits in PD since PD can be accompanied by impairments in the sensorimotor learning processes used to maintain the accuracy of skilled behaviors including arm-reaching, drawing and avoiding obstacles while walking [103,194–200]. Although L-DOPA improves motor control deficits, its effect on motor learning is less well known, with some studies suggesting it can impair adaptation in PD [310]. On the other hand, in a mouse line deprived of the PITx3 gene (leading to 90% reduction of dorsal striatal DA), administration of L-DOPA during training rescued motor learning deficits as they learned to walk on a spinning rotarod [101]. L-DOPA administration has been done in songbirds [311] but not while driving vocal learning. We predict that learning deficits induced by 6-OHDA in Area X will be alleviated by systemic treatment with L-DOPA.

Finally, it is important not to limit investigations to the BG, because DA inputs to motor cortex are also implicated in motor skill learning [77,99]. For example, ablating motor cortex DA terminals impaired learning, but not performance, when rats learned to make precision forelimb

reaching movements to obtain food [99]. We could examine DA in analogous nuclei in the songbird. The motor pathway nuclei HVC and RA are known to receive DAergic input from VTA/SNc [312,313] and DA is known to modulate synaptic plasticity in RA *in vitro* [314]. Although there is much less DAergic innervation than in Area X, DA in songbird motor nuclei could still have a significant impact on adaptive plasticity. Future work could investigate whether DA in HVC and RA is also necessary for learning. It would be especially interesting to test whether DA in HVC is necessary for learning to alter song timing, which does not require Area X and is encoded in HVC [158].

6.4 Future directions beyond Study 3

In Study 3 (Chapter 5) we analyzed how spontaneous and playback-evoked neural activity changed after 6-OHDA lesions, finding no gross differences in pallidal neuron firing rates or LFP beta power. This provided valuable preliminary data for understanding how neural firing changes under a DA-depleted condition that causes learning deficits (Study 2; Chapter 4) and for comparing effect of DA lesions with BG neurophysiology data from other model systems and human PD. However, much remains to be done to quantify neural firing and LFP changes after loss of DA. Since the overall goal of this project is to understand vocal plasticity, another important future direction is to quantify Area X's neural activity in DA-depleted awake birds during vocal learning.

The first future direction to consider is collecting more spiking data. This Study only yielded 4 well-isolated pallidal units in 6-OHDA hemispheres and only 5 striatal interneurons across birds. To reduce variance and detect small firing changes it may be necessary to increase dataset size. Having more units will also give us more statistical power for analyses of each subtype of spontaneously firing pallidal (GPe-like and GPi-like) and striatal interneuron [142–144].

Many additional analyses can be performed on this dataset. Parkinsonian pallidal neurons have increased burstiness, synchrony and oscillatory activity, and GPe and GPi neurons have decreased and increased population average firing rates, respectively [211,212]. Measuring whether these features also occur in Area X pallidal neurons will contribute to establishing songbirds as a

new model system of DA in motor behavior. We could quantify synchronicity using spike-field coherence, which measures relationship between LFP phase and spike times [315,316]. Another analysis direction is to quantify more neural firing features known to change during BOS, such as interspike interval distribution, d' between BOS and REV (a discriminability metric) and trial-to-trial spike timing variability [176,177]. These would be a more complete test of the prediction that pallidal neurons would become less responsive to BOS playbacks after DA depletion. Finally, since LFP activity in various frequency bands is a potential indicator of many functions [181,182] and currently Area X LFP literature is limited to one study [184] it would be useful to quantify spontaneous and playback-evoked LFP in non-beta bands in sham vs. 6-OHDA hemispheres, as well as transient LFP evoked by WN, individual syllables and toe pinches.

It would be informative to record from Area X when DA levels are depleted more than the ~50% we obtained with 6-OHDA (**Fig. 4.4a**). Although the time frame and degree of depletion was sufficient to cause learning deficits (Study 2; Chapter 4), perhaps we did not deplete enough DA or wait long enough for pathological activity such as beta oscillations to emerge gradually, as happens in rodent 6-OHDA models [275]. However, bilateral Area X lesions or acute DA receptor blockade in adults do not affect vocal performance [156,157] other than social-context-dependent variability (i.e. reducing variability when singing to a female) [126,127] and temporary syllable sequencing changes [159]. This suggests the possibility that complete DA lesions would not grossly affect song either, which would suggest two interesting possibilities. To review briefly, Parkinsonian motor deficits may be related not only to over-activating the indirect pathway [317] or aberrant learning caused by abnormal corticostriatal plasticity after loss of DA [102], but also to pathological synchronization spreading from the BG to motor circuits [80,190] including bradykinesia linked to the beta band [189] (but this remains controversial because motor deficits in primates appear before synchronized oscillatory neural activity [318]). Therefore, if we observe pathological activity (such as increased synchronization or higher beta band power) but no vocal motor deficits, this could mean something is preventing the spread of abnormal activity to motor nucleus RA. If we do not observe

pathological activity (controlling for possible urethane-related blunting of beta oscillations as in 6-OHDA-lesioned rats [187,275]), it could suggest the DA-dependent cellular mechanisms underlying these changes in mammals do not operate in songbirds. Future experiments studying these species differences could contribute to understanding the mechanisms of DA-dependent motor deficits.

Another critical future direction for Study 3 (Chapter 5) is to explore changes in Area X neural activity during WN learning in sham- and 6-OHDA-lesioned birds. Studies in anesthetized birds provide important data on how DA affects Area X activity. Nevertheless, the only way to show how Area X striatal and pallidal neurons adjust their firing to bias downstream motor output is by recording during learning. Neural activity differences between sham- and 6-OHDA-lesioned hemispheres will reveal the DA-dependent aspects of this biasing signal. These studies will require chronic recording over several days, so it could be difficult to maintain unit isolation throughout the baseline and learning periods. This issue can be mitigated by driving learning in younger birds, which learn more quickly [249], analyzing stable LFP activity and quantifying population activity for each neural subtype at different learning stages.

It would be especially informative to examine firing changes in MSNs, which receive glutamatergic input from LMAN and HVC [141] and spike only as birds sing specific song syllables [143]. MSNs are hypothesized to bias motor output towards rewarded actions via DA-modulated plasticity occurring at corticostriatal synapses [105]. In songbirds, DA affects MSN excitability and gates LTP of corticostriatal synapses [116,119], and Area X-projecting DA neurons code for song performance errors [115]. This could lead to MSN firing patterns changing during learning, biasing downstream motor circuits to improve performance and consolidate learning [104]. For example, in rodents performing motor skill learning, some MSN firing rates increased early in learning then decreased as performance stabilized, while a different anatomical subpopulation increased firing late in learning [92]. We predict similar changes in songbird MSNs during the syllable targeted by WN and expect these changes to be reduced in 6-OHDA-lesioned birds.

To be more specific, MSN and pallidal Area X firing patterns could vary during learning according to an "exploration-exploitation" framework [30,136,286]. During the first set of song bouts after WN reinforcement is turned on, MSNs should show increased mean firing rates (spikes per syllable) and increased firing variability (variance in the number of spikes per syllable) as the birds sing the targeted syllable relative to baseline firing during that syllable. This would match the proposed "exploration" phase, where the BG promotes behavioral variability early in learning via global activity modulation [30,136,286]. As birds learn to avoid WN by changing pitch, most of these neurons should decrease firing rates and variability again until they are at or below baseline levels. However, we predict that during late stages of learning, a subset of MSNs will acquire (or maintain) higher firing rates and fire less variably than baseline when the targeted syllable is sung. This would match the proposed "exploitation" phase, where the BG consolidates the learned behavior change by focusing and intensifying the activity of a subset of neurons [30,136,286]. Throughout learning, we predict pallidal cells to show broadly the opposite pattern, with initially decreased firing rates recovering as learning proceeds. This would also be in accordance with the "explore-exploit" framework [319]. We expect the magnitude of these firing changes to correlate with the amount learned and whether Area X was sham- or 6-OHDA-lesioned.

In addition to studying WN learning, future experiments could investigate electrophysiological changes during sensorimotor error correction and generalization (driven by headphones pitch shifts), as described in Section 6.2. WN experiments drive learning by external reinforcement instead of an internal template of the "correct pitch" [7,299]. If future experiments demonstrate DA is also necessary for internally guided sensorimotor error correction, we could investigate whether BG activity or LFP power changes in a similar way during both kinds of learning. This might indicate self-guided maintenance of vocal gestures relies on similar neural mechanisms as when learning is driven via external cues. Alternatively, if DA is not necessary for plasticity caused by headphones pitch shifts, we could determine key differences in BG activity from WN learning.

REFERENCES

1. Honda, M. Human speech production mechanisms. *NTT Tech. Rev.* (2003).
2. Stevens, K. *Acoustic phonetics. Cambridge, MA: MIT Press*. (MIT Press, 1998).
3. Houde, J. F. & Jordan, M. I. Sensorimotor adaptation in speech production. *Science* **279,** 1213–6 (1998).
4. Houde, J. F. & Jordan, M. I. Sensorimotor adaptation of speech I: Compensation and adaptation. *J. Speech. Lang. Hear. Res.* **45,** 295–310 (2002).
5. Morgan, G. Critical period in language development. *Encycl. Lang. Dev.* (2014).
6. Price, P. H. Developmental determinants of structure in zebra finch song. *J. Comp. Physiol. Psychol.* **93,** 260–277 (1979).
7. Sober, S. J. & Brainard, M. S. Adult birdsong is actively maintained by error correction. *Nat. Neurosci.* **12,** 927–31 (2009).
8. Nordeen, K. W. & Nordeen, E. J. Auditory feedback is necessary for the maintenance of stereotyped song in adult zebra finches. *Behav. Neural Biol.* **57,** 58–66 (1992).
9. Woolley, S. M. & Rubel, E. W. Bengalese finches Lonchura Striata domestica depend upon auditory feedback for the maintenance of adult song. *J. Neurosci.* **17,** 6380–90 (1997).
10. Cowie, R. & Douglas-Cowie, E. *Postlingually Acquired Deafness: Speech Deterioration and the Wider Consequences*. (Mouton De Gruyter, 1992).
11. Lane, H. & Webster, J. W. Speech deterioration in postlingually deafened adults. *Psychol. Fac. Publ. Northeast. Univ.* (1991).
12. Kandel, E. R., Schwartz, J. H. & Jessel, T. M. *Principles of Neural Science*. (McGraw-Hill, 2000).
13. Lai, C. S. L., Fisher, S. E., Hurst, J. A., Vargha-Khadem, F. & Monaco, A. P. A forkhead-domain gene is mutated in a severe speech and language disorder. *Nature* **413,** 519–523 (2001).
14. Ramig, L. O., Fox, C. & Sapir, S. Speech treatment for Parkinson's disease. *Expert Rev. Neurother.* **8,** 299–311 (2008).
15. Brainard, M. S. & Doupe, A. J. What songbirds teach us about learning. *Nature* **417,** 351–358 (2002).
16. Boughman, J. W. Vocal learning by greater spear-nosed bats. *Proc. Biol. Sci.* **265,** 227–33 (1998).
17. Poole, J. H., Tyack, P. L., Stoeger-Horwath, A. S. & Watwood, S. Animal Behavior: elephants are capable of vocal learning. *Nature* **434,** 455–456 (2005).
18. Janik, V. M. Cetacean vocal learning and communication. *Curr. Opin. Neurobiol.* **28,** 60–65 (2014).
19. Kikusui, T. *et al.* Cross fostering experiments suggest that mice songs are innate. *PLoS One* **6,** e17721 (2011).
20. Egnor, S. E. R. & Hauser, M. D. A paradox in the evolution of primate vocal learning. *Trends Neurosci.* **27,** 649–54 (2004).
21. Doupe, A. J. & Kuhl, P. K. Birdsong and human speech: common themes and mechanisms. *Annu. Rev. Neurosci.* **22,** 567–631 (1999).
22. Bolhuis, J. J., Okanoya, K. & Scharff, C. Twitter evolution: converging mechanisms in birdsong and human speech. *Nat. Rev. Neurosci.* **11,** 747–59 (2010).
23. Villacorta, V. M., Perkell, J. S. & Guenther, F. H. Sensorimotor adaptation to feedback perturbations of vowel acoustics and its relation to perception. *J. Acoust. Soc. Am.* **122,** 2306–19 (2007).
24. Jones, J. A. & Munhall, K. G. Perceptual calibration of F0 production: evidence from feedback perturbation. *J. Acoust. Soc. Am.* **108,** 1246–51 (2000).

25. Waldstein, R. S. Effects of postlingual deafness on speech production: implications for the role of auditory feedback. *J. Acoust. Soc. Am.* **88,** 2099–2114 (1990).
26. Simonyan, K., Horwitz, B. & Jarvis, E. D. Dopamine regulation of human speech and bird song: a critical review. *Brain Lang.* **122,** 142–50 (2012).
27. Fee, M. S. & Scharff, C. The songbird as a model for the generation and learning of complex sequential behaviors. *ILAR J.* **51,** 362–77 (2010).
28. Okanoya, K. The Bengalese finch: a window on the behavioral neurobiology of birdsong syntax. *Ann. N. Y. Acad. Sci.* **1016,** 724–35 (2004).
29. Sober, S. J. S. J., Wohlgemuth, M. J. & Brainard, M. S. Central contributions to acoustic variation in birdsong. *J. Neurosci.* **28,** 10370–9 (2008).
30. Kao, M. H., Doupe, A. J. & Brainard, M. S. Contributions of an avian basal ganglia-forebrain circuit to real-time modulation of song. *Nature* **433,** 638–43 (2005).
31. Feenders, G. *et al.* Molecular mapping of movement-associated areas in the avian brain: a motor theory for vocal learning origin. *PLoS One* **3,** e1768 (2008).
32. Nottebohm, F., Stokes, T. M. & Leonard, C. M. Central control of song in the canary, Serinus canarius. *J. Comp. Neurol.* **165,** 457–486 (1976).
33. Tumer, E. C. & Brainard, M. S. Performance variability enables adaptive plasticity of 'crystallized' adult birdsong. *Nature* **450,** 1240–4 (2007).
34. Krakauer, J. W., Pine, Z. M., Ghilardi, M. F. & Ghez, C. Learning of visuomotor transformations for vectorial planning of reaching trajectories. *J. Neurosci.* **20,** 8916–24 (2000).
35. Roby-Brami, A. & Burnod, Y. Learning a new visuomotor transformation: error correction and generalization. *Cogn. brain Res.* **2,** 229–242 (1995).
36. Ghahramani, Z., Wolpert, D. M. & Jordan, M. I. Generalization to local remappings of the visuomotor coordinate transformation. *J. Neurosci.* **16,** 7085–96 (1996).
37. Rochet-Capellan, A., Richer, L. & Ostry, D. J. Nonhomogeneous transfer reveals specificity in speech motor learning. *J. Neurophysiol.* **107,** 1711–7 (2012).
38. Cai, S., Ghosh, S. S., Guenther, F. H. & Perkell, J. S. Adaptive auditory feedback control of the production of formant trajectories in the Mandarin triphthong /iau/ and its pattern of generalization. *J. Acoust. Soc. Am.* **128,** 2033–48 (2010).
39. Pile, E. & Dajani, H. Talking under conditions of altered auditory feedback: does adaptation of one vowel generalize to other vowels. *Int. Congr. Phonetic Sci.* 645–648 (2007).
40. Tremblay, S., Houle, G. & Ostry, D. J. Specificity of speech motor learning. *J. Neurosci.* **28,** 2426–34 (2008).
41. Rochet-Capellan, A. & Ostry, D. J. Simultaneous acquisition of multiple auditory-motor transformations in speech. *J. Neurosci.* **31,** 2657–62 (2011).
42. Field, D. P., Shipley, T. F. & Cunningham, D. W. Prism adaptation to dynamic events. *Percept. Psychophys.* **61,** 161–76 (1999).
43. Palmer, C. & Meyer, R. K. Conceptual and motor learning in music performance. *Psychol. Sci.* **11,** 63–68 (2000).
44. Martin, T., Keating, J. & Goodkin, H. Throwing while looking through prisms II. Specificity and storage of multiple gaze—throw calibrations. *Brain* 1199–1211 (1996).
45. Kitazawa, S., Kimura, T. & Uka, T. Prism adaptation of reaching movements: specificity for the velocity of reaching. *J. Neurosci.* **17,** 1481–92 (1997).
46. Fu, Q. & Santello, M. Context-dependent learning interferes with visuomotor transformations for manipulation planning. *J. Neurosci.* **32,** 15086–92 (2012).
47. Morton, S. M., Lang, C. E. & Bastian, a J. Inter- and intra-limb generalization of adaptation during catching. *Exp. brain Res.* **141,** 438–45 (2001).
48. Baraduc, P. & Wolpert, D. Adaptation to a visuomotor shift depends on the starting posture. *J. Neurophysiol.* 973–981 (2002).

49. Goodbody, S. & Wolpert, D. Temporal and amplitude generalization in motor learning. *J. Neurophysiol.* 1825–1838 (1998).
50. Conditt, M., Gandolfo, F. & Mussa-Ivaldi, F. The motor system does not learn the dynamics of the arm by rote memorization of past experience. *J. Neurophysiol.* **78,** 554–560 (1997).
51. Alexander, M. S., Flodin, B. W. G. & Marigold, D. S. Prism adaptation and generalization during visually guided locomotor tasks. *J. Neurophysiol.* **106,** 860–71 (2011).
52. Morton, S. M. & Bastian, A. J. Prism adaptation during walking generalizes to reaching and requires the cerebellum. *J. Neurophysiol.* **92,** 2497–509 (2004).
53. Krakauer, J. W., Mazzoni, P., Ghazizadeh, A., Ravindran, R. & Shadmehr, R. Generalization of motor learning depends on the history of prior action. *PLoS Biol.* **4,** e316 (2006).
54. Shadmehr, R. Generalization as a behavioral window to the neural mechanisms of learning internal models. *Hum. Mov. Sci.* **23,** 543–68 (2004).
55. Shadmehr, R. & Mussa-Ivaldi, F. Adaptive representation of dynamics during learning of a motor task. *J. Neurosci.* **14,** 3208–3224 (1994).
56. Wainscott, S. K., Donchin, O. & Shadmehr, R. Internal models and contextual cues: encoding serial order and direction of movement. *J. Neurophysiol.* **93,** 786–800 (2005).
57. Imamizu, H. *et al.* Explicit contextual information selectively contributes to predictive switching of internal models. *Exp. Brain Res.* **181,** 395–408 (2007).
58. Wada, Y. *et al.* Acquisition and contextual switching of multiple internal models for different viscous force fields. *Neurosci. Res.* **46,** 319–331 (2003).
59. Howard, I. S., Ingram, J. N. & Wolpert, D. M. Context-dependent partitioning of motor learning in bimanual movements. *J. Neurophysiol.* **104,** 2082–91 (2010).
60. Howard, I. S., Wolpert, D. M. & Franklin, D. W. The effect of contextual cues on the encoding of motor memories. *J. Neurophysiol.* **109,** 2632–44 (2013).
61. Taylor, J. a & Ivry, R. B. Context-dependent generalization. *Front. Hum. Neurosci.* **7,** 171 (2013).
62. Poggio, T. & Bizzi, E. Generalization in vision and motor control. *Nature* **431,** (2004).
63. Darshan, R., Leblois, A. & Hansel, D. Interference and shaping in sensorimotor adaptations with rewards. *PLoS Comput. Biol.* **10,** e1003377 (2014).
64. Ghahramani, Z. & Wolpert, D. Modular decomposition in vision motor learning. *Nature* **386,** 392–395 (1997).
65. Haruno, M., Wolpert, D. M. & Kawato, M. Mosaic model for sensorimotor learning and control. *Neural Comput.* **13,** 2201–20 (2001).
66. Wolpert, D. M. & Kawato, M. Multiple paired forward and inverse models for motor control. *Neural Netw.* **11,** 1317–29 (1998).
67. Surmeier, D. J., Ding, J., Day, M., Wang, Z. & Shen, W. D1 and D2 dopamine-receptor modulation of striatal glutamatergic signaling in striatal medium spiny neurons. *Trends Neurosci.* **30,** 228–235 (2007).
68. Haber, S. N. The place of dopamine in the cortico-basal ganglia circuit. *Neuroscience* **282,** 248–257 (2014).
69. Schultz, W., Dayan, P. & Montague, P. R. A neural substrate of prediction and reward. *Science (80-.).* **275,** 1593–1599 (1997).
70. Waelti, P., Dickinson, a & Schultz, W. Dopamine responses comply with basic assumptions of formal learning theory. *Nature* **412,** 43–8 (2001).
71. Fiorillo, C. D., Tobler, P. N. & Schultz, W. Discrete coding of reward probability and uncertainty by dopamine neurons. *Science (80-.).* **299,** 1898–1902 (2003).
72. Schultz, W. Updating dopamine reward signals. *Curr. Opin. Neurobiol.* **23,** 229–238 (2013).
73. Glimcher, P. W. Understanding dopamine and reinforcement learning: The dopamine

reward prediction error hypothesis. *Proc. Natl. Acad. Sci. U. S. A.* **108,** 17569 (2011).
74. Daw, N. D. & Tobler, P. N. Chapter 15: Value learning through reinforcement: the basics of dopamine and reinforcement learning. *Neuroeconomics* 283–317 (2014).
75. Lloyd, K. & Dayan, P. Safety out of control: dopamine and defence. *Behav. Brain Funct.* **12,** 15 (2016).
76. Berridge, K. C. The debate over dopamine's role in reward: the case for incentive salience. *Psychopharmacology (Berl).* **191,** 391–431 (2007).
77. Hosp, J. a. & Luft, A. R. Dopaminergic meso-cortical projections to M1: Role in motor learning and motor cortex plasticity. *Front. Neurol.* **4 OCT,** 1–7 (2013).
78. Panigrahi, B. *et al.* Dopamine is required for the neural representation and control of movement vigor. *Cell* **162,** 1418–1430 (2015).
79. Redgrave, P. & Gurney, K. The short-latency dopamine signal: a role in discovering novel actions? *Nat. Rev. Neurosci.* **7,** 967–975 (2006).
80. Gatev, P., Darbin, O. & Wichmann, T. Oscillations in the basal ganglia under normal conditions and in movement disorders. *Mov. Disord.* **21,** 1566–1577 (2006).
81. Zhou, Q.-Y. & Palmiter, R. D. Dopamine-deficient mice are severely hypoactive, adipsic, and aphagic. *Cell* **83,** 1197–1209 (1995).
82. Blesa, J., Phani, S., Jackson-Lewis, V. & Przedborski, S. Classic and new animal models of Parkinson's disease. *J. Biomed. Biotechnol.* **2012,** 845618 (2012).
83. Mollaei, F., Shiller, D. M., Baum, S. R. & Gracco, V. L. Sensorimotor control of vocal pitch and formant trajectories in parkinson's disease. **1646,** 1 (2016).
84. Mollaei, F., Shiller, D. M. & Gracco, V. L. Sensorimotor adaptation of speech in Parkinson's disease. *Mov. Disord.* **28,** 1668–74 (2013).
85. Lang, A. E. & Obeso, J. A. Time to move beyond nigrostriatal dopamine deficiency in Parkinson's disease. *Ann. Neurol.* **55,** 761–765 (2004).
86. Jaunarajs, K. L. E. & Standaert, D. G. Removing the blinkers: Moving beyond striatal dopamine in Parkinson's disease. *J. Neurochem.* **125,** 639–641 (2013).
87. Robertson, E. M. The serial reaction time task: implicit motor skill learning? *J. Neurosci.* **27,** 10073–10075 (2007).
88. Potashkin, J. a, Blume, S. R. & Runkle, N. K. Limitations of animal models of Parkinson's disease. *Parkinsons. Dis.* **2011,** 658083 (2010).
89. Eckart, M. T., Huelse-Matia, M. C., McDonald, R. S. & Schwarting, R. K.-W. 6-hydroxydopamine lesions in the rat neostriatum impair sequential learning in a serial reaction time task. *Neurotox. Res.* **17,** 287–298 (2010).
90. Clark, G. M., Lum, J. A. G. & Ullman, M. T. A meta-analysis and meta-regression of serial reaction time task performance in Parkinson's disease. *Neuropsychology* **28,** 945–958 (2014).
91. Shiotsuki, H. *et al.* A rotarod test for evaluation of motor skill learning. *J. Neurosci. Methods* **189,** 180–185 (2010).
92. Yin, H. H. *et al.* Dynamic reorganization of striatal circuits during the acquisition and consolidation of a skill. *Nat. Neurosci.* **12,** 333–341 (2009).
93. Willuhn, I. & Steiner, H. Motor-skill learning in a novel running-wheel task is dependent on D1 dopamine receptors in the striatum. *Neuroscience* **153,** 249–258 (2008).
94. Chagniel, L., Robitaille, C., Lacharité-Mueller, C., Bureau, G. & Cyr, M. Partial dopamine depletion in MPTP-treated mice differentially altered motor skill learning and action control. *Behav. Brain Res.* **228,** 9–15 (2012).
95. Ogura, T. *et al.* Impaired acquisition of skilled behavior in rotarod task by moderate depletion of striatal dopamine in a pre-symptomatic stage model of Parkinson's disease. *Neurosci. Res.* **51,** 299–308 (2005).
96. Gambhir, H., Mathur, R. & Behari, M. Progressive impairment in motor skill learning at 12 and 20 weeks post 6-OHDA- SNc lesion in rats. *Park. Relat. Disord.* **17,** 476–478

(2011).
97. Molina-Luna, K. *et al.* Dopamine in motor cortex is necessary for skill learning and synaptic plasticity. *PLoS One* **4,** (2009).
98. Rioult-Pedotti, M. S., Pekanovic, A., Atiemo, C. O., Marshall, J. & Luft, A. R. Dopamine promotes motor cortex plasticity and motor skill learning via PLC activation. *PLoS One* **10,** 1–14 (2015).
99. Hosp, J. a, Pekanovic, A., Rioult-Pedotti, M. S. & Luft, A. R. Dopaminergic projections from midbrain to primary motor cortex mediate motor skill learning. *J. Neurosci.* **31,** 2481–2487 (2011).
100. Zhuang, X., Mazzoni, P. & Kang, U. J. The role of neuroplasticity in dopaminergic therapy for Parkinson disease. *Nat. Rev. Neurol.* **9,** 248–56 (2013).
101. Beeler, J. *et al.* Dopamine-dependent motor learning insight into levodopa's long-duration response. *Ann. Neurol.* **67,** 639–647 (2010).
102. Beeler, J. A. *et al.* A role for dopamine-mediated learning in the pathophysiology and treatment of Parkinson's disease. *Cell Rep.* **2,** 1747–1761 (2012).
103. Beeler, J. a. Preservation of function in Parkinson's disease: what's learning got to do with it? *Brain Res.* **1423,** 96–113 (2011).
104. Fee, M. S. & Goldberg, J. H. A hypothesis for basal ganglia-dependent reinforcement learning in the songbird. *Neuroscience* **198,** 152–70 (2011).
105. Fee, M. S. Oculomotor learning revisited: a model of reinforcement learning in the basal ganglia incorporating an efference copy of motor actions. *Front. Neural Circuits* **6,** 1–18 (2012).
106. Doya, K. & Sejnowski, T. in *Central Auditory Processing and Neural Modeling* 77–88 (1998).
107. Kubikova, L. & Kostál, L. Dopaminergic system in birdsong learning and maintenance. *J. Chem. Neuroanat.* **39,** 112–23 (2010).
108. Joel, D., Niv, Y. & Ruppin, E. Actor-critic models of the basal ganglia: new anatomical and computational perspectives. *Neural Netw.* **15,** 535–47 (2002).
109. Charlesworth, J. D., Warren, T. L. & Brainard, M. S. Covert skill learning in a cortical-basal ganglia circuit. *Nature* 1–6 (2012).
110. Gale, S. D. & Perkel, D. J. Physiological properties of zebra finch ventral tegmental area and substantia nigra pars compacta neurons. *J. Neurophysiol.* **96,** 2295–2306 (2006).
111. Yanagihara, S. & Yazaki-Sugiyama, Y. Auditory experience-dependent cortical circuit shaping for memory formation in bird song learning. *Nat. Commun.* **7,** 11946 (2016).
112. Gale, S. D. & Perkel, D. J. Properties of dopamine release and uptake in the songbird basal ganglia. *J. Neurophysiol.* **93,** 1871–9 (2005).
113. Goldberg, J. H. & Fee, M. S. A cortical motor nucleus drives the basal ganglia-recipient thalamus in singing birds. *Nat. Neurosci.* **15,** 620–627 (2012).
114. Andalman, A. S. & Fee, M. S. A basal ganglia-forebrain circuit in the songbird biases motor output to avoid vocal errors. *Proc. Natl. Acad. Sci. U. S. A.* **106,** 12518–23 (2009).
115. Gadagkar, V. *et al.* Dopamine neurons encode performance error in singing birds. 20–24 (2016).
116. Ding, L. & Perkel, D. J. Dopamine modulates excitability of spiny neurons in the avian basal ganglia. *J. Neurosci.* **22,** 5210–5218 (2002).
117. Ding, L., Perkel, D. J. & Farries, M. a. Presynaptic depression of glutamatergic synaptic transmission by D1-like dopamine receptor activation in the avian basal ganglia. *J. Neurosci.* **23,** 6086–95 (2003).
118. Kubikova, L., Wada, K. & Jarvis, E. D. Dopamine receptors in a songbird brain. *J. Comp. Neurol.* **518,** 741–769 (2010).
119. Ding, L. & Perkel, D. J. Long-term potentiation in an avian basal ganglia nucleus essential for vocal learning. *J. Neurosci.* **24,** 488–94 (2004).

120. Gale, S. D., Person, A. L. & Perkel, D. J. A novel basal ganglia pathway forms a loop linking a vocal learning circuit with its dopaminergic input. *J. Comp. Neurol.* **508,** 824–39 (2008).
121. Mandelblat-Cerf, Y., Las, L., Denisenko, N. & Fee, M. A role for descending auditory cortical projections in songbird vocal learning. *Elife* (2014).
122. Keller, G. B. & Hahnloser, R. H. R. Neural processing of auditory feedback during vocal practice in a songbird. *Nature* **457,** 187–90 (2009).
123. Sakata, J. T., Hampton, C. M. & Brainard, M. S. Social modulation of sequence and syllable variability in adult birdsong. *J. Neurophysiol.* **99,** 1700–11 (2008).
124. Sasaki, A., Sotnikova, T. D., Gainetdinov, R. R. & Jarvis, E. D. Social context-dependent singing-regulated dopamine. *J. Neurosci.* **26,** 9010–4 (2006).
125. Ihle, E. C., van der Hart, M., Jongsma, M., Tecott, L. H. & Doupe, A. J. Dopamine physiology in the basal ganglia of male zebra finches during social stimulation. *Eur. J. Neurosci.* **41,** 1506–1514 (2015).
126. Leblois, A. & Perkel, D. J. Striatal dopamine modulates song spectral but not temporal features through D1 receptors. *Eur. J. Neurosci.* **35,** 1771–1781 (2012).
127. Leblois, A., Wendel, B. J. & Perkel, D. J. Striatal dopamine modulates basal ganglia output and regulates social context-dependent behavioral variability through D1 receptors. *J. Neurosci.* **30,** 5730–5743 (2010).
128. Woolley, S. C. & Kao, M. H. Variability in action: Contributions of a songbird cortical-basal ganglia circuit to vocal motor learning and control. *Neuroscience* **296,** 39–47 (2015).
129. Miller, J. E., Hafzalla, G. W., Burkett, Z. D., Fox, C. M. & White, S. A. Reduced vocal variability in a zebra finch model of dopamine depletion: implications for Parkinson disease. *Physiol. Rep.* **3,** e12599–e12599 (2015).
130. Leblois, A. Social modulation of learned behavior by dopamine in the basal ganglia: insights from songbirds. *J. Physiol. Paris* **107,** 219–29 (2013).
131. Gale, S. D. & Perkel, D. J. Anatomy of a songbird basal ganglia circuit essential for vocal learning and plasticity. *J. Chem. Neuroanat.* **39,** 124–131 (2010).
132. Vicario, D. S. Organization of the zebra finch song control system: II. Functional organization of outputs from nucleus Robustus archistriatalis. *J. Comp. Neurol.* **309,** 486–94 (1991).
133. Perkel, D. Origin of the Anterior Forebrain Pathway. *Ann. N. Y. Acad. Sci.* 736–748 (2004).
134. Brainard, M. S. & Doupe, a J. Interruption of a basal ganglia-forebrain circuit prevents plasticity of learned vocalizations. *Nature* **404,** 762–6 (2000).
135. Bottjer, S. W., Miesner, E. A. & Arnold, A. P. Forebrain lesions disrupt development but not maintenance of song in passerine birds. *Science (80-.).* **224,** 901–903 (1984).
136. Olveczky, B. P., Andalman, A. S. & Fee, M. S. Vocal experimentation in the juvenile songbird requires a basal ganglia circuit. *PLoS Biol.* **3,** e153 (2005).
137. Warren, T. L., Tumer, E. C., Charlesworth, J. D. & Brainard, M. S. Mechanisms and time course of vocal learning and consolidation in the adult songbird. *J. Neurophysiol.* **106,** 1806–1821 (2011).
138. Doupe, A. J., Perkel, D. J., Reiner, A. & Stern, E. Birdbrains could teach basal ganglia research a new song. *Trends Neurosci.* **28,** 353–63 (2005).
139. Reiner, A. Functional circuitry of the avian basal ganglia: implications for basal ganglia organization in stem amniotes. *Brain Res. Bull.* **57,** 513–28 (2002).
140. Reiner, a, Medina, L. & Veenman, C. L. Structural and functional evolution of the basal ganglia in vertebrates. *Brain Res. Brain Res. Rev.* **28,** 235–85 (1998).
141. Farries, M. a, Ding, L. & Perkel, D. J. Evidence for 'direct' and 'indirect' pathways through the song system basal ganglia. *J. Comp. Neurol.* **484,** 93–104 (2005).
142. Farries, M. a & Perkel, D. J. A telencephalic nucleus essential for song learning contains

neurons with physiological characteristics of both striatum and globus pallidus. *J. Neurosci.* **22,** 3776–87 (2002).
143. Goldberg, J. H. & Fee, M. S. Singing-related neural activity distinguishes four classes of putative striatal neurons in the songbird basal ganglia. *J. Neurophysiol.* **103,** 2002–14 (2010).
144. Goldberg, J. H., Adler, A., Bergman, H. & Fee, M. S. Singing-related neural activity distinguishes two putative pallidal cell types in the songbird basal ganglia: comparison to the primate internal and external pallidal segments. *J. Neurosci.* **30,** 7088–98 (2010).
145. Luo, M., Ding, L. & Perkel, D. J. An avian basal ganglia pathway essential for vocal learning forms a closed topographic loop. *J. Neurosci.* **21,** 6836–45 (2001).
146. Butler, A. B., Reiner, A. & Karten, H. J. Evolution of the amniote pallium and the origins of mammalian neocortex. *Ann. N. Y. Acad. Sci.* **1225,** 14–27 (2011).
147. Teramitsu, I., Kudo, L. C., London, S. E., Geschwind, D. H. & White, S. a. Parallel FoxP1 and FoxP2 expression in songbird and human brain predicts functional interaction. *J. Neurosci.* **24,** 3152–63 (2004).
148. Person, A. L., Gale, S. D., Farries, M. a. & Perkel, D. J. Organization of the songbird basal ganglia, including area X. *J. Comp. Neurol.* **508,** 840–66 (2008).
149. Brainard, M. S. & Doupe, A. J. Translating birdsong: songbirds as a model for basic and applied medical research. *Annu. Rev. Neurosci.* **36,** 489–517 (2013).
150. Graybiel, A. M. Habits, rituals, and the evaluative brain. *Annu. Rev. Neurosci.* **31,** 359–87 (2008).
151. Turner, R. S. & Desmurget, M. Basal ganglia contributions to motor control: a vigorous tutor. *Curr. Opin. Neurobiol.* **20,** 704–716 (2010).
152. Kojima, S., Kao, M. H. & Doupe, a. J. Task-related 'cortical' bursting depends critically on basal ganglia input and is linked to vocal plasticity. *Proc. Natl. Acad. Sci.* **2013,** 1–6 (2013).
153. Censor, N., Sagi, D. & Cohen, L. G. Common mechanisms of human perceptual and motor learning. *Nat. Rev. Neurosci.* **13,** 658–64 (2012).
154. Nixdorf-Bergweiler, B. E. Divergent and parallel development in volume sizes of telencephalic song nuclei in male and female zebra finches. *J. Comp. Neurol.* **375,** 445–456 (1996).
155. Mooney, R. Neural mechanisms for learned birdsong. *Learn. Mem.* 655–669 (2009).
156. Sohrabji, F., Nordeen, E. J. & Nordeen, K. W. Selective impairment of song learning following lesions of a forebrain nucleus in the juvenile zebra finch. *Behav. Neural Biol.* **53,** 51–63 (1990).
157. Scharff, C. & Nottebohm, F. A comparative study of the behavioral deficits following lesions of various parts of the Zebra finch song system: implications for vocal learning. *J. Neurosci.* **11,** 2896–2913 (1991).
158. Ali, F. *et al.* The basal ganglia is necessary for learning spectral, but not temporal, features of birdsong. *Neuron* **80,** 1–13 (2013).
159. Kobayashi, K., Uno, H. & Okanoya, K. Partial lesions in the anterior forebrain pathway affect song production in adult Bengalese finches. *Neuroreport* **12,** 353–8 (2001).
160. Reiner, A., Laverghetta, A. V., Meade, C. a., Cuthbertson, S. L. & Bottjer, S. W. An immunohistochemical and pathway tracing study of the striatopallidal organization of area X in the male zebra finch. *J. Comp. Neurol.* **469,** 239–61 (2004).
161. Carrillo, G. D. & Doupe, A. J. Is the songbird Area X striatal, pallidal, or both? An anatomical study. *J. Comp. Neurol.* **473,** 415–437 (2004).
162. Beatty, J. A., Sullivan, M. A., Morikawa, H. & Wilson, C. J. Complex autonomous firing patterns of striatal low-threshold spike interneurons. *J. Neurophysiol.* **108,** 771–781 (2012).
163. Hessler, N. a & Doupe, a J. Singing-related neural activity in a dorsal forebrain-basal

ganglia circuit of adult zebra finches. *J. Neurosci.* **19,** 10461–81 (1999).
164. Luo, M. & Perkel, D. J. A GABAergic, strongly inhibitory projection to a thalamic nucleus in the zebra finch song system. *J. Neurosci.* **19,** 6700–11 (1999).
165. Luo, M. & Perkel, D. J. Long-Range GABAergic projection in a circuit essential for vocal learning. *J. Comp. Neurol.* 68–84 (1999).
166. Leblois, A., Bodor, A. L., Person, A. L. & Perkel, D. J. Millisecond timescale disinhibition mediates fast information transmission through an avian basal ganglia loop. *J. Neurosci.* **29,** 15420–33 (2009).
167. Fujimoto, H., Hasegawa, T. & Watanabe, D. Neural coding of syntactic structure in learned vocalizations in the songbird. *J. Neurosci.* **31,** 10023–33 (2011).
168. Castelino, C. B., Diekamp, B. & Ball, G. F. Noradrenergic projections to the song control nucleus area X of the medial striatum in male zebra finches (Taeniopygia guttata). *J. Comp. Neurol.* **562,** 544–562 (2007).
169. Lovell, P. V., Kasimi, B., Carleton, J., Velho, T. a. & Mello, C. V. Living without DAT : Loss and compensation of the dopamine transporter gene in sauropsids (birds and reptiles). *Nat. Publ. Gr.* **5,** 1–12 (2015).
170. Person, A. L. & Perkel, D. J. Unitary IPSPs drive precise thalamic spiking in a circuit required for learning. *Neuron* **46,** 129–140 (2005).
171. Reiner, A. *et al.* Revised nomenclature for avian telencephalon and some related brainstem nuclei. *J. Comp. Neurol.* **473,** 377–414 (2004).
172. Peng, Z. *et al.* Ultrastructural and electrophysiological analysis of Area X in the untutored and deafened Bengalese finch in relation to normally reared birds. *Brain Res.* **1527,** 87–98 (2013).
173. Doupe, A. J. & Konishi, M. Song-selective auditory circuits in the vocal control system of the zebra finch. *Neurobiology* **88,** 11339–11343 (1991).
174. Doupe, a J. & Solis, M. M. Song- and order-selective neurons develop in the songbird anterior forebrain during vocal learning. *J. Neurobiol.* **33,** 694–709 (1997).
175. Solis, M. M. & Doupe, a J. Anterior forebrain neurons develop selectivity by an intermediate stage of birdsong learning. *J. Neurosci.* **17,** 6447–6462 (1997).
176. Person, A. L. & Perkel, D. J. Pallidal neuron activity increases during sensory relay through thalamus in a songbird circuit essential for learning. *J. Neurosci.* **27,** 8687–8698 (2007).
177. Koumura, T., Seki, Y. & Okanoya, K. Local structure sensitivity in auditory information processing in avian song nuclei. *Neuroreport* **25,** 1–7 (2014).
178. Seki, Y., Hessler, N. a, Xie, K. & Okanoya, K. Food rewards modulate the activity of song neurons in Bengalese finches. *Eur. J. Neurosci.* **39,** 975–983 (2014).
179. Jenkinson, N. & Brown, P. New insights into the relationship between dopamine, beta oscillations and motor function. *Trends Neurosci.* **34,** 611–618 (2011).
180. Chalk, M., Gutkin, B. & Denève, S. Neural oscillations as a signature of efficient coding in the presence of synaptic delays. *Elife* **5,** 1–23 (2016).
181. Friston, K. J., Bastos, A. M., Pinotsis, D. & Litvak, V. LFP and oscillations-what do they tell us? *Curr. Opin. Neurobiol.* **31,** 1–6 (2015).
182. Buzsáki, G., Anastassiou, C. a & Koch, C. The origin of extracellular fields and currents--EEG, ECoG, LFP and spikes. *Nat. Rev. Neurosci.* **13,** 407–20 (2012).
183. Einevoll, G. T., Kayser, C., Logothetis, N. K. & Panzeri, S. Modelling and analysis of local field potentials for studying the function of cortical circuits. *Nat. Rev. Neurosci.* **14,** 770–85 (2013).
184. Yanagihara, S. & Hessler, N. a. Phasic basal ganglia activity associated with high-gamma oscillation during sleep in a songbird. *J. Neurophysiol.* **107,** 424–432 (2012).
185. Brown, P. *et al.* Dopamine dependency of oscillations between subthalamic nucleus and pallidum in Parkinson's disease. *J. Neurosci.* **21,** 1033–1038 (2001).

186. Costa, R. M. *et al.* Rapid alterations in corticostriatal ensemble coordination during acute dopamine-dependent motor dysfunction. *Neuron* **52,** 359–369 (2006).
187. Mallet, N. *et al.* Parkinsonian beta oscillations in the external globus pallidus and their relationship with subthalamic nucleus activity. *J. Neurosci.* **28,** 14245–14258 (2008).
188. Tachibana, Y., Iwamuro, H., Kita, H., Takada, M. & Nambu, A. Subthalamo-pallidal interactions underlying parkinsonian neuronal oscillations in the primate basal ganglia. *Eur. J. Neurosci.* **34,** 1470–1484 (2011).
189. Oswal, A., Brown, P. & Litvak, V. Synchronized neural oscillations and the pathophysiology of Parkinson's disease. *Curr. Opin. Neurol.* **26,** 662–70 (2013).
190. Hammond, C., Bergman, H. & Brown, P. Pathological synchronization in Parkinson's disease: networks, models and treatments. *Trends Neurosci.* **30,** 357–364 (2007).
191. Duffy, J. R. *Motor Speech Disorders: Substrates, Differential Diagnosis, and Management*. (Elsevier Health Sciences, 2013).
192. NIH. What you need to know about stroke. *National Institutes of Health* (2004). at <https://stroke.nih.gov/materials/needtoknow.htm>
193. De Diego-Balaguer, R. *et al.* Striatal degeneration impairs language learning: evidence from Huntington's disease. *Brain* **131,** 2870–81 (2008).
194. Nieuwboer, A., Rochester, L., Müncks, L. & Swinnen, S. P. Motor learning in Parkinson's disease: limitations and potential for rehabilitation. *Parkinsonism Relat. Disord.* **15 Suppl 3,** S53-8 (2009).
195. De Nunzio, A. M., Nardone, A. & Schieppati, M. The control of equilibrium in Parkinson's disease patients: delayed adaptation of balancing strategy to shifts in sensory set during a dynamic task. *Brain Res. Bull.* **74,** 258–270 (2007).
196. Krebs, H. I., Hogan, N., Hening, W., Adamovich, S. V & Poizner, H. Procedural motor learning in Parkinson's disease. *Exp. brain Res.* **141,** 425–437 (2001).
197. Wilkinson, L. & Jahanshahi, M. The striatum and probabilistic implicit sequence learning. *Brain Res.* **1137,** 117–30 (2007).
198. Marinelli, L. *et al.* Learning and consolidation of visuo-motor adaptation in Parkinson's disease. *Parkinsonism Relat. Disord.* **15,** 6–11 (2009).
199. Cohen, H. & Pourcher, E. Intact encoding, impaired consolidation in procedural learning in Parkinson's disease. *Exp. Brain Res.* **179,** 703–8 (2007).
200. Agostino, R. *et al.* Prolonged practice is of scarce benefit in improving motor performance in Parkinson's disease. *Mov. Disord.* **19,** 1285–93 (2004).
201. Abbruzzese, G., Trompetto, C. & Marinelli, L. The rationale for motor learning in Parkinson's disease. *Eur. J. Phys. Rehabil. Med* **45,** 209–214 (2009).
202. Katzenschlager, R. & Lees, A. J. Treatment of Parkinson's disease: levodopa as the first choice. *J. Neurol.* **249 Suppl,** II19-24 (2002).
203. Wichmann, T. & Delong, M. Deep-brain stimulation for basal ganglia disorders. *Basal Ganglia* 65–77 (2011).
204. Goodwin, V. A., Richards, S. H., Taylor, R. S., Taylor, A. H. & Campbell, J. L. The effectiveness of exercise interventions for people with Parkinson's disease: A systematic review and meta-analysis. *Mov. Disord.* **23,** 631–640 (2008).
205. Lötzke, D., Ostermann, T. & Büssing, A. Argentine tango in Parkinson disease - a systematic review and meta-analysis. *BMC Neurol.* **15,** 226 (2015).
206. Fox, C. M., Morrison, C. E., Ramig, L. O. & Sapir, S. Current perspectives on the Lee Silverman Voice Treatment (LSVT) for individuals with idiopathic Parkinson disease. *Am. J. Speech-Language Pathol.* **11,** 111–124 (2002).
207. Fox, C., Ebersbach, G., Ramig, L. & Sapir, S. LSVT LOUD and LSVT BIG: Behavioral treatment programs for speech and body movement in Parkinson disease. *Parkinsons. Dis.* **2012,** (2012).
208. Hoffmann, L. A., Kelly, C. W., Nicholson, D. A. & Sober, S. J. A lightweight,

headphones-based system for manipulating auditory feedback in songbirds. *J. Vis. Exp.* e50027 (2012).
209. Colombo, M. Deep and beautiful. The reward prediction error hypothesis of dopamine. *Stud. Hist. Philos. Biol. Biomed. Sci.* **45,** 57–67 (2014).
210. Leventhal, D. K. D. D. K. *et al.* Dissociable effects of dopamine on learning and performance within sensorimotor striatum. *Basal Ganglia* **4,** 43–54 (2014).
211. Galvan, A. & Wichmann, T. Pathophysiology of parkinsonism. *Clin. Neurophysiol.* **119,** 1459–1474 (2008).
212. Rubin, J. E., McIntyre, C. C., Turner, R. S. & Wichmann, T. Basal ganglia activity patterns in parkinsonism and computational modeling of their downstream effects. *Eur. J. Neurosci.* **36,** 2213–28 (2012).
213. Hoffmann, L. A. & Sober, S. J. Vocal generalization depends on gesture identity and sequence. *J. Neurosci.* **34,** 5564–5574 (2014).
214. Hahnloser, R. H. R., Kozhevnikov, A. A. & Fee, M. S. An ultra-sparse code underlies the generation of neural sequences in a songbird. *Nature* **419,** 65–70 (2002).
215. Leonardo, A. & Fee, M. S. Ensemble coding of vocal control in birdsong. *J. Neurosci.* **25,** 652–61 (2005).
216. Wohlgemuth, M. J., Sober, S. J. & Brainard, M. S. Linked control of syllable sequence and phonology in birdsong. *J. Neurosci.* **30,** 12936–12949 (2010).
217. Yu, A. C. & Margoliash, D. Temporal hierarchical control of singing in birds. *Science* **273,** 1871–5 (1996).
218. Sober, S. J. & Brainard, M. S. Vocal learning is constrained by the statistics of sensorimotor experience. *Proc. Natl. Acad. Sci. U. S. A.* **109,** 21099–103 (2012).
219. Taylor, J. A., Hieber, L. L. & Ivry, R. B. Feedback-dependent generalization. *J. Neurophysiol.* **109,** 202–15 (2013).
220. Margoliash, D. & Fortune, E. Temporal and harmonic combination-sensitive neurons in the zebra finch's HVc. *J. Neurosci.* **12,** 4309–4326 (1992).
221. Lewicki, M. S. & Arthur, B. J. Hierarchical organization of auditory temporal context sensitivity. *J. Neurosci.* **16,** 6987–98 (1996).
222. Dave, A. S. & Margoliash, D. Song replay during sleep and computational rules for sensorimotor vocal learning. *Science* **290,** 812–6 (2000).
223. Hogden, J., Lofqvist, A. & Gracco, V. Accurate recovery of articulator positions from acoustics: new conclusions based on human data. *J. Acoust. Soc. Am.* **100,** 1819–1834 (1996).
224. Mitra, V., Nam, H., Espy-Wilson, C., Saltzman, E. & Goldstein, L. Retrieving tract variables from acoustics: a comparison of different machine learning strategies. *IEEE J. Sel. Top. Signal Process.* **4,** 1027–1045 (2010).
225. Goller, F. & Suthers, R. A. Role of syringeal muscles in controlling the phonology of bird song. *J. Neurophysiol.* **76,** 287–300 (1996).
226. Gardner, T., Cecchi, G., Magnasco, M., Laje, R. & Mindlin, G. Simple motor gestures for birdsongs. *Phys. Rev. Lett.* **87,** 1–4 (2001).
227. Laje, R., Gardner, T. & Mindlin, G. Neuromuscular control of vocalizations in birdsong: a model. *Phys. Rev. E* **65,** 1–8 (2002).
228. Suthers, R. A., Goller, F. & Hartley, R. S. Motor stereotypy and diversity in songs of mimic thrushes. *J. Neurobiol.* **30,** 231–45 (1996).
229. Secora, K. R. *et al.* Syringeal specialization of frequency control during song production in the bengalese finch (Lonchura striata domestica). *PLoS One* **7,** e34135 (2012).
230. Charlesworth, J. D., Tumer, E. C., Warren, T. L. & Brainard, M. S. Learning the microstructure of successful behavior. *Nat. Neurosci.* **14,** 373–80 (2011).
231. Wolpert, D. M., Diedrichsen, J. & Flanagan, J. R. Principles of sensorimotor learning. *Nat. Rev. Neurosci.* **12,** 739–51 (2011).

232. Hoffmann, L. A., Saravanan, V., Wood, A. N., He, L. & Sober, S. J. Dopaminergic contributions to vocal learning. *J. Neurosci.* **36,** 2176–2189 (2016).
233. Schultz, W. Behavioral dopamine signals. *Trends Neurosci.* **30,** 203–210 (2007).
234. Peh, W. Y. X., Roberts, T. F. & Mooney, R. Imaging auditory representations of song and syllables in populations of sensorimotor neurons essential to vocal communication. *J. Neurosci.* **35,** 5589–5605 (2015).
235. Vallentin, D. & Long, M. a. Motor origin of precise synaptic inputs onto forebrain neurons driving a skilled behavior. *J. Neurosci.* **35,** 299–307 (2015).
236. Graybiel, A. M. The basal ganglia: learning new tricks and loving it. *Curr. Opin. Neurobiol.* **15,** 638–44 (2005).
237. Schober, A. Classic toxin-induced animal models of Parkinson's disease: 6-OHDA and MPTP. *Cell Tissue Res.* **318,** 215–224 (2004).
238. Soha, J. a., Shimizu, T. & Doupe, A. J. Development of the catecholaminergic innervation of the song system of the male zebra finch. *J. Neurobiol.* **29,** 473–89 (1996).
239. Mello, C. V, Pinaud, R. & Ribeiro, S. Noradrenergic system of the Zebra finch brain : immunocytochemical study of dopamine-b-hydroxylase. *J. Comp. Neurol.* **400,** 207–28 (1998).
240. Kutner, M. H., Nachtsheim, C. J., Neter, J. & Li, W. *Applied Linear Statistical Models*. (McGraw-Hill, 2005).
241. Preibisch, S., Saalfeld, S. & Tomancak, P. Globally optimal stitching of tiled 3D microscopic image acquisitions. *Bioinformatics* **25,** 1463–1465 (2009).
242. Karten, H. J. *et al.* Digital atlas of the zebra finch (Taeniopygia guttata) brain: A high-resolution photo atlas. *J. Comp. Neurol.* **521,** 3702–15 (2013).
243. Palkovits, M. Isolated removal of hypothalamic or other brain nuclei of the rat. *Brain Res.* **59,** 449–450 (1973).
244. Pozdeyev, N. *et al.* Dopamine modulates diurnal and circadian rhythms of protein phosphorylation in photoreceptor cells of mouse retina. *Eur. J. Neurosci.* **27,** 2691–2700 (2008).
245. Lowry, O. H., Rosebrough, N. J., Farr, L. A. & Randall, R. J. Protein measurement with the folin phenol reagent. *J Biol Chem* **193,** 265–275 (1951).
246. Murugan, M., Harward, S., Scharff, C. & Mooney, R. Diminished FoxP2 levels affect dopaminergic modulation of corticostriatal signaling important to song variability. *Neuron* **80,** 1464–76 (2013).
247. Kao, M. H. & Brainard, M. S. Lesions of an avian basal ganglia circuit prevent context-dependent changes to song variability. *J. Neurophysiol.* **96,** 1441–55 (2006).
248. Nieuwenhuis, S., Forstmann, B. U. & Wagenmakers, E.-J. Erroneous analyses of interactions in neuroscience: a problem of significance. *Nat. Neurosci.* **14,** 1105–7 (2011).
249. Kelly, C. W. & Sober, S. J. A simple computational principle predicts vocal adaptation dynamics across age and error size. *Front. Integr. Neurosci.* **8,** 1–9 (2014).
250. Bottjer, S. W. & Altenau, B. Parallel pathways for vocal learning in basal ganglia of songbirds. *Nat. Neurosci.* **13,** 153–5 (2010).
251. Iyengar, S., Viswanathan, S. S. & Bottjer, S. W. Development of topography within song control circuitry of zebra finches during the sensitive period for song learning. *J. Neurosci.* **19,** 6037–6057 (1999).
252. Hara, E., Kubikova, L., Hessler, N. A. & Jarvis, E. D. Role of the midbrain dopaminergic system in modulation of vocal brain activation by social context. *Eur. J. Neurosci.* **25,** 3406–3416 (2007).
253. Canopoli, A., Herbst, J. a. & Hahnloser, R. H. R. A higher sensory brain region is involved in reversing reinforcement-induced vocal changes in a songbird. *J. Neurosci.* **34,** 7018–7026 (2014).
254. Deumens, R., Blokland, A. & Prickaerts, J. Modeling Parkinson's disease in rats: an

evaluation of 6-OHDA lesions of the nigrostriatal pathway. *Exp. Neurol.* **175,** 303–317 (2002).
255. Debeir, T. *et al.* Effect of intrastriatal 6-OHDA lesion on dopaminergic innervation of the rat cortex and globus pallidus. *Exp. Neurol.* **193,** 444–54 (2005).
256. Brown, P. & Williams, D. Basal ganglia local field potential activity: Character and functional significance in the human. *Clin. Neurophysiol.* **116,** 2510–2519 (2005).
257. Xu, X., Zheng, C. & Zhang, T. Reduction in LFP cross-frequency coupling between theta and gamma rhythms associated with impaired STP and LTP in a rat model of brain ischemia. *Front. Comput. Neurosci.* **7,** 27 (2013).
258. Silberstein, P. *et al.* Oscillatory pallidal local field potential activity inversely correlates with limb dyskinesias in Parkinson's disease. *Exp. Neurol.* **194,** 523–529 (2005).
259. Theunissen, F. E. *et al.* Song selectivity in the song system and in the auditory forebrain. *Ann. N. Y. Acad. Sci.* **1016,** 222–245 (2004).
260. Gale, S. D. S. & Perkel, D. J. D. A basal ganglia pathway drives selective auditory responses in songbird dopaminergic neurons via disinhibition. *J. Neurosci.* **30,** 1027–1037 (2010).
261. Ellis, D. P. W. A phase vocoder in Matlab. http://www.ee.columbia.edu/~dpwe/resources/matlab/ (2002).
262. Srivastava, K. H., Elemans, C. P. H. & Sober, S. J. Multifunctional and context-dependent control of vocal acoustics by individual muscles. *J. Neurosci.* **35,** 14183–94 (2015).
263. Alvarez-Fischer, D. *et al.* Characterization of the striatal 6-OHDA model of Parkinson's disease in wild type and alpha-synuclein-deleted mice. *Exp. Neurol.* **210,** 182–93 (2008).
264. Stott, S. R. W. & Barker, R. a. Time course of dopamine neuron loss and glial response in the 6-OHDA striatal mouse model of Parkinson's disease. *Eur. J. Neurosci.* 1–15 (2013).
265. Rolston, J. D., Gross, R. E., Potter, S. M. & Surgery, A. Common median referencing for improved action potential detection with multielectrode arrays. *Proc. 31st Annu. Int. Conf. IEEE Eng. Med. Biol. Soc. Eng. Futur. Biomed. EMBC 2009* 1604–1607 (2009).
266. Rossant, C. *et al.* Spike sorting for large, dense electrode arrays. *Nat. Neurosci.* **19,** 634–641 (2016).
267. Kadir, S. N., Goodman, D. F. & Harris, K. D. High-dimensional cluster analysis with the Masked EM Algorithm. *Neural Comput.* **26,** 2379–2394 (2014).
268. Purpura, K. P. & Bokil, H. Neural Signal Processing: Tutorial 1. *Neural Signal Process.* (2008).
269. Bokil, H., Andrews, P., Kulkarni, J. E., Mehta, S. & Mitra, P. P. Chronux: A platform for analyzing neural signals. *J. Neurosci. Methods* **192,** 146–151 (2010).
270. Doupe, A. J. Song-and order-selective neurons in the songbird anterior forebrain and their emergence during vocal development. *J. Neurosci.* **17,** 1147–1167 (1997).
271. Solis, M. M. M. & Doupe, A. J. A. J. Contributions of tutor and bird's own song experience to neural selectivity in the songbird anterior forebrain. *J. Neurosci.* **19,** 4559–4584 (1999).
272. Kojima, S. & Doupe, A. J. Neural encoding of auditory temporal context in a songbird basal ganglia nucleus, and its independence of birds' song experience. *Eur. J. Neurosci.* **27,** 1231–1244 (2008).
273. Kojima, S. & Doupe, A. J. Song selectivity in the pallial-basal ganglia song circuit of zebra finches raised without tutor song exposure. *J. Neurophysiol.* **98,** 2099–2109 (2007).
274. Fukushima, M., Rauske, P. L. & Margoliash, D. Temporal and rate code analysis of responses to low-frequency components in the bird's own song by song system neurons. *J. Comp. Physiol. A Neuroethol. Sensory, Neural, Behav. Physiol.* **201,** 1103–1114 (2015).
275. Mallet, N. *et al.* Disrupted dopamine transmission and the emergence of exaggerated beta oscillations in subthalamic nucleus and cerebral cortex. *J Neurosci* **28,** 4795–4806 (2008).
276. Vicario, D. S. & Yohay, K. H. Song-selective auditory input to a forebrain vocal control

nucleus in the zebra finch. *J. Neurobiol.* **24,** 488–505 (1993).
277. Lewandowski, B. C. & Schmidt, M. Short bouts of vocalization induce long-lasting fast gamma oscillations in a sensorimotor nucleus. *J. Neurosci.* **31,** 13936–13948 (2011).
278. Markowitz, J. E. *et al.* Mesoscopic patterns of neural activity support songbird cortical sequences. *PLoS Biol.* **13,** e1002158 (2015).
279. Beckers, G. J. L. & Gahr, M. Neural processing of short-term recurrence in songbird vocal communication. *PLoS One* **5,** (2010).
280. Chen, X. *et al.* Sensorimotor control of vocal pitch production in Parkinson's disease. *Brain Res.* (2013).
281. Liu, H., Wang, E. Q., Metman, L. V. & Larson, C. R. Vocal responses to perturbations in voice auditory feedback in individuals with Parkinson's disease. *PLoS One* **7,** e33629 (2012).
282. Kobayasi, K. I. & Okanoya, K. Context-dependent song amplitude control in Bengalese finches. *Neuroreport* **14,** 521–4 (2003).
283. Osmanski, M. S. & Dooling, R. J. The effect of altered auditory feedback on control of vocal production in budgerigars (Melopsittacus undulatus). *J. Acoust. Soc. Am.* **126,** 911–9 (2009).
284. Kakade, S. & Dayan, P. Dopamine: generalization and bonuses. *Neural Netw.* **15,** 549–59 (2002).
285. Kahnt, T. & Tobler, P. N. Dopamine regulates stimulus generalization in the human hippocampus. *Elife* **5,** 1–20 (2016).
286. Barnes, T. D., Kubota, Y., Hu, D., Jin, D. Z. & Graybiel, A. M. Activity of striatal neurons reflects dynamic encoding and recoding of procedural memories. *Nature* **437,** 1158–61 (2005).
287. Torres-Oviedo, G. Muscle synergies characterizing human postural responses. *J. Neurophysiol.* 2144–2156 (2007).
288. Basteris, A., Bracco, L. & Sanguineti, V. Robot-assisted intermanual transfer of handwriting skills. *Hum. Mov. Sci.* **31,** 1175–1190 (2012).
289. Fleckenstein, A. E., Volz, T. J., Riddle, E. L., Gibb, J. W. & Hanson, G. R. New insights into the mechanism of action of amphetamines. *Annu. Rev. Pharmacol. Toxicol.* **47,** 681–698 (2007).
290. Isaias, I. U. *et al.* Dopaminergic striatal innervation predicts interlimb transfer of a visuomotor skill. *J. Neurosci.* **31,** 14458–62 (2011).
291. Shiner, T. *et al.* Dopamine and performance in a reinforcement learning task: Evidence from Parkinson's disease. *Brain* **135,** 1871–1883 (2012).
292. Verschueren, S. M., Swinnen, S. P., Dom, R. & De Weerdt, W. Interlimb coordination in patients with Parkinson's disease: motor learning deficits and the importance of augmented information feedback. *Exp. Brain Res.* **113,** 497–508 (1997).
293. Myers, C. E. *et al.* Dissociating hippocampal versus basal ganglia contributions to learning and transfer. *J. Cogn. Neurosci.* **15,** 185–93 (2003).
294. Shohamy, D., Myers, C. & Geghman, K. L-dopa impairs learning, but spares generalization, in Parkinson's disease. *Neuropsychologia* **44,** 774–784 (2006).
295. Bello, O., Sanchez, J. A. & Fernandez-del-Olmo, M. Treadmill walking in Parkinson's disease patients: adaptation and generalization effect. *Mov. Disord.* **23,** 1243–9 (2008).
296. Heremans, E. *et al.* Impaired retention of motor learning of writing skills in patients with Parkinson's disease with freezing of gait. *PLoS One* **11,** 1–13 (2016).
297. Thenganatt, M. A. & Jankovic, J. Parkinson disease subtypes. *JAMA Neurol.* **71,** 499–504 (2014).
298. Del Tredici, K., Rüb, U., De Vos, R. a I., Bohl, J. R. E. & Braak, H. Where does parkinson disease pathology begin in the brain? *J. Neuropathol. Exp. Neurol.* **61,** 413–426 (2002).
299. Adret, P. In search of the song template. *Ann. N. Y. Acad. Sci.* **324,** 303–324 (2004).

300. Hisey, E., Kearney, M. & Mooney, R. A midbrain-basal ganglia circuit is critical to externally and internally reinforced vocal learning. in *Society for Neuroscience annual meeting (conference poster)* (2016).
301. Shen, W., Flajolet, M., Greengard, P. & Surmeier, D. J. Dichotomous dopaminergic control of striatal synaptic plasticity. *Science* **321,** 848–51 (2008).
302. Yuan, H., Sarre, S., Ebinger, G. & Michotte, Y. Histological, behavioural and neurochemical evaluation of medial forebrain bundle and striatal 6-OHDA lesions as rat models of Parkinson's disease. *J. Neurosci. Methods* **144,** 35–45 (2005).
303. Thiele, S. L., Warre, R. & Nash, J. E. Development of a unilaterally-lesioned 6-OHDA mouse model of Parkinson's disease. *J. Vis. Exp.* 1–10 (2012).
304. PubChem Compound Database. Cyperquat (MPP+). *National Center for Biotechnology Information* (2017). at <https://pubchem.ncbi.nlm.nih.gov/compound/39484>
305. Meredith, G. E. & Rademacher, D. J. MPTP mouse models of Parkinson's disease: an update. *J Park. Dis* **1,** 19–33 (2011).
306. Shimohama, S., Sawada, H., Kitamura, Y. & Taniguchi, T. Disease model: Parkinson's disease. *Trends Mol. Med.* **9,** 360–365 (2003).
307. Espino, A. *et al.* Chronic effects of single intrastriatal injections of 6- hydroxydopamine or 1-methyl-4-phenylpyridinium studied by microdialysis in freely moving rats. *Brain Res.* **695,** 151–157 (1995).
308. Visanji, N. & Brotchie, J. MPTP-induced models of Parkinson's disease in mice and non-human primates. *Curr. Protoc. Pharmacol.* **1983,** 1–13 (2005).
309. Liu, W. *et al.* Human mutant huntingtin disrupts vocal learning in transgenic songbirds. *Nat. Neurosci.* **18,** 1–9 (2015).
310. Semrau, J. a, Perlmutter, J. S. & Thoroughman, K. a. Visuomotor adaptation in Parkinson's disease: effects of perturbation type and medication state. *J. Neurophysiol.* **111,** 2675–87 (2014).
311. Prasad, S., Thapliyal, J. & Chaturvedi, C. The effects of daily injections of l-dihydroxyphenylalanine and 5-hydroxytryptophan in different temporal relationships on thyroid-gonadal interaction in an Indian finch, Spotted Munia, Lonchura punctulata. *Gen. Comp. Endocrinol.* **86,** 335–343 (1992).
312. Appeltants, D., Ball, G. F. & Balthazart, J. The origin of catecholaminergic inputs to the song control nucleus RA in canaries. *Neuroreport* **13,** 649–653 (2002).
313. Appeltants, D., Absil, P., Balthazart, J. & Ball, G. F. Identification of the origin of catecholaminergic inputs to HVc in canaries by retrograde tract tracing combined with tyrosine hydroxylase immunocytochemistry. *J. Chem. Neuroanat.* **18,** 117–133 (2000).
314. Wang, S., Liao, C., Meng, W., Huang, Q. & Li, D. Activation of D1-like dopamine receptors increases the NMDA-induced gain modulation through a PKA-dependent pathway in the premotor nucleus of adult zebra finches. *Neurosci. Lett.* **589,** 37–41 (2015).
315. Pesaran, B. Spectral Analysis for Neural Signals. *Short Course III* (2007). at <http://neurophysics.ucsd.edu/courses/physics_173_273/SfN_Short_Course_c1.pdf>
316. Li, Z., Ouyang, G., Yao, L. & Li, X. Estimating the correlation between bursty spike trains and local field potentials. *Neural Networks* **57,** 63–72 (2014).
317. Mikell, C. B. & McKhann, G. M. Regulation of Parkinsonian motor behaviors by optogenetic control of basal ganglia circuitry. *Neurosurgery* **67,** 622–626 (2010).
318. Leblois, A. *et al.* Late emergence of synchronized oscillatory activity in the pallidum during progressive parkinsonism. *Eur. J. Neurosci.* **26,** 1701–1713 (2007).
319. Sheth, S. & Abuelem, T. Basal ganglia neurons dynamically facilitate exploration during associative learning. *J. Neurosci.* **31,** 4878–4885 (2011).